In presenting the dissertation as a partial fulfillment of the requirements for an advanced degree from the Georgia Institute of Technology, I agree that the Library of the Institute shall make it available for inspection and circulation in accordance with its regulations governing materials of this type. I agree that permission to copy from, or to publish from, this dissertation may be granted by the professor under whose direction it was written, or, in his absence, by the Dean of the Graduate Division when such copying or publication is solely for scholarly purposes and does not involve potential financial gain. It is understood that any copying from, or publication of, this dissertation which involves potential financial gain will not be allowed without written permission.

_____

_____

7/25/68

A STUDY OF AIRFLOW CHARACTERISTICS IN BUILT-UP FAN ROOMS

A THESIS

Presented to

The Faculty of the Division

of Graduate Studies and Research

by

Robert Douglas Stone

In Partial Fulfillment

of the Requirements for the Degree

Master of Science in Mechanical Engineering

Georgia Institute of Technology

January, 1971

A STUDY OF AIRFLOW CHARACTERISTICS

IN BUILT-UP FAN ROOMS

Approved:

Date approved by Chairman: Jan 29 1971

ACKNOWLEDGEMENTS

I extend my sincere appreciation to my advisor, Professor W. A. Hinton. Prof. Hinton was a constant source of technical assistance and moral encouragement. I would also like to thank Dr. A. Bergles for his comments and advisement and Dr. T. Kethley for his comments.

I thank the American Society of Heating, Refrigerating and Air Conditioning Engineers. Without A.S.H.R.A.E. financial support this study would not have been possible. I appreciate the assistance of members of the Atlanta Chapter of A.S.H.R.A.E. I especially appreciate the contributions of equipment and materials.

A special note of thanks goes to Britt Alderman, Jr., my uncle, who has taught me the many facets of design of air conditioning systems, while providing a means to finance my education.

Finally I thank my wife for helping with the preparation of this paper. Most of all, I thank Gail for the understanding and encouragement she has given me.

TABLE OF CONTENTS

TABLE OF CONTENTS (CONTINUED)

LIST OF TABLES

LIST OF ILLUSTRATIONS

LIST OF ILLUSTRATIONS (CONTINUED)

LIST OF ILLUSTRATIONS (CONTINUED)

LIST OF ILLUSTRATIONS (CONTINUED)

SUMMARY

A dual duct air conditioning system is one method of providing many zones of control from centrally located equipment. Satisfactory design information is available for all components of the dual duct system except the central equipment. In particular, there have only been recommendations for arrangement with no design information available for the central air handling equipment or fan room.

The purpose of this study is to take the first step toward providing adequate design information for the built-up dual duct fan room. After initial testing, it became apparent that construction of a model would be useful. The model provided a means of varying the arrangements of the fan room to determine the effect on the system performance.

Field tests measured 100 percent variation of the velocity of air through the cooling coil, the model having a similar variation. Secondary flow set-up by the interaction of the expanding mainstream flow from the fan to the coils produced wiping at the coil surface four times greater than the through-flow velocity. Supply air temperature stratification and moisture carry-over could result from poor distribution of air to the coils.

A perforated plate of about 50 percent free area provided satisfactory distribution of air from the fan to the coils, without an effective decrease in flow rate or pressure. The position of the plate was optimized to be 2/3 the distance from the fan to the coils. A vaned outlet diffuser performed satisfactory for several distances, but did not at closer than two fan wheel diameters.

NOMENCLATURE

A_a	-	Area of cross section at position "a," ft.^{2}
A_o	-	Open area of perforated plate
A_t	-	Total area of perforated plate
b	-	Characteristic dimension for screen Reynolds number, bar width, ft.
C_c	-	Contraction coefficient
C_o	-	Orifice contraction coefficient
D	-	Fan wheel diameter
g	-	Acceleration due to gravity in ft./sec.^{2}
g_c	-	Gravitational constant, lbm-ft./lb-sec.^{2}
H_t	-	Total head loss in feet of fluid flowing
H_s	-	Static head loss
H_v	-	Velocity head loss
H_r	-	Static head regain
h_t	-	Total head loss, inches of water
h_s	-	Static head loss
h_v	-	Velocity head loss
h_r	-	Static head regain
k	-	Loss coefficient for a diverging section
K	-	Perforated plate loss coefficient
L	-	Characteristic dimension of Reynolds number

$\dot{m}$ - Mass flow rate

N_R - Reynolds number

Q - Flow rate, cu. ft./min.

P_a - Static pressure at position "a"

P_s - Stagnation pressure

ΔP_c - Pressure drop across a coil

ΔP_p - Pressure drop across a perforated plate

S - Solidity ratio, $1-A_o/A_t$

V_o - Mean Velocity

V_a - Mean velocity at position "a," ft./sec

u, v - Velocity at points in velocity profile

VP_e - Acceptable velocity pressure at coil face

VP_c - Velocity pressure for coil through-flow velocity

W - Width of two dimensional expansion channel

μ - Dynamic viscosity

ν - Kinetic viscosity

ρ - Density

Subscripts

a - Air

w - Water

p - Prototype

m - Model

u - Upstream

1, 2, . . Position in flow path

ABBREVIATIONS

R.A.	Return air
S.A.	Supply air
O.A.	Outside air
D.W.D.I.	Double width, double inlet fan
fpm	Feet per minute
cfm	Cubic feet per minute
C	Cold
H	Hot

CHAPTER I

INTRODUCTION

Background

In the past 20 years the dual duct air conditioning system has emerged as one answer to the requirements of modern commercial air conditioning systems. The dual duct system is applicable to buildings having a multiplicity of zoning requirements.

Basically the dual duct system consists of two complete duct systems, one conveying cold air while the other carries warm air. Individual rooms or groups of rooms which compose a zone are supplied with a mixture of cold air and warm air from a mixing box controlled by the zone thermostat. The ability to provide simultaneous heating and cooling from central equipment to different zones makes the dual duct system a popular choice for large multi-zone applications.

The factor contributing most to widespread use of dual duct systems was the introduction of high velocity air distribution (1). With high velocity airflow, duct sizes could be reduced, thus fitting the space limitations imposed by the building architecture. Since duct losses are a function of velocity, the dual duct system is also a medium-to-high-pressure system (2-1/2 to 10 inches of water). Along with reduced space requirements, the central location of major equipment is an advantage of dual duct systems. Most maintenance is confined to the central location. Piping and electrical wiring are limited to central locations away from

tenant spaces.

The dual duct air conditioning system consists of essentially three components; these are: the central equipment, the high velocity duct system, and terminal mixing box with associated low velocity duct and distribution system. This study is concerned with the central air handling equipment. In particular, the arrangement of supply air fan and coils with associated plenums will be considered.

In general, the consulting engineer has adequate design information for dual duct systems. Performance data has been published for duct components and duct systems as applied to high velocity air distribution. Manufacturers have about 20 years to refine the design of dual duct terminal mixing boxes. Looking at the central system and assuming that it is a "built-up" system to fit the space, there is little design information available. A built-up system would be one containing various components, such as filters, fan, and coils, which were selected and arranged to fit the space by the designer. The consulting engineer must generally rely on past experience in adapting fan, coil, filters, etc., to a space, allowing maximum rental space. The components are all subject to elaborate rating procedures, none of which make allowances for the built-up dual duct fan room type application.

Though experience can inform a consulting engineer as to what design worked or did not work, the complexity of the dual duct fan room often makes it difficult to evaluate performance. Such things as moisture carry-over are easy to observe, but the cause, poor velocity distribution, is more difficult to

comprehend. Furthermore, any attempt by a designer to evaluate, by field testing, fan and/or coil performance in the dual duct system would require elaborate test equipment and excessive time.

Survey of Literature

Much of the design information for high velocity dual duct systems included in the 1970 ASHRAE Guide and Data Book (2) was originated by Shataloff and Waterfill (1, 3, 4). Shataloff (1) has considered the total problem of designing dual duct systems. The thermodynamics of the dual duct system present no difficult problem to the consulting engineer. The dual duct cycles and psychrometrics have been covered extensively by Shataloff (1, 3) and others (2, 5). The operating characteristics of dual duct mixing boxes were also covered by Shataloff (1, 3). The mixing box has become a standard item with companies that manufacture air distribution equipment. Mixing box performance is cataloged and assumed to be accurate.

Major drawbacks in the application of dual duct systems included the lack of accurate knowledge about losses in air distribution systems, heat loss and gain in the duct system, and noise of high velocity air in the ducts. Duct and duct components losses have been measured and compiled (6, 7, 8). A study of heat loss and gain in high velocity ductwork has been made (9). Several reports on noise in dual duct systems are available to the consulting engineer (10, 11).

Thus far it is seen that design information is available for most of the components of dual duct systems, except the central equipment. Shataloff (1) gives a typical arrangement of a fan room and suggests using a perforated plate to distribute air to the coil face. Other than this, there is very little information available

for use in design of the fan room. Recently one manufacturer has published recommendations for using perforated plates and a method of estimating the distance from fan to coils for an acceptable velocity distribution at the coils (12). Aside from the above mentioned work, very little has been written about the design of built-up fan rooms.

Out of necessity the performance of the components of a fan room must be looked at individually, since most information is presented in this manner. The fan performance has been considered by Farquhar (13) and others (12, 14). Distribution of high velocity air out of the fan is considered by Gilman and Graham (15, 16) using diffusers and perforated plates, respectively. Losses for perforated plates have been measured by Stone (17) and the performance of perforated plates predicted and measured by Baines (18) and Lipstein (19). Friction and dynamic losses of abrupt or diverging expansions and contractions are considered by Kratz and Fellows (20). The performance of cooling and heating coils which are subjected to poor air entrance has not been considered (21). Methods of improving distribution of air from the fan to the coils in a dual duct fan room have not been studied.

Statement of Objective and Scope of Investigation

In order to establish design parameters for built-up dual duct fan rooms, a study of airflow characteristics is required. Airflow characteristics encompass the flow magnitude and direction of air as it leaves the fan, passes through any flow correction device, and enters and leaves the cooling and heating coils. This

study deals with the first step in evaluating the performance of a built-up fan room, that is, the airflow within the plenum. This study will establish how well air is distributed from the fan outlet to the cooling and heating coils of a built-up fan room.

Case studies initiated in built-up fan rooms pointed to the need to vary the arrangement of the components of such rooms. Out of necessity a model was constructed to study various arrangements of the fan, coils, and duct connections. This paper correlates the performance of the model with the actual system or prototype. Information currently available is used to estimate the performance of the components which make up a built-up fan room. Based on the performance of the model, design parameters for a built-up fan room are recommended.

Case Studies of Actual Systems

Description of Actual Systems

The arrangement of equipment which makes up the built-up fan is dependent on the available space. A typical layout would be Fig. 1 as suggested by Shataloff (1). In this typical layout, a rectangular duct is used; but currently machine-formed round and flat-oval duct are popular. In this arrangement return air is ducted to the return air fan. For large systems the return air duct might be replaced with a masonry shaft, arriving in a plenum which contains the return air fan. Where head room is limited, two supply air fans might be used. Appendix A contains a brief survey of various arrangements of built-up fan rooms.

In order to consider the performance of fan rooms, a means of comparing the size and general dimensions of the equipment is required. In other words, a

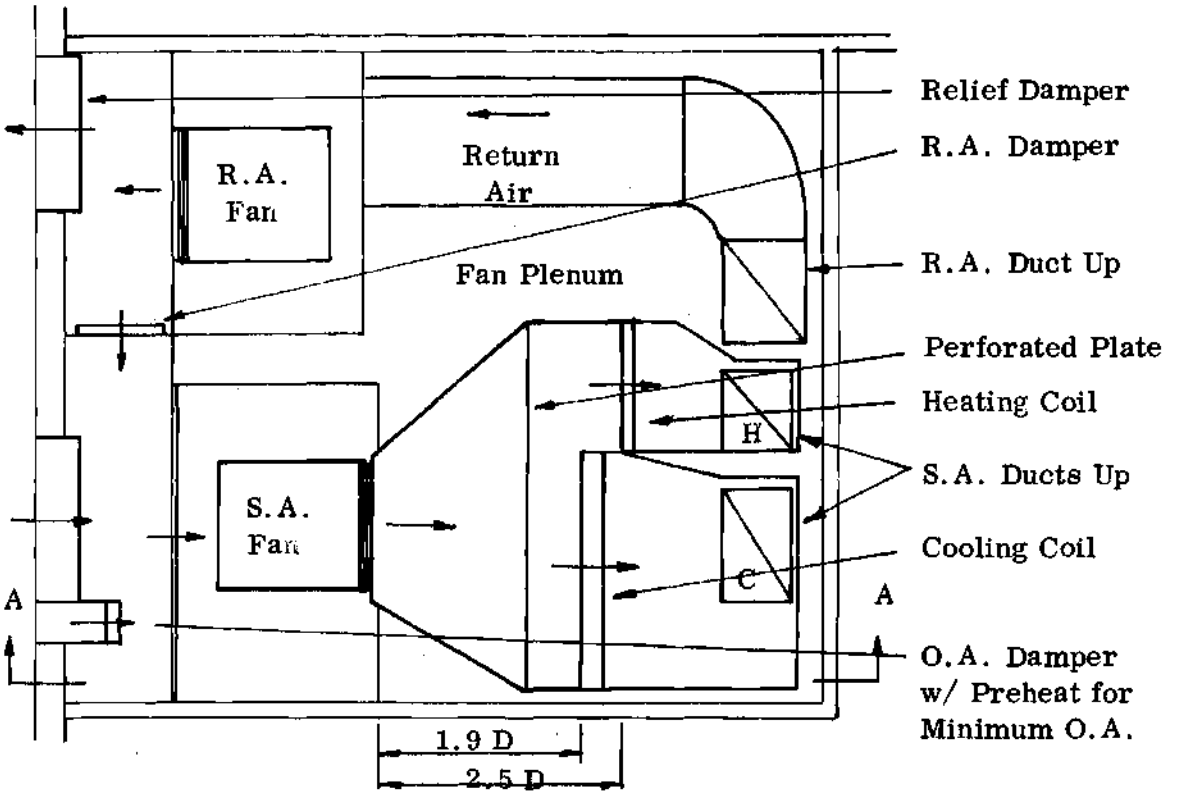

FAN ROOM FLOOR PLAN

Scale = 1/8" = 1'-0"

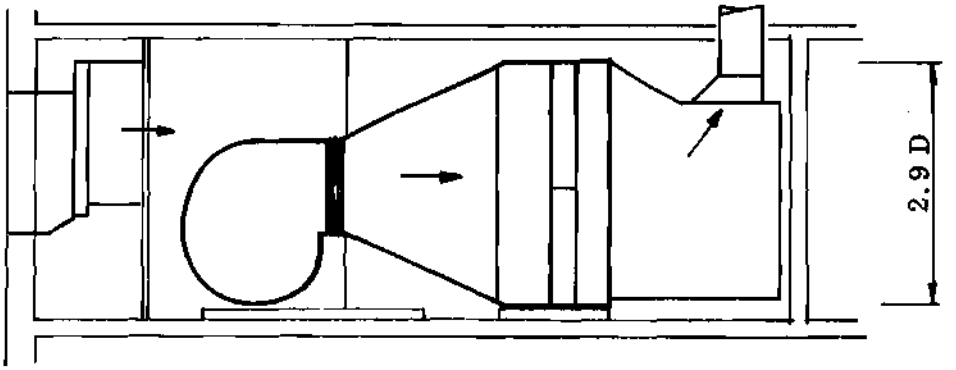

SECTION A.A

Figure 1. Shataloff's Suggested Dual Duct Fan Room Arrangement.

characteristic dimension of the dual duct fan room is needed. Looking at the fan plenum section of the fan room, there are only two possible characteristic dimensions available, either the fan or the coils. The size and shape of the coils is subject to much variation due to such factors as, face velocity, number of rows, fin spacing, and height or width limitations. Thus, the only logical choice of a characteristic dimension came from the fan. It is customary to catalog centrifugal fans by wheel diameter. Wheel diameter is also used as the characteristic dimension of fans in dimensional analysis. Logically, wheel diameter was considered first when looking for a characteristic dimension. Outlet dimensions might have been applicable, but analysis of the outlet dimensions of various fans show that the outlet size is dependent on wheel diameter. The ratio of dimensions of the fan plenum to the wheel diameter gives a dimension in terms of fan diameters, Fig. 1. Appendix A contains various fan room arrangements dimensioned in terms of fan diameters. For example, the distance from fan outlet to the cooling coil face varies from 2.0 D to 1.45 D (D - fan wheel diameter) for fan rooms of 70,000 to 100,000 cfm capacity (cubic feet per minute).

The fan room arrangement chosen for taking data was the actual system of Building A shown in Fig. 2. The arrangement in Fig. 2 is similar to the recommendations of Shataloff (Fig. 1). Since the recommendations of Shataloff have been used extensively in the field of dual duct systems, it seemed appropriate to use a fan room similar to Fig. 1 for field testing. Both systems use an offset of the coils to allow for piping and to eliminate wiping of the heating coil. "Wiping" of the coil refers to flow across the face of the coil which does not go through the coil. The dimensions

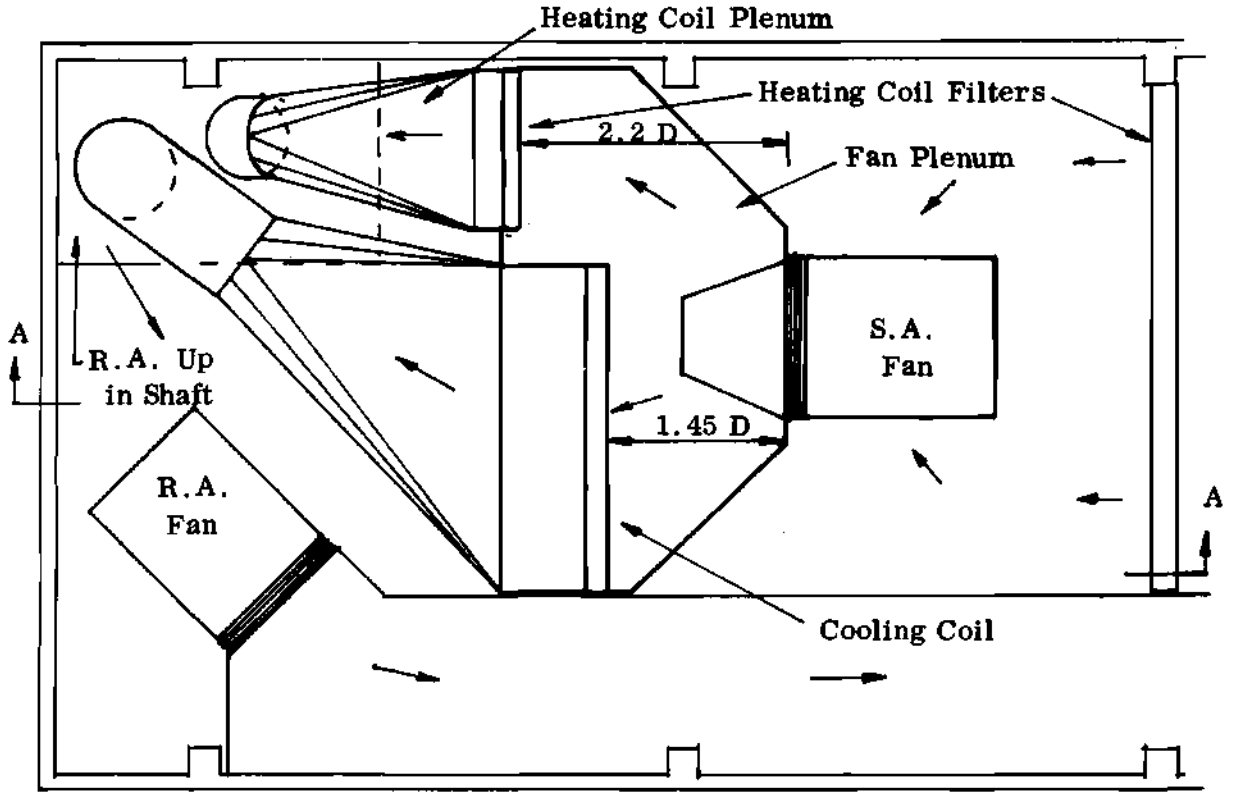

BUILDING A FAN ROOM FLOOR PLAN

Scale: 1/8" = 1'-0"

Note: Dampers not shown.

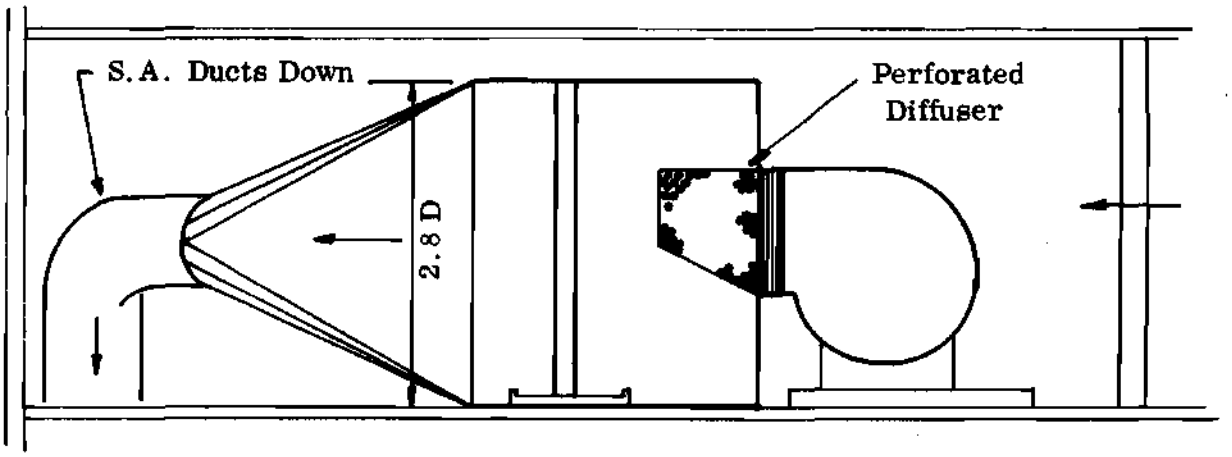

SECTION A.A

Figure 2. Building A Upper West Fan Room Arrangement.

in terms of wheel diameters vary, but the general sizes compare favorably. Therefore, data for the Building A fan room should be of interest to engineers who have used Shataloff's recommended arrangement as a guideline for designing dual duct fan rooms. The Building A fan design operating point is about 70 percent of the wide-open cfm, this appears to be about the selection point of most dual duct fan rooms considered in Appendix A. Refer to Appendix A for other actual systems where data were taken.

Description of Field Tests

The actual fan rooms tested were five of the 12 high velocity dual duct fan rooms that serve a group of three high rise office buildings (28). The Upper West Fan Room of Building A was thoroughly tested. The velocity measurements and airflow direction tests were made in five general areas, as follows: fan inlet, fan outlet, fan plenum, immediate vicinity of the coils, and downstream of the cooling coils. All of the fan rooms in the group of buildings used a perforated metal diffuser over the fan outlet. Refer to Appendix A for details of the fan rooms. The perforated diffuser was removed in Building A Upper West Fan Room to provide a comparison between airflow characteristics with and without a diffusing device.

While the majority of field testing involved one particular fan room, testing of four other fan rooms provided data for comparison purposes. The other upper Building A fan room is a mirror image to the west fan room, and provides a means of substantiating data taken in the west fan room. Two other fan rooms tested were in the twin building to Building A; Building B is a mirror image of Building A. The arrangement and size of these fan rooms are similar in all respects to Building A

except the fan is one size smaller, i.e. a six inch reduction in the fan wheel diameter. While Building A and B have fan rooms with non-symmetric coil arrangements, the fan room of Building C has symmetry, providing test data for a symmetric arrangement. Also the fan room in Building C was the largest in which tests were made.

The tests included obtaining both qualitative and quantitative measurements of the airflow characteristics. Due to the size of the fan rooms being studied (see Appendix A), observers were required to make tests from inside the fan plenum.

Field Testing Procedure

To study the movement of air within the fan room required using flow visualization techniques. In many instances a hand-held pocket hankerchief indicated air motion. Tufts of nylon cord attached to a metal rod were also used for determining air motion. The tufts or hankerchief indicated flow separation, secondary and reverse flow, high and low velocity regions, and stagnation regions within the fan plenum. In areas of low velocity, such as downstream of the cooling coil, smoke was used to observe the direction of flow. Smoke was generated by a M.S.A. Ventilation Smoke Tube.* Since the smoke dissipated rapidly in moderate velocity streams (500 fpm and up), bits of paper were released to trace the paths of streams of air.

---

*Tradename, Mine Safety Appliances Co.

Several techniques were used to make velocity measurements. A standard A.M.C.A. pitot tube (24) was used to measure velocity pressure for velocities above 500 fpm. An Anemotherm Air Meter,* a common hot wire meter used in air conditioning field testing, was used for velocities below 500 fpm. A vaned velometer was also used to measure velocity over the range of velocity found in the fan rooms. The general procedure was to read velocity at pre-selected points. The points where readings were taken usually formed a cross-sectional profile of the fan room. In order to minimize variations in location of points in the profile, a grid of numbered lines was drawn on the fan plenum walls and floor. When taking measurements observers remained clear of the main air streams, as much as possible. One observer held the test probe, usually a pitot tube, while a second observer would direct the first in positioning the probe. A third observer would read and record the data. A detailed discussion of measurements and instruments is contained in Appendix C.

Prototype Observations

Building A Upper West Fan Room. The majority of detailed observations were made in the Upper West Fan Room of the Building A. (A list of tests is included in Appendix F.) As mentioned previously, the areas under consideration were the fan outlet, the fan plenum, and the coil plenum. The fan outlet flow characteristics were measured and observed in tests P-1, P-2, P-4, P-6, and P-11. These tests, which included velocity measurements and flow visualization, consistently show poor velocity profiles. The velocity profiles with and without the perforated diffuser are

---

*Tradename, Dynamics Corp. of America.

shown in Figure 44. Based on visual observations, reversal of flow at the outlet occurred over more than 16 percent of the outlet area. The reversal occurred both with and without the diffuser over the fan outlet.

The airflow in the Upper West Fan Room was found to be turbulent and erratic. There existed secondary flows, whose boundaries with the mean flow were fairly stable. At the face of the cooling coil, the velocity of air wiping the coil in many locations was three or four times greater than the design coil face velocity. The magnitude of the wiping of the coil prevented the use of smoke to visualize airflow entrance into the coil. The removal of the diffuser had no significant effect on the coil wiping. However, the flow in the plenum was affected by the removal of the diffuser. Velocities in the direction of the heating coil ranged from 20 to 30 percent higher without the diffuser. No general trend in the data indicated any significant changes in velocity at the cooling coil. The flow pattern in the fan plenum is indicated in Fig. 45.

Due to the turbulence and wiping at the face of the coil, measurements of the coil velocity were made on the downstream side of the coil. Visual observations with the diffuser in place did not indicate any improvement in the velocity profile of air at the cooling coil. The profile of the downstream velocity of air at the coil without the diffuser is shown in Fig. 46. Note that the velocity at the section of the coil in front of the fan discharge is about 100 percent greater than the velocity at the outside edge of the coil section.

Other Built-Up Fan Room Observations

Observations were made in the Upper East Fan Room of the Building A to

verify the observations made in the West Fan Room. The velocity measurements were made inside the diffuser. The velocity profile of the fan outlet is shown in Fig. 47. Recall that the fan rooms are mirror,images when comparing Fig. 47 and 44, so the velocity profiles are reversed. The airflow in these two fan rooms appeared similar.

In order to further verify the airflow characteristics of the Building A fan room observations were made in the Building B, the twin building to the Building A. The results of velocity profiles at the fan outlet are given in Fig. 48. Visual observations indicated extensive wiping of the cooling coil, and the heating coil to a lesser extent. Generally the airflow in the various fan rooms was similar.

Thus far all the fan rooms considered have had non-symmetric arrangements of coils. Observations in a symmetric arrangement show a different pattern of airflow in the fan plenum. The profile downstream from the diffuser as well as the outlet velocity profile is given in Fig. 49. Comparing this profile with the profile for a non-symmetric fan room it is apparent that symmetry improves airflow in this incidence. The symmetric fan room did not exhibit wiping and smoke tests indicated good entrance into the coils.

Several limitations imposed by the actual systems required the construction of a model. With the actual system it was not possible to control the ratio of cooling to heating flow. The actual system had limitations such as, size and the inability to rearrange the fan or the coils. It became apparent that a study of built-up fan rooms required control over variables in fan operation such as, the flow rates through the coils. Also control over design of the fan room was required, although not possible with the actual system. All this pointed to the need for a model.

CHAPTER II

THE MODEL FAN ROOM

Certain economic and space limitations were imposed on the design and construction of the model. The fan, motor, and the coils for the model were donated by a manufacturer, therefore selection was limited to standard equipment. This restriction presented a problem in modeling the system. First of all, fan speeds available were too slow. The size and shape of coils was limited. Space limitations of the lab imposed less than ideal flow measuring techniques.

Modeling

To obtain complete simulitude between the model and prototype (Building A fan room) geometric, kinematic, and dynamic similarity are required (22). Geometric similarity requires all dimensions to be expressed in terms of a single dimension. It has been stated previously that the fan diameter was chosen as the characteristic dimension of the fan room. Figure 3 is a comparison of the geometric shape of the model and prototype. The model is drawn at a scale that makes it appear to be the same size as the prototype. The dimensions of the model are based on the wheel diameter of the model's fan. The only geometric difference was a slight variation in the overall height of the fans in relation to the coils.

Kinematic similarity requires the velocities at the same relative point in each system be related.

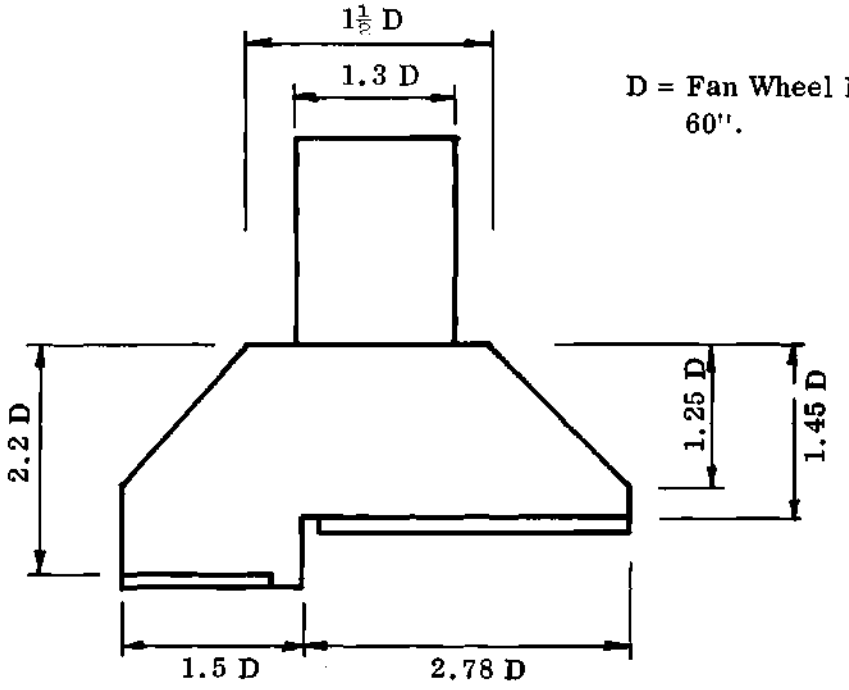

BUILDING A FAN ROOM*

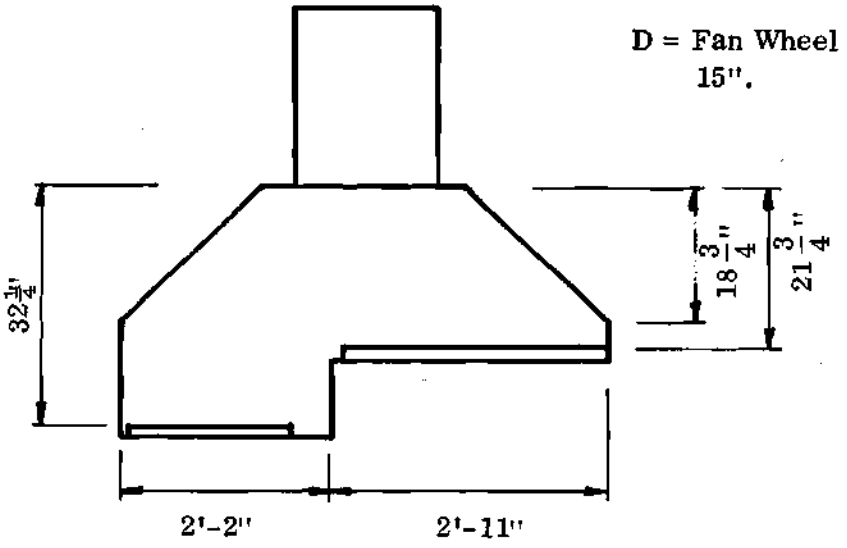

MODEL OF BUILDING A**

*Dimensioned in terms of the fan wheel diameter.

**Dimensions based on the size of the model's fan.

Figure 3. The Comparison of Geometric Shape of Model and Prototype.

$$\frac{u_p}{v_p} = \frac{u_m}{v_m} \tag{1}$$

Therefore velocity gradients and profiles in each system will appear similar. For example, the velocity profile at the coil face for the model should be similar to the profile of the Building A coil. In establishing operating conditions for the model, the ratio of fan outlet velocity to coil average face velocity for the prototype was used.

Dynamic similarity requires the systems to have similar relationships between force fields. For the fan room model and prototype to be dynamically similar, several relationships must hold. The first requirement is the following equation,

$$Re_p = Re_m \tag{2}$$

If the Reynolds numbers for the model and prototype were made equal, the model's fan would have been required to deliver twice the maximum catalog rating. The Reynolds number is a ratio of inertia to viscous forces, but other force fields are present. The Euler number is a dimensionless group, relating inertia to static pressure forces. In this study and in the work of Gilman (15) and Graham (16) airflow in plenums has been independent of static pressure. The third dynamic relationship is that of the inertia and wall shear forces. This would include the cooling and heating coil pressure loss. To increase the velocity to obtain correlation of Reynolds numbers for the model and prototype would have significantly increased the wall shear and form drag through the coil. For the model cooling

coil, a narrow fin spacing was used to simulate the wet fins of a wider fin spacing usually encountered in built-up systems. Although the fan was not operated at sufficient speed to produce equal Reynolds numbers, the flow through the coil was similar in the model and prototype. For the Building A model, the fan operated at 70 percent of wide-open cfm, which is about the same point on the fan curve as the prototype.

The Building A model was only one of many arrangements considered. The modeling techniques have been discussed in relation to the Building A model, since data were available from the prototype to compare with data from the model. The model of the Building A fan room was one of several models in this study. Results of comparisons of airflow in the Building A model with the prototype showed the airflow to be similar. Distribution of air to the cooling coil was found to be similar. With the Building A model as a basis, other models of different sizes could be evaluated.

Fan Room Variables

There are a number of variables associated with a dual duct built-up fan room, both as regards physical design and operation. Geometrically, the size and shape is influenced by the space available. Usually either the height or width is fixed by the space, establishing the other dimensions. The cooling coil size is established by a maximum desirable velocity across the face of the coil. The distance between the different components; fan, coils, filters, etc., is established by the available space. Therefore to obtain a greater distance between the fan and coils, a reduction must be made between the fan and filters or between the coils

and duct connections. Besides the shape of the coils varying, the number of rows of tubes and the fin spacing are also physical variables. For any one operating condition of the fan, the choice of the fan size results in establishing the outlet velocity and rotational speed. Once the physical characteristics of the fan room have been established, the operating characteristics become the important variables.

The variables associated with the fan, the total flow and pressure vary depending on the cooling flow ratio. This is due to the difference in resistance between the cooling and heating duct systems. Resistance of the coils varies as a function of velocity. The cooling coil resistance is also affected by the amount of moisture condensing on the fins.

From the viewpoint of heat transfer, the operation of the coils is influenced by several variables. Assuming the airflow rate and cross-sectional area are fixed, the heat transfer rate can be established. A combination of the entering and leaving water conditions, water flow rates, fin spacing, and the number of rows of tubes in the coil will establish the heat transfer rate. Similar variables affect the heating coil heat transfer rate for a hot water coil. For the steam heating coil, the heat transfer rate is dependent on the fin spacing, number of tubes, steam pressure, and flow rates. The leaving air conditions are dependent on the entering wet and dry bulb temperatures. The usual method of control will vary the leaving coil temperature depending on the outside air temperature.

Aside from the major variables just discussed, a number of less significant variables are present. These include variations in barometric pressure, outside air temperature, and the return air conditions. The effects of age on the system

results in scaling in the coil tubes and belt wear of the fan drive. Poor distribution of water to a bank of coils results from improper balancing of water flow through the coils.

Description of Model

The multiplicity of possible arrangements of built-up fan rooms necessitated construction of a model that could be rearranged with a minimum of work. The model was capable of changing the following aspects of a fan room: distance from fan to cooling and heating coils (independently), distance from coils to duct connection, coil face area, aspect ratio (ratio of height to width) of fan plenum, divergence of plenum walls, and angle between the plane of the fan and the plane of the coils. In terms of fan and coil air flow, the model should be capable of changing the total flow as well as the ratio of cooling to total flow, the cooling flow ratio. The airflow rate for any particular model was established on the basis of fan outlet velocity and coil face velocities.

The model consists of three boxes, the largest box is open at both ends and the smaller boxes are open at one end, the other containing a coil, see Figure 4. The smaller boxes containing the coils have a moveable wall in the open end containing a bellmouth duct fitting, and form the heating and cooling plenums. The largest box accommodates the coil plenums at one end in a manner that allows the coils to be moved independently. The fan is mounted through a moveable wall which fills the other open end of the large box or fan plenum. The duct system, consisting of a square edge orifice flow meters and dampers, provided a means of simulating a varying cooling flow ratio. The fan was belt driven, using a variable speed sheave

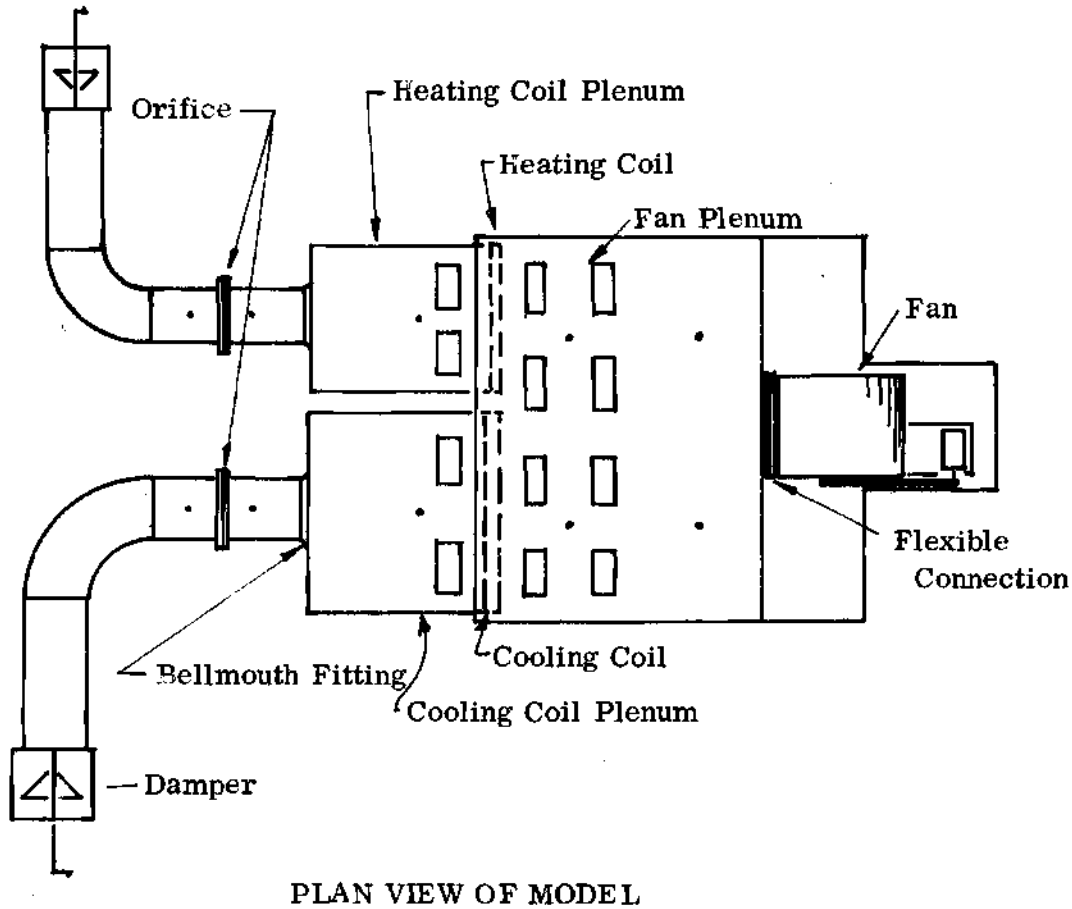

PLAN VIEW OF MODEL

Scale: $\frac{1}{4}$" = 1'-0"

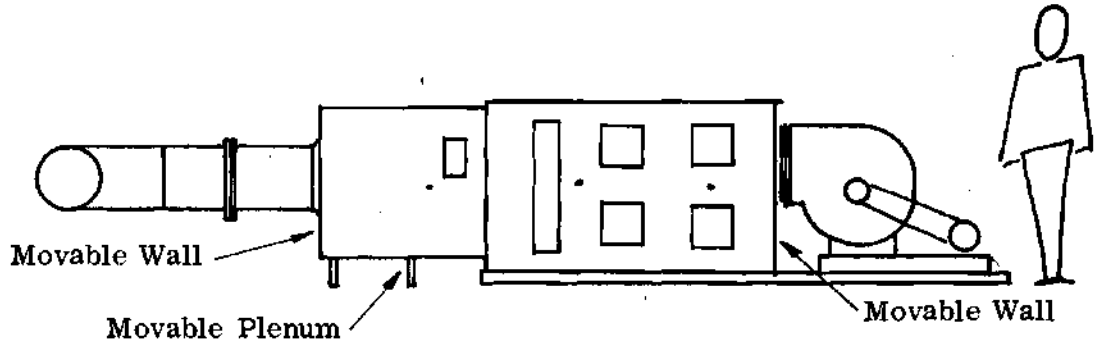

ELEVATION

Note: "•" Denotes fixed static pressure taps.

Figure 4. The General Model.

to change speeds.

The primary material used in the construction of the model was interior plywood. Plywood panels were installed inside the fan plenum to change the aspect ratio of the plenum. At the same time portions of the cooling and heating coils could be sealed off to change the coil face area. Plywood panels could also be installed inside the plenum at various angles from the fan to the coils. Roughness of the plywood walls was not felt to be a factor in contributing any additional friction at the plenum wall surface. The friction loss based on a velocity five times the average plenum velocity is 0.10 percent of the minimum head developed by the fan. Therefore skin friction in the plenum was neglected.

The model was operated without heating or cooling coils functioning. There are several reasons for not providing heating and cooling to the model coils. First of all, the number of variables affecting the system performance required reduction to allow the studying of a complicated system. Through the use of "dead" coils, approximately one-half of the variables, previously mentioned, are eliminated. As a result, the model construction was simplified, omitting the following: piping and control valves, waterproof plenum construction, maintaining operating temperatures, and a source of chilled water. By avoiding the problems of operating the cooling and heating coils, the simplier approach allowed concentration on the air side of the coils, therefore a better study of the airflow was possible.

The Factors Affecting Fan Plenum Performance

Three major factors affect the fan plenum performance; they are: space

requirements, plenum losses, and air distribution. The fan plenum must first meet the space limitations. The size of the fan room can be the single most important factor governing how well a particular fan plenum will perform. The fan plenum can be considered an extension of the fan to the coils, it can be thought of as part of the fan or part of the system. Thus, the performance of the fan and plenum combination could be presented in a manner similar to a head-flow curve used for the fan alone. This approach would include the plenum losses within the fan performance. On the other hand, the plenum losses could be considered as part of the system losses. The plenum losses reduce fan performance, regardless of how the plenum is to distribute air over the face of the coils. The distribution of air from the fan outlet affects the overall performance of the fan plenum.

Corrective Measures to Improve Air Distribution

Several corrective measures used in fan rooms can affect the overall performance. Most corrective measures are aimed at improving air distribution where space is limited, and at the same time holding losses to a minimum. Ideally, the use of an outlet diffuser on the fan offers the greatest potential of improving performance. The ideal diffuser would distribute the air and regain pressure normally lost in the abrupt expansion at the fan outlet. Gilman (15) investigated diffusers for distribution of air and reduction of losses in box plenums, similar to a fan plenum. Gilman's apparatus flow rate was approximately one fourth the model flow rate.

Fan Outlet Diffusers

The study by Gilman, which is considered in more detail in Appendix B,

concerned: (1) the turbulent mixing of air in a plenum, (2) effect of outlets on plenum performance, and (3) the effect of the physical dimensions on losses and air flow characteristics. Of the diffusers tested by Gilman, a vaned internal (inside the plenum) expansion diffuser proved to be superior to all others. The losses with the diffuser were 50 percent less than the abrupt expansion loss. Also the diffuser eliminated a rotational flow in the plenum. Gilman found no logical method of separating the entrance and turbulent losses for box plenums, but estimates of entrance loss account for less than 40 percent of the plenum loss. An evaluation of losses for the closed-coupled and remote positions of the fan did not show measurable changes in plenum losses, distribution of air, or rotational flow. Box plenum losses were found to be a function of entrance velocity head. Static pressure did not affect the plenum performance. A diffuser similar to the one used by Gilman was considered in this study.

Although a plenum with diverging walls is similar to one of Gilman's diffusers, it was considered separately. The practice of using a plenum with diverging walls by Shataloff (see Appendix A) is open to some question. The efficiency of pressure recovery of diverging expansions is no greater than the abrupt expansion recovery if the included angle between the walls is 60° or greater (20). For the arrangement in Figures 1 and 2, the included angle is 75° and 85°, respectively. Theoretically, the use of a plenum with diverging walls in dual duct systems of the size and arrangement considered in this study would not reduce expansion loss. Using a diverging wall does reduce plenum wall material in some cases, as well as improve the appearance of the fan plenum, in the eyes of a reviewing authority. To evaluate the reduction in

turbulence that could be attributed to the use of diverging plenum walls would be extremely difficult.

Perforated Plates

The most widely recommended corrective device for air distribution in applications similar to the fan plenum has been a perforated plate (1, 2, 16, 17, 18). Recently Graham (16) considered the use of a perforated plate to distribute air over a bank of filters immediately downstream of a fan. To obtain optimum performance of high efficiency filters a relatively uniform velocity profile is required at the face of the filters. Graham observed the velocity profile at the fan outlet to be very non-uniform, a fact that this paper will substantiate. Graham evaluated the performance of the perforated diffuser plate in terms of effectiveness in breaking up the high velocity profile of the fan. Due to the high velocity blast area (the area directly ahead of the fan outlet), the plate was doubled in front of the fan outlet to allow a variation in free area by moving one plate. Horizontal vanes in the fan outlet were used to deflect airflow vertically to improve distribution by the perforated plate. The vanes would be required in an arrangement such as a top horizontal discharge where the top of the fan was not near the top of the plenum. This is a result of the air tending to follow the direction of rotation of the fan, thus not diffusing upward. Graham recommends a minimum fan to plate distance of approximately 0.8 D to 0.5 D depending on the size of the fan and the outlet velocity. For a detailed review of the use of perforated plates by Graham, refer to Appendix B. Graham's apparatus flow rate was three to five times greater than the model flow rate.

Additional Correction Methods

Generally, space limitations require the heating and cooling coils to be offset to allow for piping, (Fig. 1 and 2). Depending on the method of piping several feet in width can be saved by offsetting the coils. Shataloff (1) recommends that the heating coil be the farther distance from the fan so as to minimize the chance of the air wiping the heating coil and then going through the cooling coil. For operation of the system using outside air for cooling and the heating coil, wiping of the heating coil can result in air temperature rises of 25 to 40 percent of full capacity (12). Another approach to eliminate extensive wiping of the coils would be the installation of an anti-wipe baffle. The anti-wipe baffle is essentially a partition between the heating and cooling coils. Presently there is no information as to the effectiveness of either coil offsetting or anti-wipe baffles in reducing air wiping of the coils.

Correction Devices Applied to the Model

As mentioned previously, the model was designed with the capability of testing various airflow correction devices. To test the diverging walls, plywood walls were installed inside the model. A small opening in the diverging wall allowed the model walls to hold the pressure, requiring the diverging wall to direct airflow only. The anti-wipe baffle consisted of a piece of plywood placed between the coils, extending into the fan plenum.

Since the study of box plenums by Gilman (15) determined that a vaned internal expansion diffuser performed best, a similar diffuser was installed and tested in the fan plenum. The box plenum required only horizontal expansion while the

fan plenum requires both horizontal and vertical expansion. Therefore a modified version of Gilman's diffuser was designed and constructed (Fig. 5). Since a detailed analysis of vaned diffusers is beyond the scope of the study, no analytical analysis of performance was made.

Choice of perforated plates was restricted to patterns normally carried in stock by metal perforating companies. By using stock patterns the cost is less, and generally the same stock patterns are carried by most suppliers, allowing competitive bidding. The patterns used in this study are listed in Table 1. The perforated plates were mounted on a frame, which could be moved to vary the position of the plate between the fan and the coils.

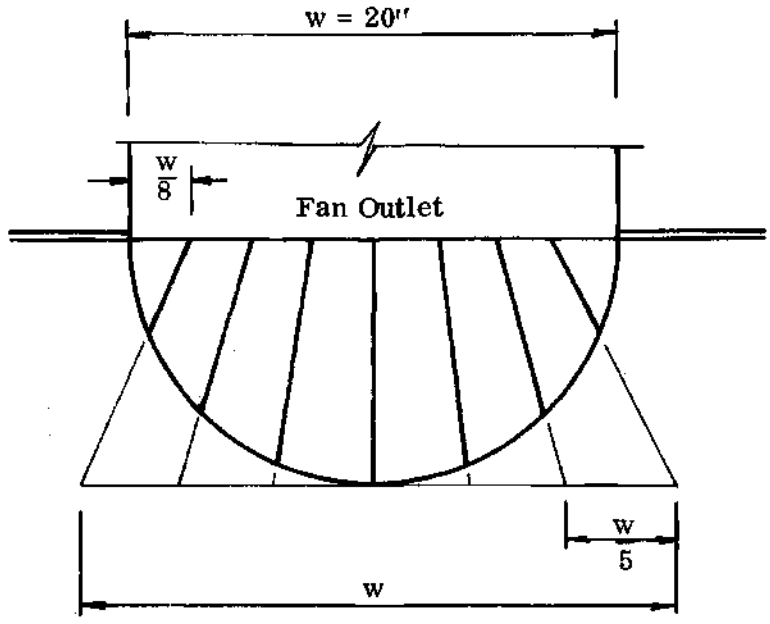

PLAN VIEW

Scale: $1\frac{1}{2}$" = 1'-0"

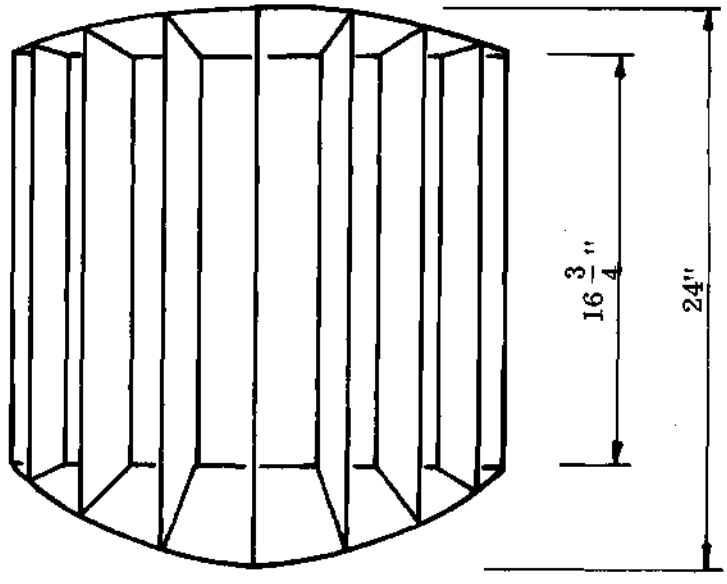

FRONT ELEVATION

Figure 5. The Modified Version of Gilman's Internal Vaned Diffuser.

Table 1. Perforated Plate Patterns

Plate No.	Perforation Description	Percent Free Area	Gauge
1	½" diameter, 11/16" centers	47	22
2	¼" diameter, 5/16" centers	58	22
3	¼" x 1½" slot, 3/8" centers	67	18
4	29/64" square, ½" centers	80	22

CHAPTER III

MODEL TESTS AND PROCEDURE

Model Tests

The model was used to evaluate different arrangements of the components of the fan plenum, including any correction device that might be used. The position of the fan and coils was measured in terms of fan diameter. For a particular series of tests, the fan and coil position were held constant. The total flow and the cooling flow ratio were varied by adjusting cooling and heating dampers. When a greater variation was required, the fan speed was changed. Table 3 lists the tests using the model (Appendix G).

Procedure

Flow Visualization

Measurement techniques follow along the same line as those used in the actual system, except the model allowed use of more refined methods. A good example is the improvement in flow visualization possible with the model. Usually the flow visualization technique was a fixed grid of yarn tufts. Four tuft grids were used, two were fixed below the cooling coil (six inch square grid) and heating coil (five inch square grid). The coil plenum yarn tuft grids provided an excellent view of the coil velocity profiles. The fan plenum grid (five inch square grid) was attached to a rigid frame that could be moved between the fan and coils. A grid

of tufts (three inch square grid) on the fan outlet was also used. For spot checks of flow direction, single and multiple yarn tufts attached to a metal rod were used. As in the actual system, smoke tests were limited to points of low velocity, such as downstream of the coils. The smoke dissipated too rapidly to be used effectively in the fan plenum. The laboratory ventilation was such that the use of large quantities of smoke to overcome the dissipation problems was not feasible.

Flow Rate Measurement

Another improvement in taking measurements, which the model provided, was controllable flow rates in the heating and cooling plenums. Since the damper positions were fixed for a particular test, the cooling flow ratio was held constant. This was not possible in an actual system since the individual mixing boxes control the ratio of cooling flow to the total flow, which is supplied to the conditioned space.

The flow rates were measured with an orifice meter. Due to the relatively wide range of cooling and heating flow rates, each duct system required the use of two sizes of orifices. The orifices were calibrated by measuring flow rates using A.M.C.A. standards (24) for pitot tube velocity determinations. Details of the calibration are a part of Appendix C.

Velocity Profiles

Velocity profiles were measured either by pitot tube traverses or hot wire probe traverses. Both the pitot tube and the hot wire probe are sensitive to direction, requiring that yarn tufts determine direction of flow. Due to airflow other than parallel to the static pressure sensing holes, the pitot tube did not work successfully in the fan plenum. For this reason, the velocity profile was taken at the exit of the

coil. The hot wire probe is not as sensitive to static pressure variations and provided velocity measurements in the fan plenum. Velocity profile techniques are based on recommendation of ASHRAE (25). Total and velocity pressure profiles were made at the fan outlet and the immediate vicinity with a pitot tube or kiel tube. Appendix C contains information about velocity measurements.

Pressure Measurements

The measurement of static pressure was accomplished by using two type of pressure sensing elements. The pressure sensing taps for the orifice flow meter were manufactured static pressure probes, similar to a small pitot tube without a total pressure opening. All other static pressure taps are round tubing flush with the inside surface of the plenum. This type of pressure tap would be less likely affected by secondary flows and turbulence in the plenum. Static pressure readings were taken at the fan outlet using a pitot tube. The fan plenum pressure was measured on either of two sets of wall pressure taps. Each set consists of eight taps connected in parallel. Coil plenum pressures were measured on a set of four wall taps connected in parallel. Pressure drop across perforated plates was measured from secondary taps located on either side of the plate in the fan plenum.

Pressures on the model were measured with Magnehelic* gages. The eleven gages used had pressure ranges from 0-0.25 to 0-10.0 inches of water. For orifice pressure drop measurement, two gages of different pressure ranges

*Tradename -- Dwyer Co.

were used in parallel to obtain better accuracy at lower pressures. This method was also used for measuring velocity pressure. Since the Magnehelic gages do not produce accurate measurements in the range of velocity pressure encountered downstream of the coil, a micromanometer was used for low velocity pressure measurements. Since the micromanometer contained a nulling device, stable measurements were possible in turbulent air streams. The micromanometer was also used to measure pressure drop across the perforated plate. A more detailed discussion of measurement techniques is in Appendix C.

CHAPTER IV

ANALYSIS OF SYSTEM LOSSES AND FLOW CHARACTERISTICS

System Losses

The losses in the dual duct fan room can be grouped as follows: fan plenum loss, coil friction loss, coil plenum loss, and duct loss. Fan plenum losses are the most important group in this study. Fan plenum losses were placed ahead of the others because the fan outlet, diffusers, and perforated plates all affect the fan plenum loss. Next in order of importance to this study is the coil pressure loss, which was also affected by what happens in the fan plenum. The coil plenum and duct losses were secondary to the other losses, and only considered to determine the overall system losses for the model.

The fan plenum loss is the sum of several losses of different forms occurring in the fan plenum. The fan plenum losses include: (1) the abrupt expansion loss as air leaves from the fan into the plenum, (2) the turbulent mixing loss within the plenum, (3) the resistance of the flow correction device, if used, and (4) the friction loss along the plenum wall. In order to estimate the fan plenum loss, the airflow was assumed to be uniform. This assumption was required because all present methods of loss calculations are based on a uniform velocity profile. An analysis of the turbulent mixing loss is beyond the scope of this paper, but estimates were made.

Abrupt Expansion and Mixing Losses

The abrupt expansion of air as it leaves from the fan was of primary importance in considering losses in the fan plenum. Due to the non-uniformity of the velocity at the fan outlet, only estimates were possible. For the general model the loss due to expansion was estimated to be 0.85 to 0.9 velocity heads. Some recommendations (12) appear to attribute too much loss to the abrupt expansion, when in reality the losses might be due to turbulent mixing in the plenum. A detailed analysis of expansion loss is contained in Appendix D.

The turbulent mixing in the plenum might be the major loss in the fan plenum. The turbulent mixing is characterized by three-dimensional vortex action in the region close to the fan outlet. Farther downstream, two-dimensional separation occurs and remains until the flow reattaches to the plenum wall. Actually reattachment does not occur, because the coil is placed closer to the fan than the reattachment point. The flow interacts with the coil, wiping the face of the coil. Along the plenum walls, a secondary flow moves opposite the mainstream flow. Other secondary flow, such as crossflow, exist in the plenum.

In Gilman's study of box plenums (15), turbulent mixing was neglected, but this proved to be a poor assumption. Based on the losses measured for a box plenum, some recommendations for fan expansion loss (12) appear to be in actuality the loss for the fan and plenum. Friction loss at the plenum wall is small; however the turbulence might tend to increase the friction. There is no way of knowing what portion of the turbulent loss is due to increased friction at the wall. Also the turbulence and wiping of the air at the coil face produces less than

desirable airflow entrance into the coil. The portion of the turbulent loss which arises from increased coil friction, is not separable from the total turbulent loss.

The General Model Overall System Resistance

The airflow resistance of the general model system is the sum of the losses for the system components, such as, the abrupt expansion, coil pressure loss, and duct pressure loss. The overall system resistance is easily estimated once the fan plenum loss has been established. Data is available for the coil friction from the coil manufacturer. Design information is also available for duct and duct fitting losses. A complete analysis of the system resistance is contained in Appendix D. Figure 34 is a calculated system resistance curve for the model. In addition to the resistance normally encountered in dual duct systems, the model also had losses as a result of flow measuring orifices and dampers. Standard methods of estimating the pressure loss of a square edge orifice were used (25). The pressure drop due to the abrupt expansion at the conical dampers was estimated for the open damper position (25, 21). The losses for the open damper and orifice are included in Figure 34.

Losses of Correction Devices

Once the system losses are established, it becomes important to know the effect an airflow correction device would have on the system losses. The use of a diverging transition from the fan to the coils could provide static regain and eliminate some of the turbulent mixing loss in the plenum. The diverging transition or diverging plenum wall, when designed properly, reduces the fan outlet velocity resulting in static pressure regain. The efficiency of static regain is

dependent on the included angle between the diverging sides of the transition. The diverging transition is not effective for included angles greater than 40^{o}, since the static regain for large angles is no better than an abrupt expansion (20). The study by Gilman (15) indicates that turbulent mixing losses are reduced by using a diverging transition of 58^{o} included angle, which is not in agreement with Ref. 20. A further discussion of diverging transitions is included in Appendix D.

The use of vaned internal diffusers (see Fig. 5) has been analyzed in terms of distribution of air without regard to losses. Gilman was successful in reducing losses by half, using the diffuser described earlier in this study (15). A discussion of Gilman's work with diffusers is found in Appendix B.

Since perforated diffusing plates have been recommended for distributing air over coils, etc., this study has considered the perforated plate as the prime corrective device. The perforated plate, while improving airflow distribution of a non-uniform velocity profile, introduces resistance to the flow. The resistance caused by the plates distributing the airflow is often the limiting factor in perforated plate applications. Therefore it became necessary to have a method of calculating the pressure drop across a perforated plate. The following equation agrees quite well with experimental data,

$$\frac{\Delta P}{\rho V_o^2/2} = \frac{1}{C_c(A_o/A_t)} - 1 \qquad (3)$$

A derivation and discussion of the use of Eqn. (3) is found in Appendix D. For use where upstream flow is non-uniform, an effective velocity is used in place of the

mean velocity V_o. Figure 38 is a plot of the ratio of the effective velocity to the mean velocity versus a dimensionless distance from the expansion or fan outlet (19).

Airflow

Poor heat and mass transfer performance can result from a poor velocity profile at the cooling and heating coils. The prediction of velocity profiles within the fan plenum is beyond the scope of this study, but general statements can be made concerning the distribution of air in the fan plenum. The velocity profile measured at the outlet of a large centrifugal fan is irregular (16). Although many manufacturers would like to claim a uniform profile, this is not found in field testing. In order to make any sort of analysis regarding airflow in the fan plenum, a uniform velocity profile at the fan outlet has been assumed. By assuming a uniform velocity profile, the results of Lipstein's study of expansion with obstructions in the area of expansion can be applied (19).

For the case of interrupting an expansion of flow, such as a coil downstream of an abrupt expansion, it has been shown that the flow resembles unobstructed expansion flow (19). Three flow regions have been identified for a two dimensional expansion (26). In the immediate vicinity of the expansion interface, there exists a region of strong three-dimensional vortex action. Next follows a region of two-dimensional separation, that is, flow along the floor and walls moves opposite the flow of the expanding air stream. The third region of flow is the point of reattachment at the wall. Refer to Appendix E for more detailed consideration of flow regions.

An important question is that of what type airflow is acceptable for good

performance of a fan and coil arrangement. One manufacturer (12) has published an empirical relationship for acceptable velocity at the coil face that states,

$$VP_e \leq 0.4\ (\Delta P_c + VP_c) \tag{4}$$

for cooling coils of $\Delta P_c/VP_c \geq 27.0$ and

$$VP_e \leq 0.25\ (\Delta P_c + VP_c) \tag{5}$$

for heating coils with $\Delta P_c/VP_c \geq 5$. The data used was a result of studies conducted with packaged air handlers. The data was in terms of distance from fan to coils and fan diameter. An analysis of the flow distribution using this method is included in Appendix E. With this method, a perforated plate of 50 percent free area is used if the conditions of Eqn. (4) and (5) cannot be satisfied.

There has been success in predicting correction of airflow velocity profiles using perforated plates (18, 19). Mean flow conditions are considered by the velocity modification equations, not the random irregular motion of air. Aside from the irregular motion or turbulence upstream of the perforated plate, turbulence is actually generated downstream. A number of individual jets which spread and finally coalesce is representative of flow through a perforated plate. The energy of turbulence is converted from the energy of the mean flow. As the turbulence in the form of eddies decays, the energy of turbulence changes to heat. The theoretical temperature rise was estimated to be on the order of $0.001^{\circ}F$. Several equations predict the velocity modification, and are given in Appendix E. These equations fit the experimental data for high percentages of free areas. For

low percentage of free area (25 percent) irregularities in screens and perforated plates have produced local zones of high and low velocity at quite unpredictable locations (18). Test results have shown that perforated plates distribute the air from a fan to high efficiency filters with acceptable performance (16).

Heat Transfer

The ratings for coils are based on uniform face velocities (21). The performance is affected by non-uniform airflow at the face of the coil. The cause of poor coil performance could be the entrance of air at odd angles and wiping of the coil face. Fouling of coils by dirt also reduces performance, but this is a maintenance, not a design problem. Poor entrance conditions can cause reverse airflow through the coils which would reduce performance (21).

A poor velocity profile affects the outlet temperature profile of steam coils. Based on the manufacturer's data for the steam coil used in the model, Figure 6 shows how the outlet temperature varies with the average coil face velocity. In this example, the temperature variation is 26^{o} F. Other choices of coils and entering conditions can result in greater exit temperature variations. The poor temperature distribution is more significant if the result is stratification of air in the heating duct. As an example, consider the arrangements of coils and ducts shown in Figure 7. Secondary flow in the duct fittings would mix the air to some extent. These arrangements could result in substantial temperature differences at branch ducts, a problem with which the author is familiar. Another problem resulting from poor airflow distribution is the possibility of freezing the coil.

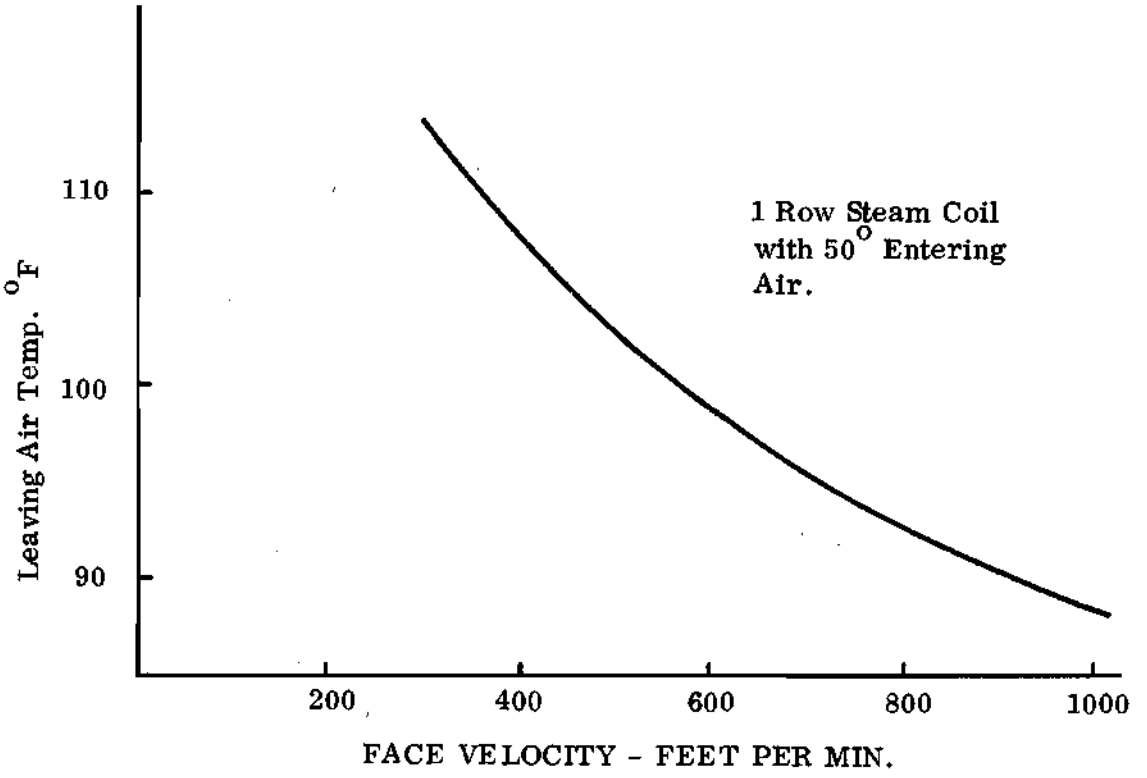

Figure 6. Effect of Velocity on Leaving Air Temperature of a Heating Coil.

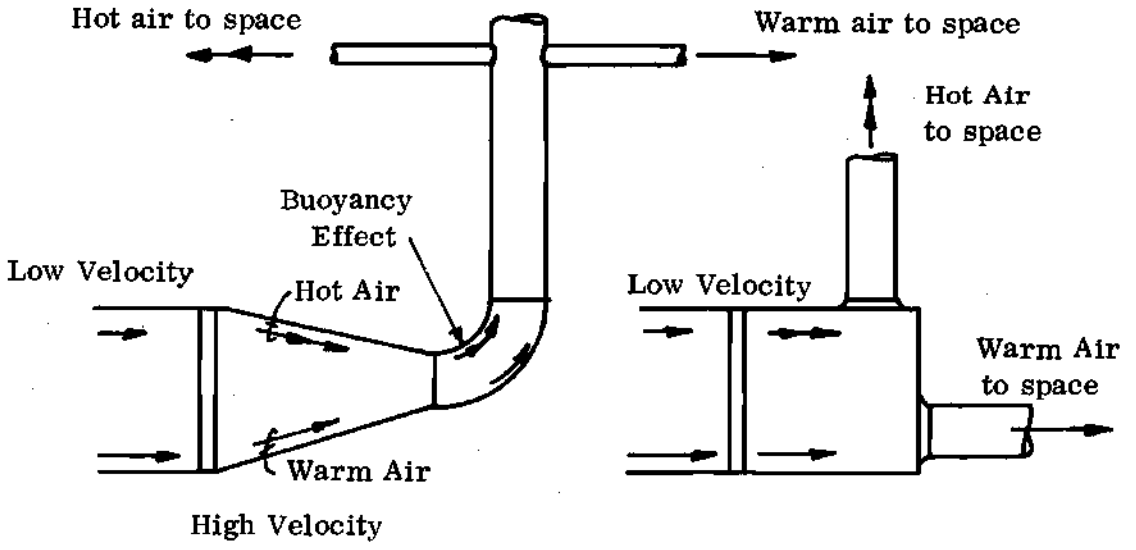

Figure 7. Effect of Stratification of Air in the Heating Supply Ducts.

Although coil freezing is not generally a problem of dual duct systems, it should still be considered when designing the fan room.

The cooling coil also requires good airflow distribution to perform as rated. The face velocity determines the friction as well as heat transfer for a cooling coil. For a cooling and dehumidifying coil moisture carryover, the blowing of condensed water from the fins of the coil, can be a major problem. Due to carryover, face velocities should be limited to 700 fpm (21). The ratio of sensible to latent cooling is affected by the face velocity. This characteristic of a cooling and dehumidifying coil could tend to decrease moisture carryover since for high velocity the sensible heat ratio is higher (see Figure 10). The differences in sensible and latent cooling are not large, but the portion of the coil with high velocity is also the portion with lower moisture removal. Therefore the coil characteristics would tend to reduce the moisture carryover.

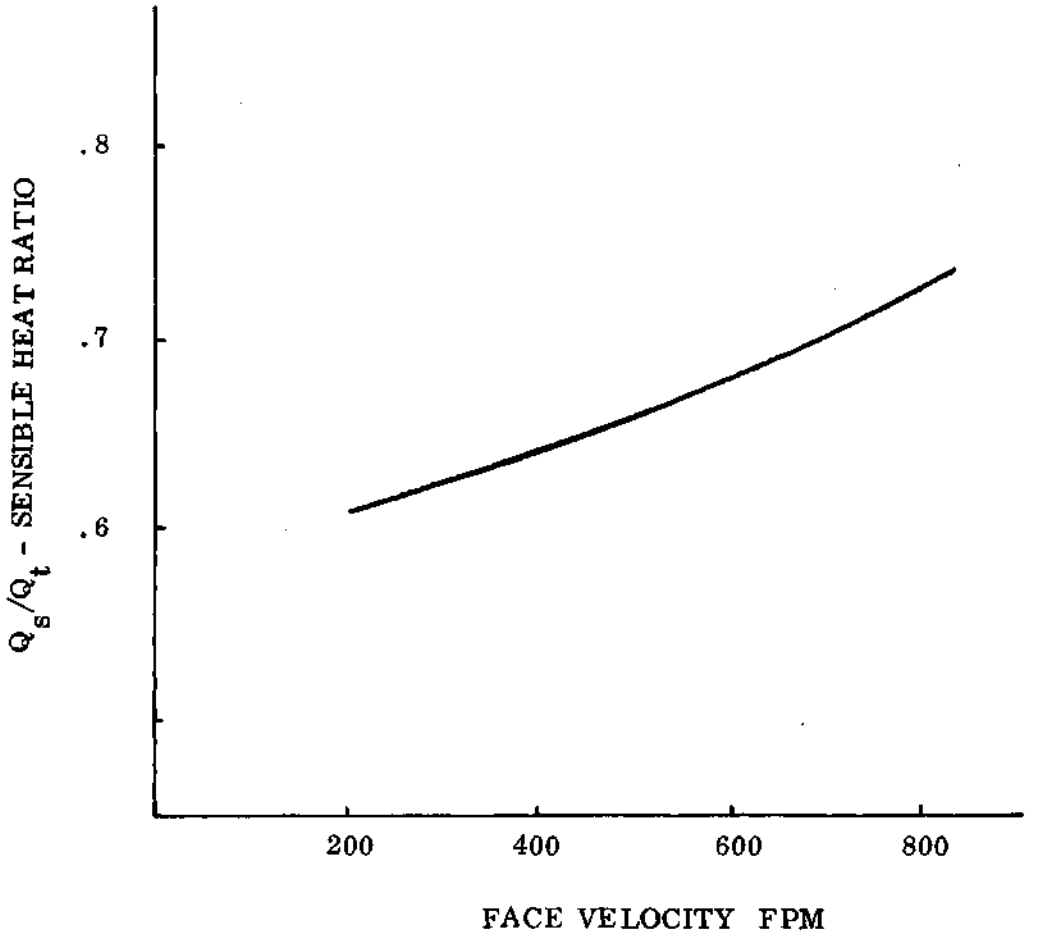

Figure 8. The Effect of the Face Velocity on the Coil Sensible Heat Ratio.

CHAPTER V

RESULTS AND OBSERVATIONS

Building A Model

As pointed out in Chapter II, dynamic similarity was not possible between the Building A prototype and model. For a fan room a Reynolds number could be based on the fan outlet velocity. One characteristic dimension for a fan outlet Reynolds number is the fan diameter, since the dimensions of the outlet are functions of the diameter. Using this approach, the Reynolds number for the model requires the fan to operate at three times the rated speed. The relatively low Reynolds number of the fan affected the quantitative measurements. Geometrically and kinematically the model was good. Tests show qualitative agreement between the model and prototype airflow characteristics.

Fan Outlet

The model did not exhibit reverse flow at the outlet as did the Building A prototype. The outlet velocity profile was non-uniform and did not have points of zero velocity pressure. No significant change in this profile was observed as the cooling flow ratio was changed. A typical profile is given in Fig. 9. The point of zero velocity recurred with different cooling flow ratios.

Fan Plenum Airflow

The airflow in the fan plenum of the model was very similar to the flow in the Building A prototype. The regions of expansion flow as discussed in Chapter IV, were apparent, except for the point of reattachment. Fig. 10 shows the airflow

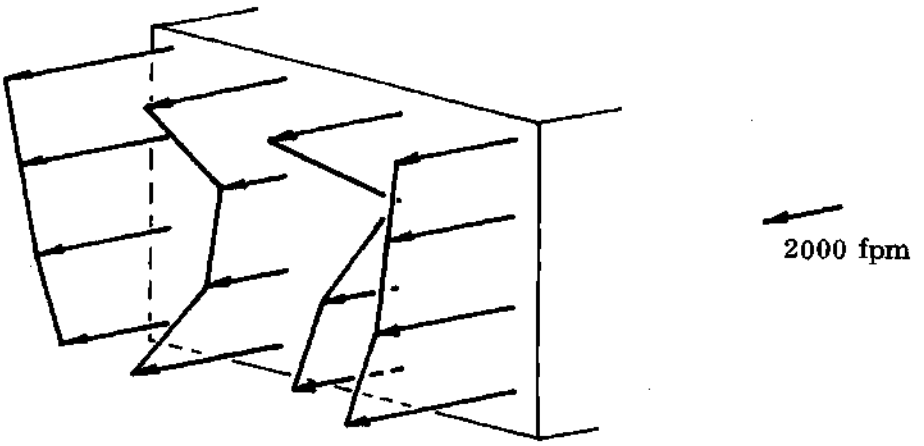

Figure 9. Building A Model Fan Room, Fan Outlet Velocity Profile.

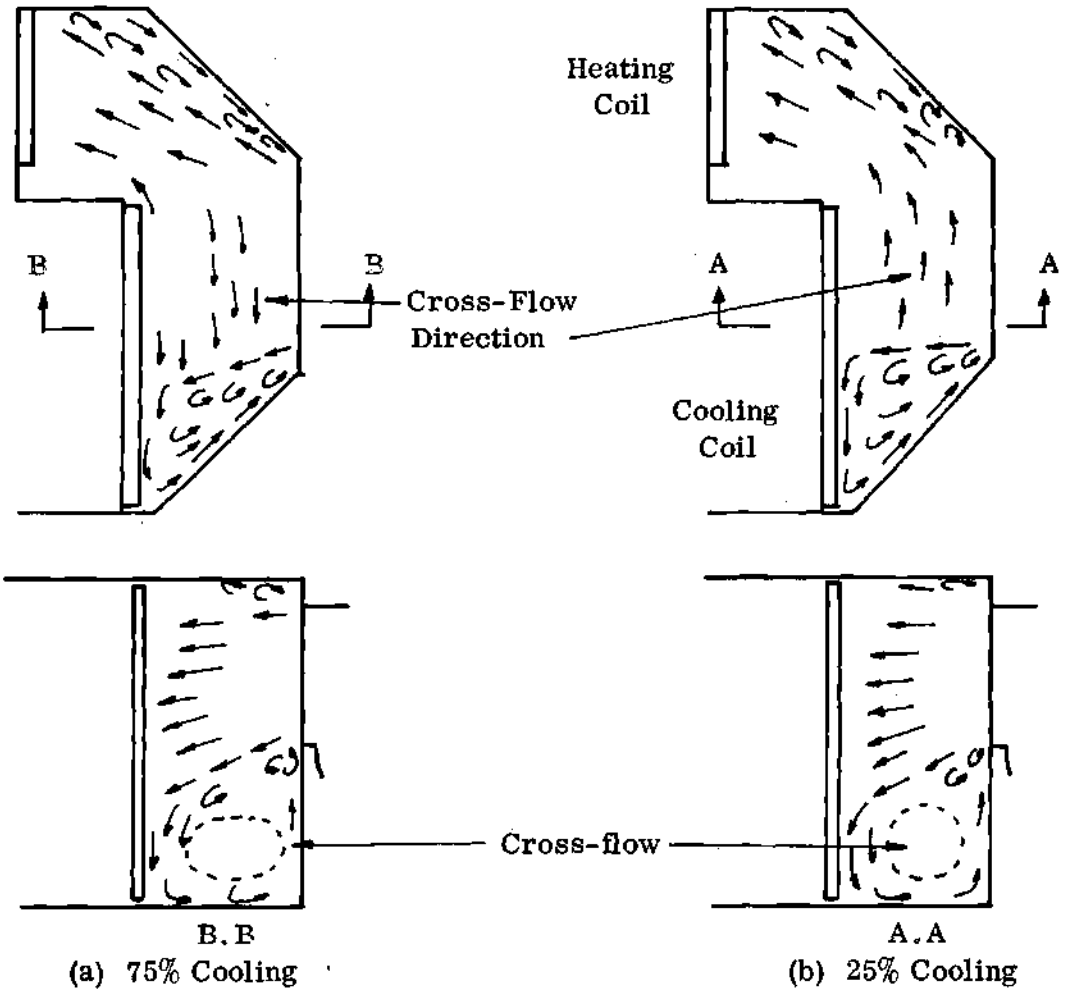

Figure 10. Building A Fan Room Model, Fan Plenum Airflow Patterns.

pattern for the Building A model, refer to Fig. 45 for comparison with the prototype. The airflow pattern for the model shows a region of crossflow, which was not recorded for the prototype, although there were several crossflows observed in the prototype. The crossflow is not stable; its direction of movement is determined by the cooling flow ratio. For 60 percent or higher cooling flow ratio, the crossflow moves toward the cooling coil. At 55 percent cooling flow ratio, there was no crossflow observed. As the flow was increased through the heating coil the crossflow reappeared, moving in the direction of the heating coil.

The crossflow results from air wiping either the cooling or heating coil. After wiping a coil the air moves back across the plenum to the other coil. The coil with the lower flow rate was more heavily wiped. Offsetting the coils did not appreciably affect the wiping of the individual coils. The anti-wipe baffle, a partial partition placed between the coils to eliminate wiping, reduced wiping, but did not eliminate it.

Coil and Coil Plenum Airflow

The velocity profiles for the cooling and heating coil airflow were determined by measuring the velocity leaving the coils. Due to turbulence and secondary flows, a velocity measurement upstream of the coils would be meaningless. The profile of the velocity for the Building A model was similar to the profile for the prototype. The variation of the velocity from the section directly ahead of the fan outlet to the outer edge is less for the model. This is illustrated in Fig. 11. The profile of the velocity for the prototype is included for comparison purposes. It can be seen that the model velocity profile is similar in most respects.

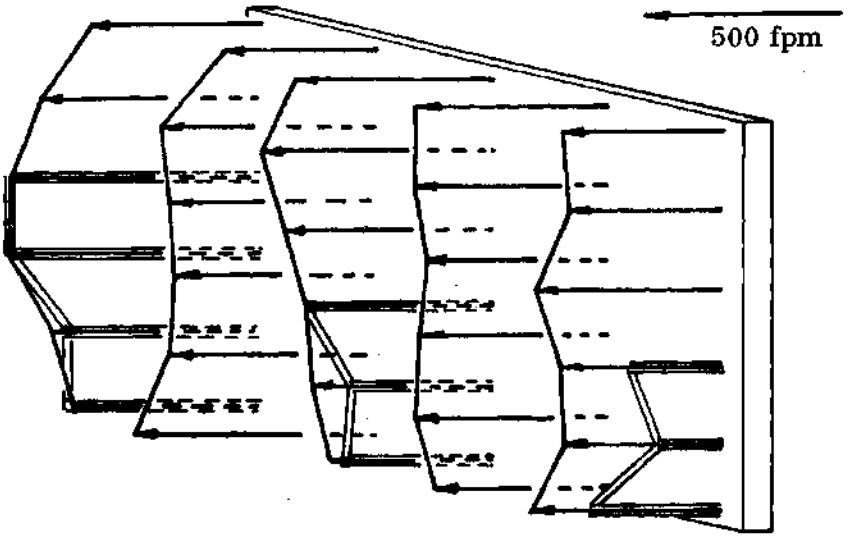

Prototype
Model

0.55 Cooling Flow Ratio

Figure 11. Building A Fan Room Model, Downstream Cooling Coil Velocity Profile.

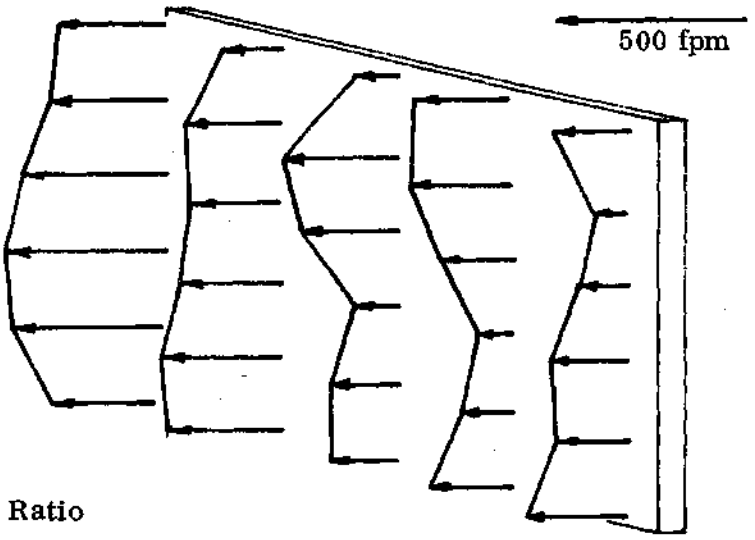

0.25 Cooling Flow Ratio

Figure 12. Building A Fan Room Model, Downstream Cooling Coil Velocity Profile.

For the velocity profile shown in Fig. 11, the cooling flow ratio was approximately the same as in the Building A prototype. This profile is actually better than the Building A velocity profile. For a different cooling flow ratio, say 0.25, the profile is significantly poorer, as Fig. 12 illustrates.

The velocity profiles, which have been considered thus far, were made without any sort of diffusing device in the plenum. Results show a very significant improvement when a perforated plate was placed between the coils and the fan outlet. The improvement in distribution of the air to the cooling coil was better for lower flow rates, see Figs. 13 and 50. For the arrangement using the perforated plate, the wiping at the face of the heating coil was substantially reduced. The direction of approach to the cooling coil was stable and more nearly perpendicular entry of air was observed. For low flow rates through the cooling coil, substantial wiping was evident as shown in Figure 13b. Also the cross-flow became erratic for low flow through the cooling coil. Subsequent tests were made without the diverging walls and without the perforated plate. Results show no measurable difference when the perforated plate is used and the diverging walls removed. This result was not unexpected since the diverging angle of the walls is quite high, about 90°. When neither a perforated plate nor diverging walls were used, the turbulence was highest. The flow just downstream of the fan was not affected for all arrangements. Also the point of reversal of flow was not affected appreciably by any changes in the arrangement.

The results presented thus far have ignored airflow downstream of the heating coil, since field data were not available for comparison purposes. Lack

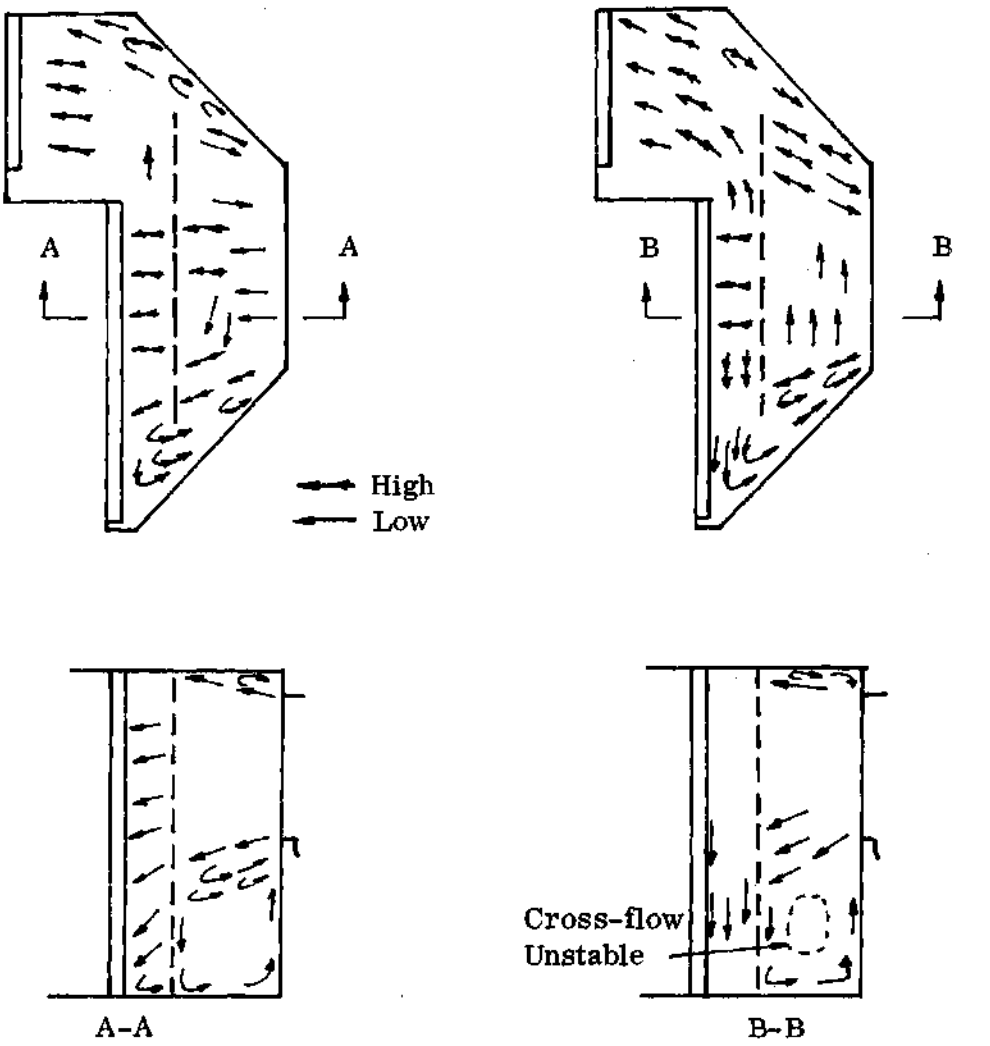

(a) 0.75 Cooling Flow Ratio

(b) 0.25 Cooling Flow Ratio

Figure 13. Building A Fan Room Model, Fan Plenum Airflow Patterns with a Perforated Plate.

of emphasis on the heating coil airflow should not be construed to mean that the flow is satisfactory. In fact, quite the contrary is the case, as illustrated in Fig. 50. This figure shows the velocity profile downstream of the heating coil for 25 percent and 75 percent of the total air through the coil. For these particular tests the velocity varies as much as 50 percent from the average velocity.

The results of the various tests using the model of the Building A fan room are similar in most respects to the measurements in the actual system. Since the airflow for the geometric and kinematic model was similar to the prototype, other models of the size of the Building A model provided information about airflow in a large fan room. All subsequent testing used the general model arrangement (Fig. 4).

The General Model

Fan Outlet

The fan outlet velocity was observed to be erratic. The variation from the average outlet velocity, as published by the fan manufacturer, was 100 percent below the average and 85 percent above the average. The fan outlet velocity profile is shown in Figure 14. The results of the velocity measurement indicate unexplained points of zero velocity. The fan outlet velocity profile was similar for all arrangements, that is, high velocity at the top and outer edges of the outlet with low velocity at the interior and bottom of the outlet.

Fan Plenum Airflow

Airflow within the fan plenum was difficult to observe and measure. For this reason the observations were limited to those which provide a general

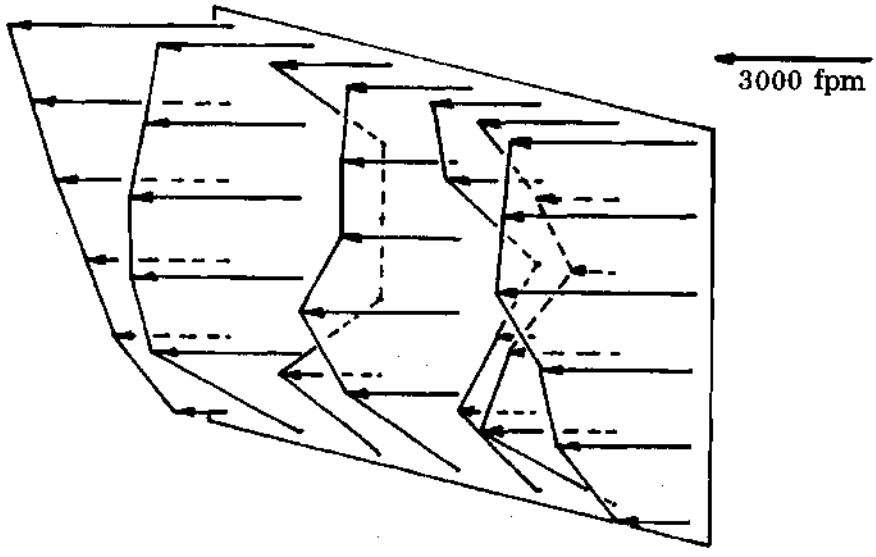

Figure 14. General Model, Fan Outlet Velocity Profile.

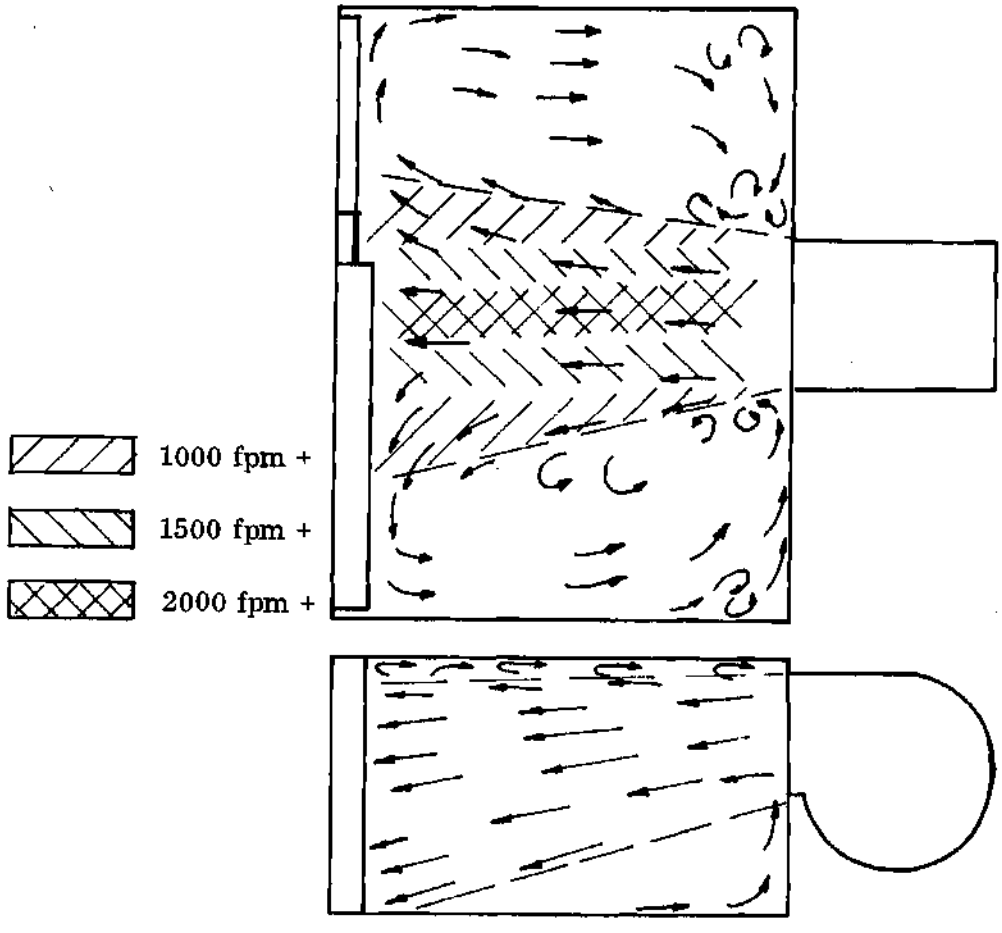

Figure 15. General Model, Fan Plenum Airflow Patterns.

understanding of the airflow patterns between the fan and the coils. Turbulence and secondary flows existed in the fan plenum. There was extensive wiping of both the heating and cooling coil. The airflow pattern for a 50 percent cooling flow ratio is shown in Figure 15. The region of highest velocity is in the blast area. As the flow was changed to either high heating or cooling flow rates, the flow pattern shifted slightly in the direction of the increased flow. For high cooling flow ratios the wiping of the heating coil was more predominant. For the opposite situation, the wiping of the cooling coil was less predominant.

The use of distributing devices generally improved airflow in the fan plenum. The visualization of airflow patterns downstream of a perforated plate was hampered by the physical arrangement of the windows and the perforated plate position. Therefore a detailed study of the movement of air in the fan plenum with a perforated plate was omitted. Observations indicated a significant reduction in the turbulence and wiping on both the heating and cooling coil for a perforated plate placed across the fan plenum. The vaned diffuser did afford the opportunity for detail flow observation which is shown in Fig. 16. The diffuser increased the included angle of expansion about twice that of the angle when no correction was used. Results of the airflow pattern tests, when diverging walls were installed showed insignificant improvement.

Coil Plenum

As was the case with the Building A model, the determination of the velocity profile at the coil required the measuring of the velocity downstream of the coil. The wiping and erratic secondary flow prevented the measurement of the

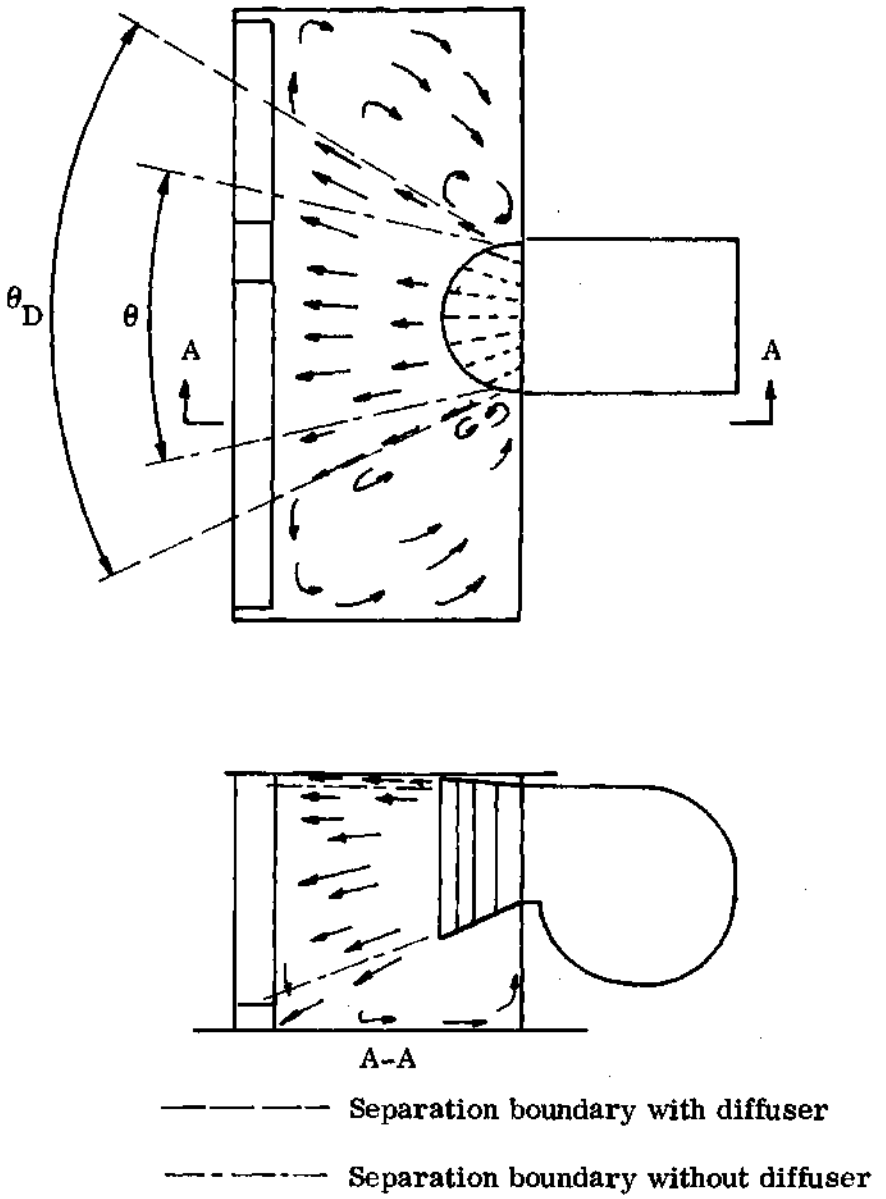

Figure 16. General Model, Fan Plenum Airflow Patterns with a Vaned Diffuser.

through-flow velocity of the coil from an upstream position. The test results for an arrangement without any correction device was the basis for comparison. The effect a correction device made on airflow was compared with the velocity profile without the correction device. Besides the tests using either a perforated plate or the vaned diffuser, the various positions of the fan and the duct connections were evaluated.

General Model Without Correction Devices. The airflow through the coils was non-uniform for an arrangement which used neither a vaned diffuser nor a perforated plate. Typical velocity profiles for the cooling coil and heating coil are shown in Fig. 51. For the heating coil the variation from the average face velocity was 120 percent while the cooling coil variation was 43 percent. This difference in the velocity profiles of the coil attributed to the differences in fin spacing and the number of rows of tubes. The much higher air resistance of the cooling coil aids in reducing the non-uniformity of airflow through the coil.

For low flow rates through the heating coil, extremely poor velocity profiles were observed and measured. Not only was the flow distributed unevenly downstream of the coil but also the flow reversed and passed back through the coil into the fan plenum. The reversed flow was observed with smoke and yarn tufts. The heating coil airflow profiles for two low heating conditions are shown in Fig. 52. In the figure, the reversed flow is plotted as zero velocity, but estimates place the magnitude at 100 to 150 fpm. The reversed flow existed with the flow through the heating coil being as high as 30 percent of the total fan flow rate. Even at very low flow as in Fig. 52b, the velocity of reversed flow was

estimated to be about 300 fpm. The reversed flow was observed for the heating coil only.

The Vaned Diffuser. The vaned diffuser performed fairly well, provided the fan was about 2-1/3 D or farther from the coil. The cooling coil velocity profile using the vaned diffuser was observed and measured; results are shown in Fig. 53. Figure 53a presents the velocity profile for the cooling coil. The profile appears relatively uniform when compared to Figure 51a. The improvement in the cooling coil velocity is quite apparent. Unfortunately the vaned diffuser did not improve the heating coil velocity profile; see Figure 53. The vaned diffuser also failed to give a uniform cooling coil velocity profile for the position of the fan at 1-1/3 D from the coil.

Perforated Distributing Plates. The perforated distributing plate provided the best correction for non-uniform velocity profiles. For an arrangement with the fan placed at 1-1/3 D the velocity profile of the cooling coil was uniform, as shown in Fig. 54a. Although the heating coil profile retained some of the non-uniformity seen in Fig. 53b, overall the profile was improved. The evidence of the effect of the perforated plate was obtained by comparing Fig. b with Fig. 53b. For the fan positioned 2-1/3 D from the coils, relatively good velocity profiles were measured for both coils. The results of the 2-1/3 D observations are given in Figure 55.

After the results had established the perforated plate as superior to the diffuser and by far superior to the system without any correction device, the position of the perforated plate in the fan plenum was considered. For the fan positioned

at 2-1/3 D the velocity profiles of four different plate positions were measured. Results are contained in Appendix G. The best position was 1-1/2 D from the fan to the perforated plate. Positions of 1 and 1/2 D also give acceptable results, while the 2 D position resulted in a relatively poor velocity profile.

The data in Appendix D indicates that the size of the hole in a perforated plate is not the important factor. Commercial perforated plate patterns are available from stock with holes sizes ranging from 1/20" to 1/2". It is the free area that is significant. Since the perforation and pattern are not significant, data from four plates were compared on the basis of free area. The four plates were tested at 1-1/2 D from the fan. From the results it was evident that the plate of 48 percent free area was superior (Appendix G). In fact, as the free area increased the relative improvement in velocity profile decreased. For a perforated plate of 80 percent free area, the velocity profile was totally unacceptable.

Other Factors Influencing Coil Velocity Profiles. As pointed out in the discussion of results for the Building A model, no improvement was observed with the addition of diverging walls in the fan plenum. This is not to say that diverging walls have no value. For this study when a tapered or diverging wall was used the angle of divergence was too large for theoretical improvement (Appendix D). Any improvement in pressure recovery was not detected. The diverging wall did eliminate the vortex flow in the corners at the fan end of the plenum.

The position of the duct connection downstream of the coil was evaluated. In this case the connection was a standard machine-formed bellmouth fitting. No effect on the velocity profile was observed when the bellmouth was moved to within

one duct diameter of the coil. Evaluation of positions closer than one diameter were not possible with the methods used to measure velocity profiles. The approach velocity to the bellmouth entrance and the velocity in the wake of flow over the coil tubes were not conducive to establishing any sort of velocity profile downstream of the coil. Observation of a grid of yarn tufts did not show any affect of the bellmouth fitting on airflow immediately downstream of the coils.

System Performance

The performance of the system in terms of airflow for various damper settings was evaluated. Any effect on the system performance of correction device was not measurable in terms of either a reduction of losses or an increase of in airflow. As expected the head-flow curve measured for the fan is somewhat less than the A.M.C.A. rated head-flow curve published by the manufacturer. Several head-flow curves were measured for the model, a representative head-flow curve is given in Fig. 17, and additional data is contained in Appendix G. Note that for constant cfm the static pressure for the model is about 11 percent less than the rated pressure. For the same static pressure the flow is reduced by 8 percent from the rated flow. A reduction of 8 percent might not seem significant, but 8 percent is about equivalent to the supply air quantity for one floor of a twelve story building. Results of this study did not show significant quantitative differences in system performance for various positions of the fan or for the different correction devices used in the fan plenum.

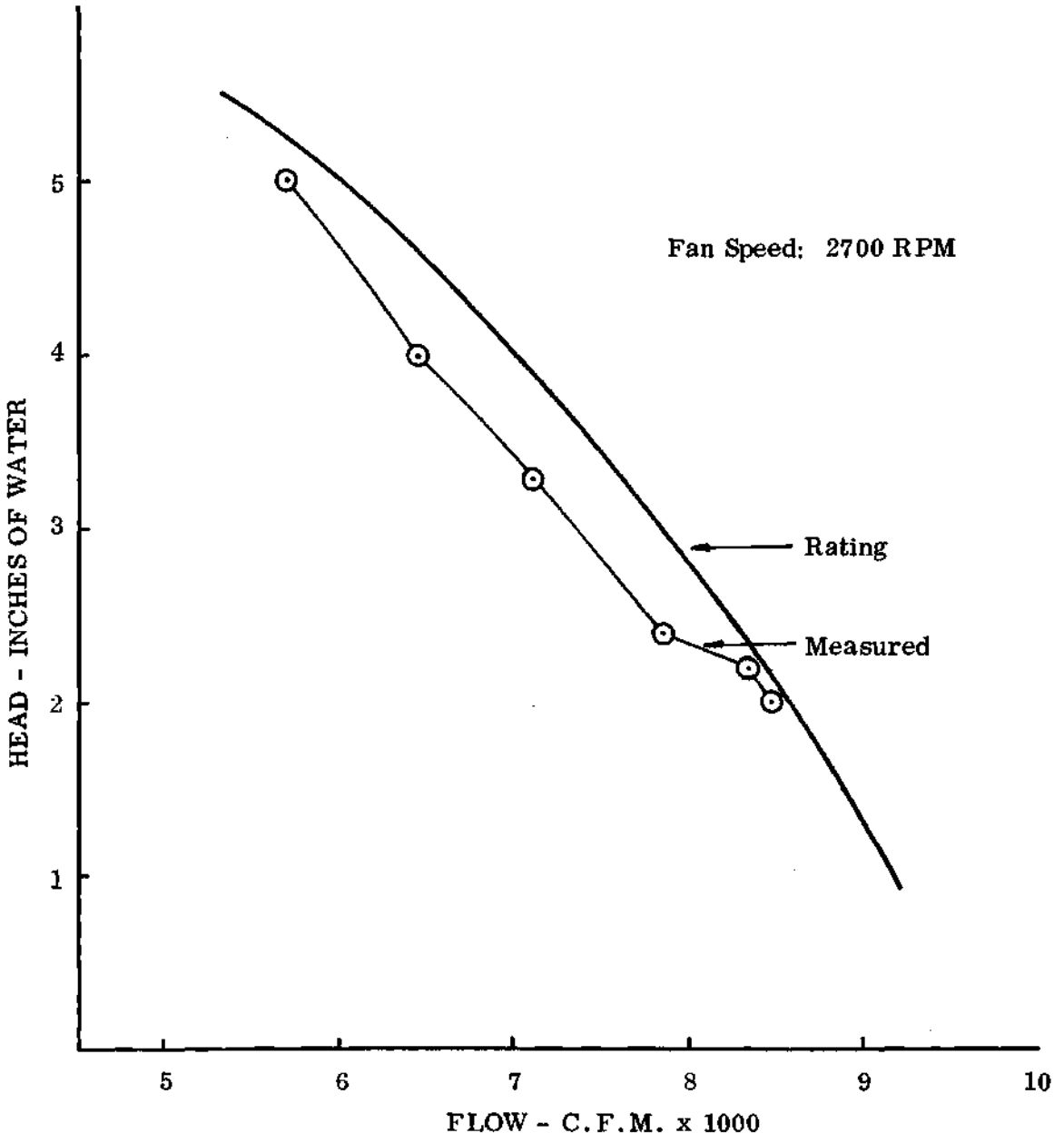

Figure 17. General Model, Typical Head-Flow Curve for the Model Fan Room.

CHAPTER VI

CONCLUSION AND RECOMMENDATIONS

The many possible variables associated with the built-up fan as well as the complicated airflow characteristics make field observations difficult. When cooling and heating coils are located in the region of expanding flow downstream of a fan; air distribution is poor. The velocity through the cooling coil was observed to vary as much as 100 percent across the width of the coil. The velocity of air wiping the face of the coils ranges up to four times the average face velocity.

Field evaluation of the dual duct fan room performance requires observations of airflow rate, static pressure, and airflow characteristics. Flow rates are easier measured in a supply air duct, but when this is not practical measurements in the coil plenums would be adequate. Static pressure should be the average of the measurements at several locations in the fan plenum, away from the mainstream of flow. Generally, for the prototypes considered in this study the flow was 8 percent less than the specified system flow, while static pressure was 15 percent less than the specified fan static pressure. Distribution of air to the coils could be observed with smoke downstream of the coil. Of course, as long as there are no problems, such as, moisture carry-over from the coil, supply air temperature stratification, or tenants complaining about heating and cooling, field testing would not be necessary.

When a fan is located so as to discharge directly at the cooling and heating

coils, uneven distribution of air occurs. Based on the results of model studies the use of a perforated plate located in the expanding airstream from the fan gives satisfactory airflow distribution. A perforated plate of about 50 percent free area gave the best distribution of the plates tested. The perforated plate performed best when placed about two-thirds the distance from the fan to the coils. This recommendation agrees with that of a manufacturer, published after this work was complete (12). To aid in eliminating wiping of the heating coils, the coils should be offset with the heating coil placed farther downstream from the fan. Significant differences in flow or pressure were not observed for different fan positions or correction devices.

The results of the vaned diffuser performance indicate a further study of optimum design parameters would be useful. At this time the perforated plate would be considered superior to other correction devices tested. But the vaned diffuser offers the potential to regain static pressure at the same time the air distribution is being improved. Since a detailed analysis of the diffuser design was not made, a redesign might improve the diffuser performance. The diffuser worked for the cooling coil at 2-1/3 D and a change of the vane angles would no doubt produce better distribution of air to the coil for closer fan positions. A perforated plate used to increase the resistance of the heating coil would probably be required when a vaned diffuser is used.

The performance of the fan plenum is dependent on how well the high velocity air stream from the fan discharge is distributed to the coils. Problems such as moisture carry-over, coil wiping, and air stratification are related to poor

distribution of air. The losses in a fan plenum are difficult to predict. The designer must be mindful of the fact that the fan is not installed in a manner similar to the way it is rated. The correction for the fan plenum loss can take the form of the recommendations by the Air Balancing Council (12). The losses through perforated plates are in agreement with experimental results of several investigations (17, 18, 19). The velocity downstream of the fan outlet should be considered as an effective velocity, when losses for perforated plates are considered (Fig. 38).

Additional work is needed to evaluate the quantitative performance of the perforated plate and design modifications for the vaned diffuser. Also the problem of turning the airstream from the fan to the coils through 90^{o} should be considered.

APPENDIX A

A SURVEY OF TYPICAL FAN ROOM ARRANGEMENTS

Since the arrangement of the fan and coils of a dual duct fan room are dependent on the architecture of the building, a variety of fan room arrangements are used. Basically there are two arrangements, symmetric and non-symmetric. Several types of symmetric arrangements are possible, including: parallel fans, coils at 90^{o} to the fan, coils directly ahead of the fan, and others. Generally for non-symmetric fan rooms the coils are arranged ahead of the fan or at some angle to the fan. For spaces with limited height, coils have been stacked diagonally. A more interesting problem is arrangement of a fan room for a tall, narrow space. The author is familar with one such design, which used two parallel fans, one above the other with the cooling coil above the heating coil.

For arrangements to be presented here, all dimensions are in terms of fan wheel diameter. Chapter II introduces the concept of fan wheel diameter being the characteristic dimension of the fan room.

The first arrangements are symmetric, and are shown in Figure 18, 19, and 20. Figure 18 is the only arrangement from which data were collected for this study. The other two symmetric arrangements are the designs recommended by Shataloff (1), Fig. 20 and an actual fan room built very similar to Shataloff's recommendation, Fig. 19. Both of the parallel fan arrangements attempt to direct the outside air through the cooling and dehumidifying coil. This is done

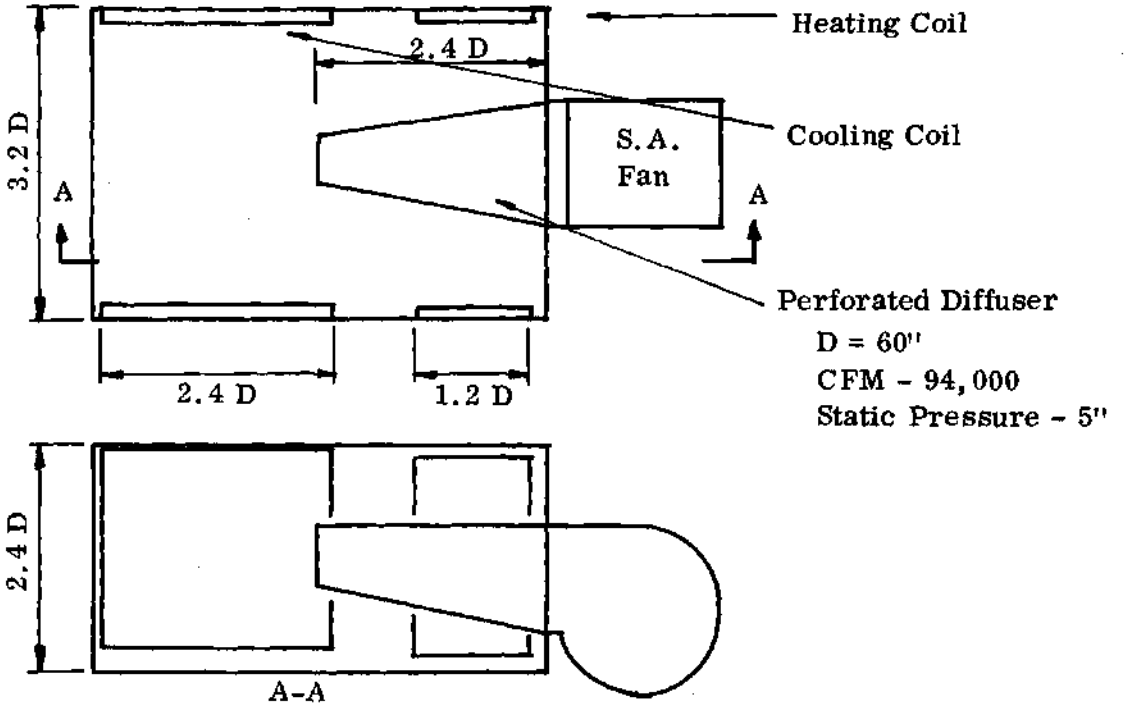

Figure 18. Building C, A Symmetric Fan Room Arrangement.

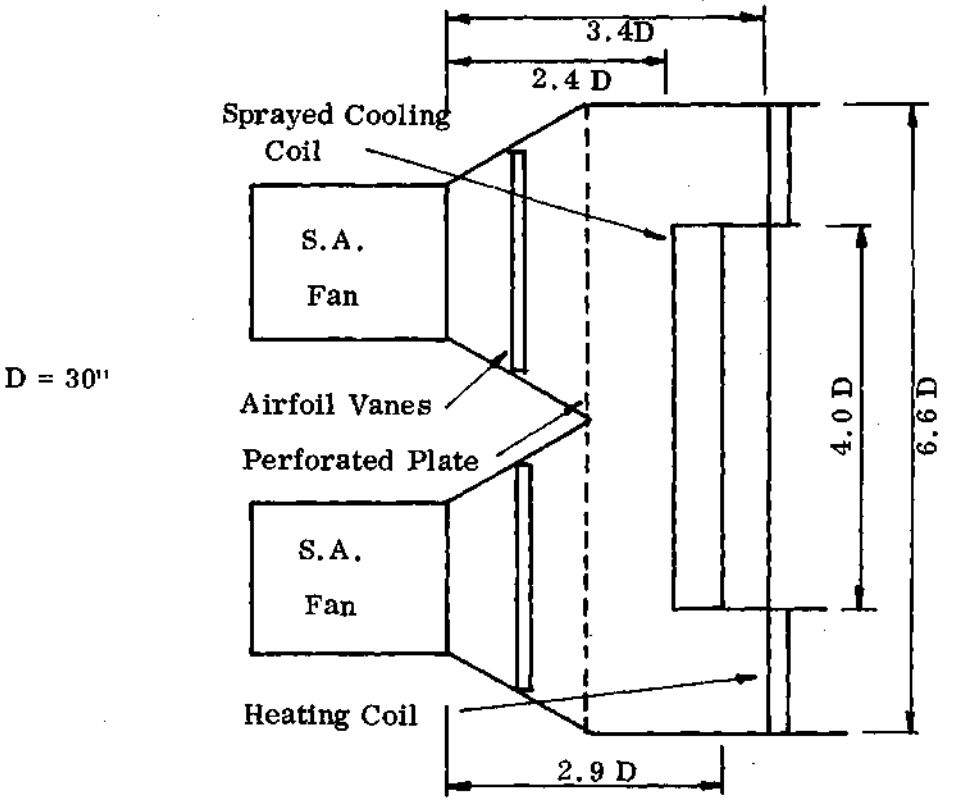

Figure 19. Small Symmetric Parallel Fan Room Arrangement.

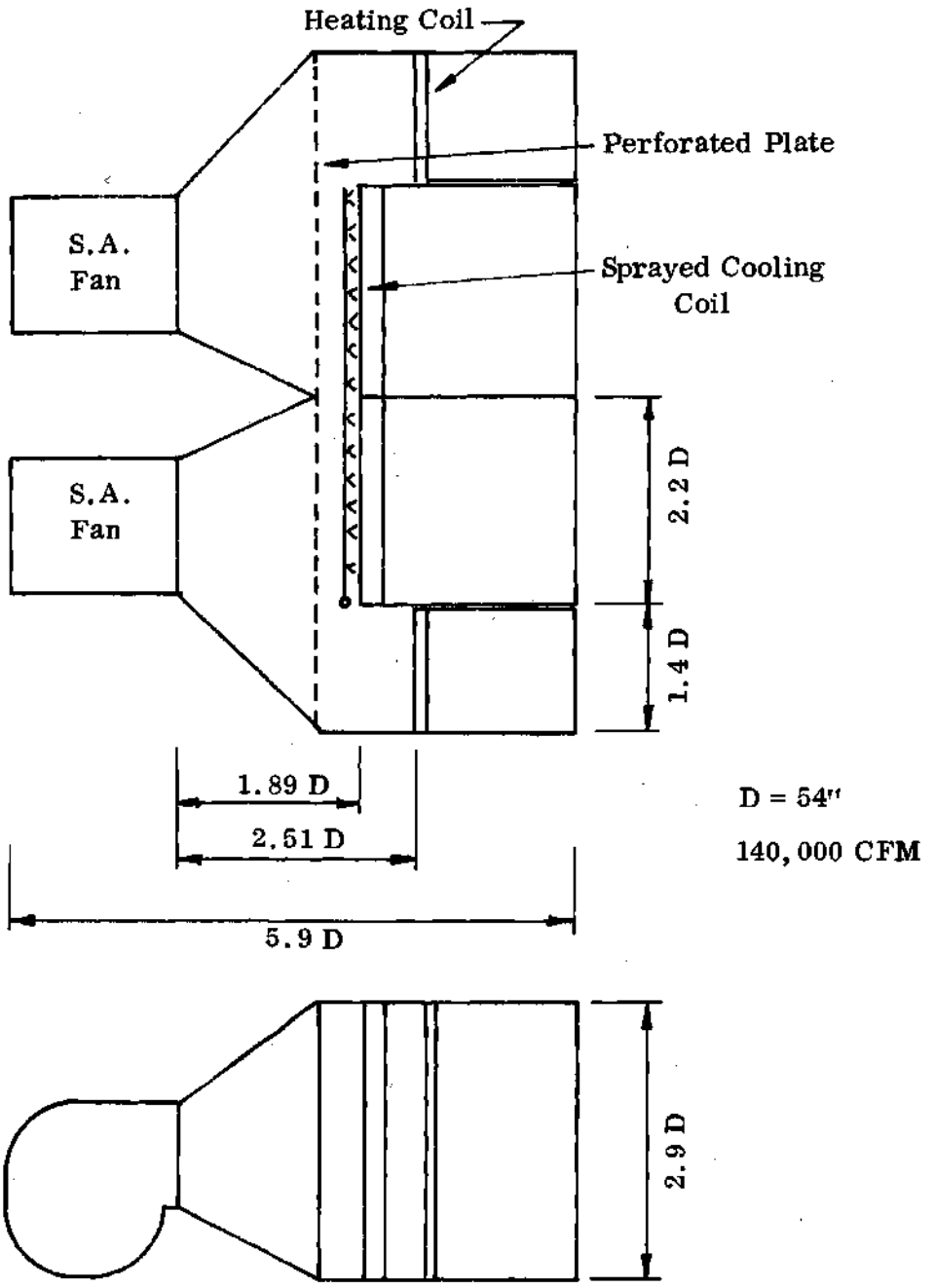

Figure 20. Large Symmetric Parallel Fan Room Arrangement as Recommended by Shataloff (29).

so that outside air can be used for cooling and return air used for heating at certain times.

Arrangements of non-symmetric fan rooms were given in the introduction, Figures 1 and 2. Several more are considered here. Similar to Figures 1 and 2 are arrangements by Shataloff for a larger fan room, Fig. 21 and the other non-symmetric fan room where data was taken for this study, Fig. 22. Figure 23 presents an actual arrangement, designed after the general model was constructed, which is similar to the general model in configuration.

The remaining arrangements vary much more than previously discussed arrangements from Shataloff's recommended arrangement. Due to height limitations in the arrangement in Fig. 24 the coils were stacked diagonally. Although the airflow should appear good for diagonal coils, the flow of moisture is questionable. There is a possibility of moisture dripping back into the fan plenum or tending to fill a portion of the coil, if the coil is placed in the top-to-the-front diagonal position, as in Fig. 24. On the other hand, for the top-to-the-back diagonal position the moisture would be blow off rather than run down the fins. Where space is limited and does not allow the fan room to have the coils in the plane parallel to the plane of the fan outlet, arrangements shown in Figures 25 and 26 have been used. Reports to the author from field inspections indicate that the subway grating aids in turning the direction of air toward the coils (Figs. 25 and 26).

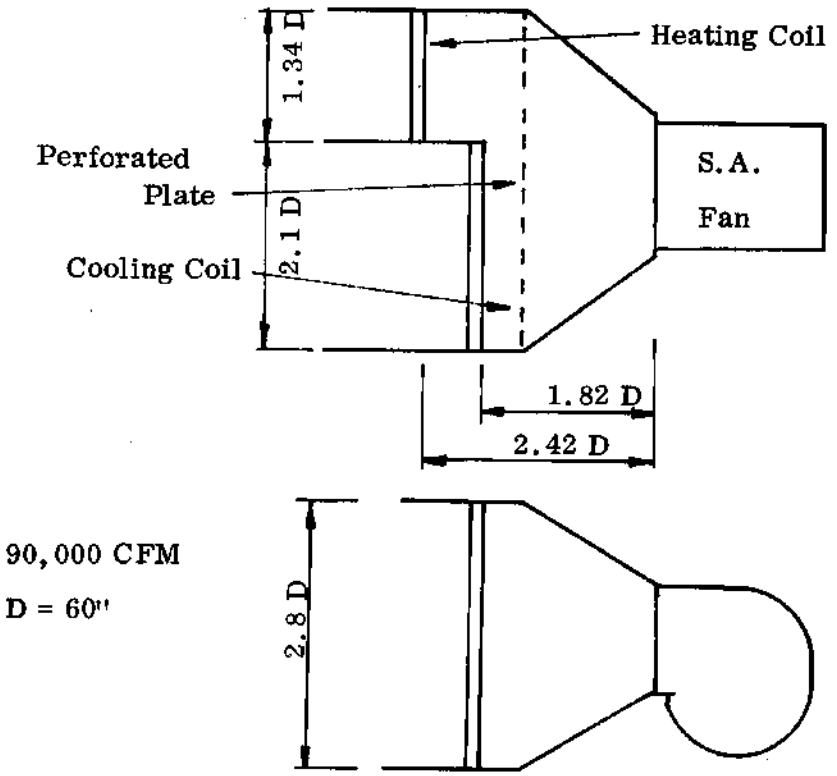

Figure 21. A Non-symmetric Fan Room as Recommended by Shataloff (4).

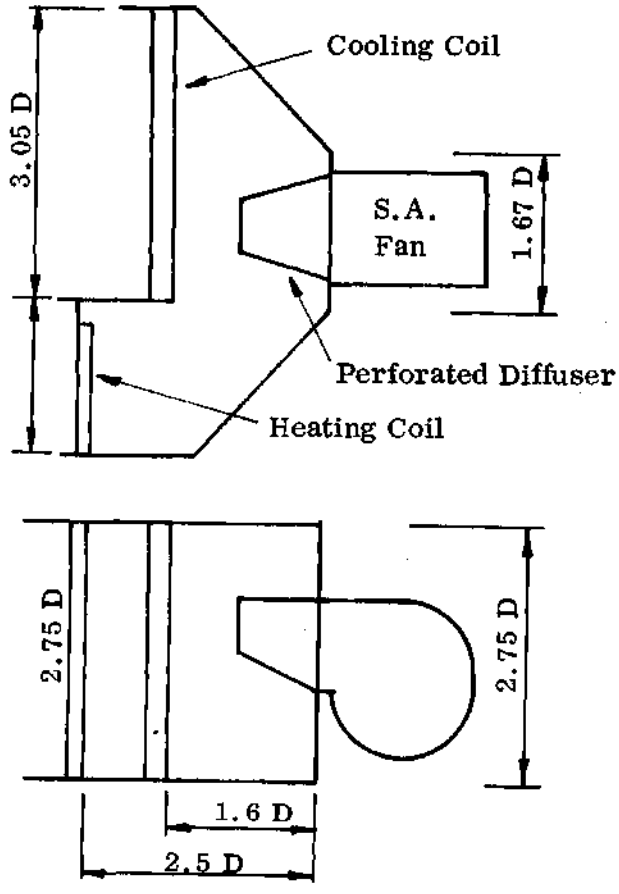

D = 54"

83,000 CFM

Figure 22. Building B, Non-symmetric.

D = 60"

94,000 CFM

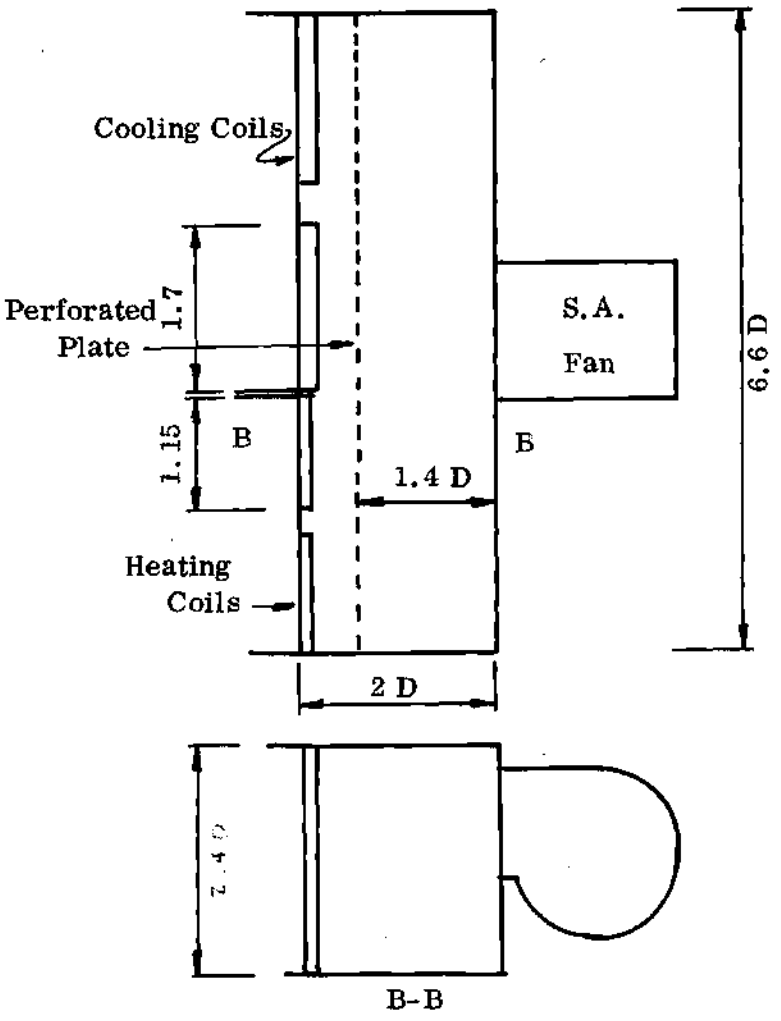

Figure 23. A Fan Room Arrangement Similar to the General Model.

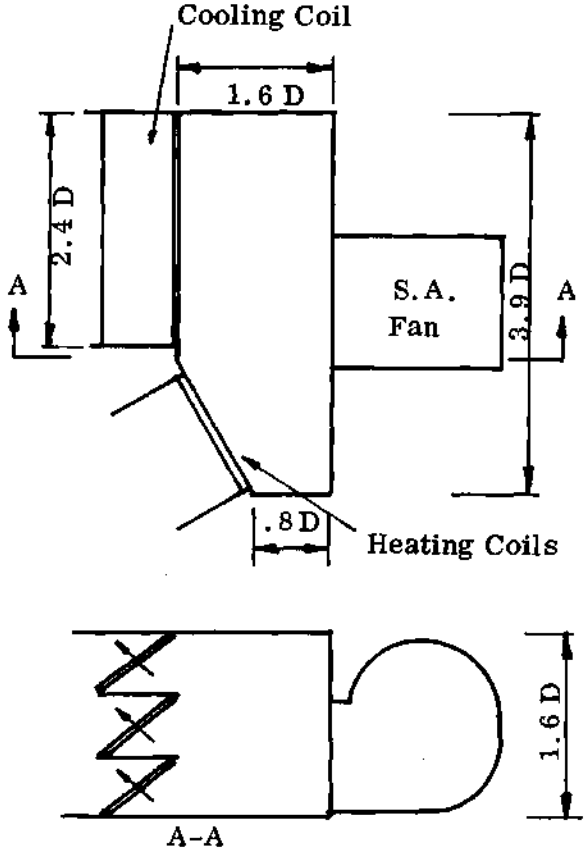

Figure 24. A Non-symmetric Fan Room Arrangement Using Vertical Offsetting of Coils.

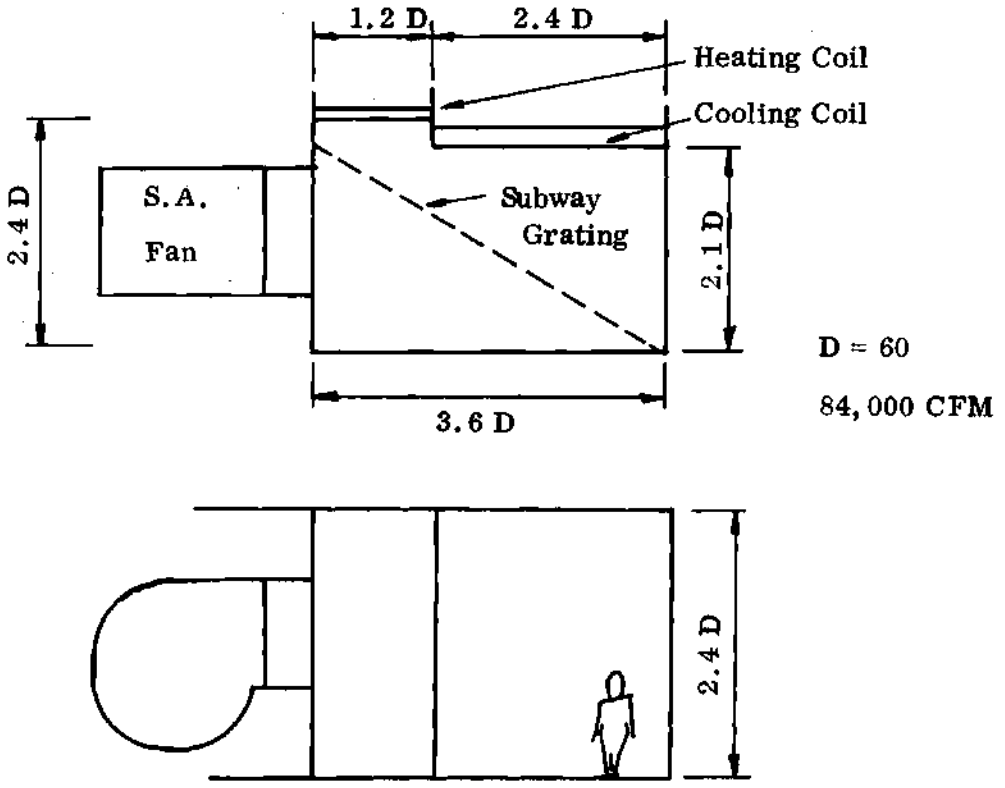

Figure 25. Fan Room Arrangement Requiring Airflow to Turn 90° to Enter the Coils.

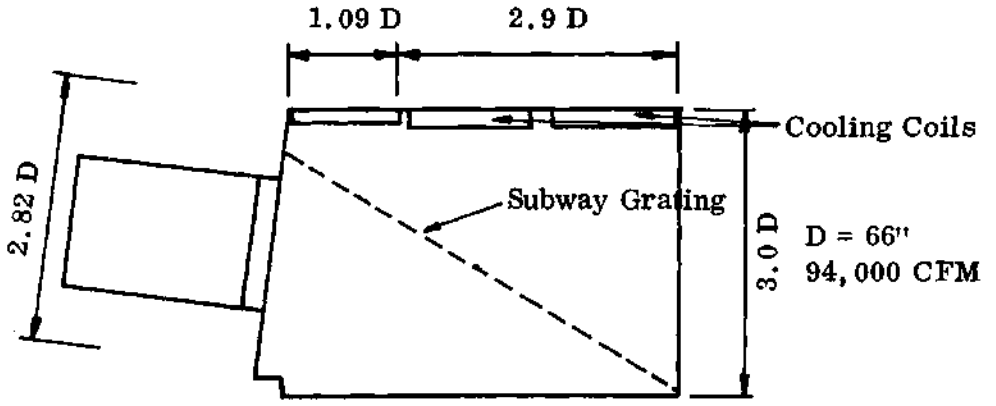

Figure 26. A Fan Room Arrangement Requiring Airflow to Turn Greater than 90° to Enter the Coils.

APPENDIX B

PREVIOUS STUDIES OF CORRECTION DEVICES IN FAN PLENUMS

There has been only a minimal amount of work done in the area of improving airflow characteristics in plenums. The most significant work dealt with airflow in box plenums used to distribute air to several ducts (15). The performance of five types of entrances to the plenum were evaluated. Figure 27 shows the different entrances to the plenum used in the study. The performance of each inlet is shown in Figure 28, note the additional pressure imposed on the system to balance the airflow in all ducts.

Most of Gilman's work had the fan placed in a remote position upstream of the plenum. A perforated plate and eggcrate straighteners were installed in the duct between the fan and the plenum to obtain a uniform velocity at the entrance to the plenum. For the fan in the close-coupled position, system loss was higher than the remote position, but not significantly so. The distribution to the outlets was the same, also the rotational flow observed in the plenum still existed. The vaned internal diffuser performed similarly for both remote and close-coupled fan positions. No significant differences were observed with the straighteners and perforated plate removed.

One surprising fact represented by Fig. 28 is the poor performance of vanes placed in the area immediately downstream of the abrupt expansion. Gilman's data indicates that the abrupt expansion is better than the external vanes for the

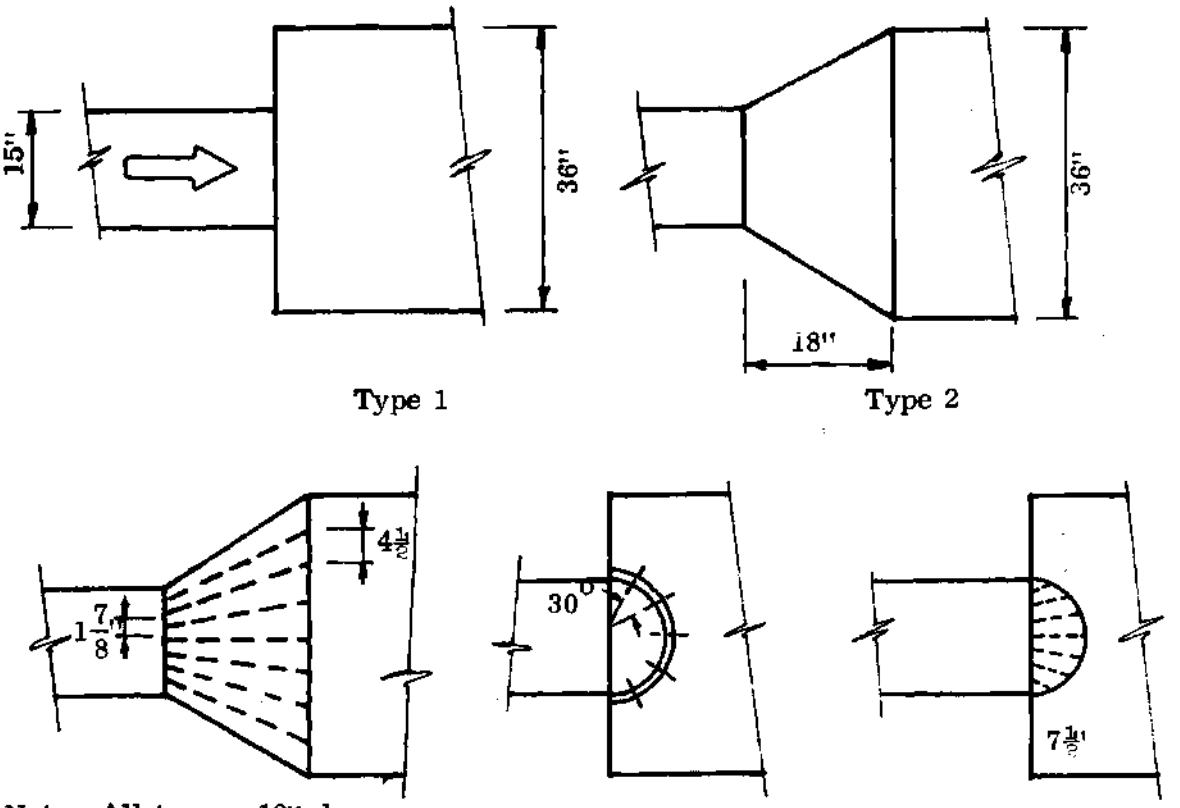

Note: All types, 12" deep.

Figure 27. Entrance Sections Studied by Gilman (Ref. 15, Fig. 3)

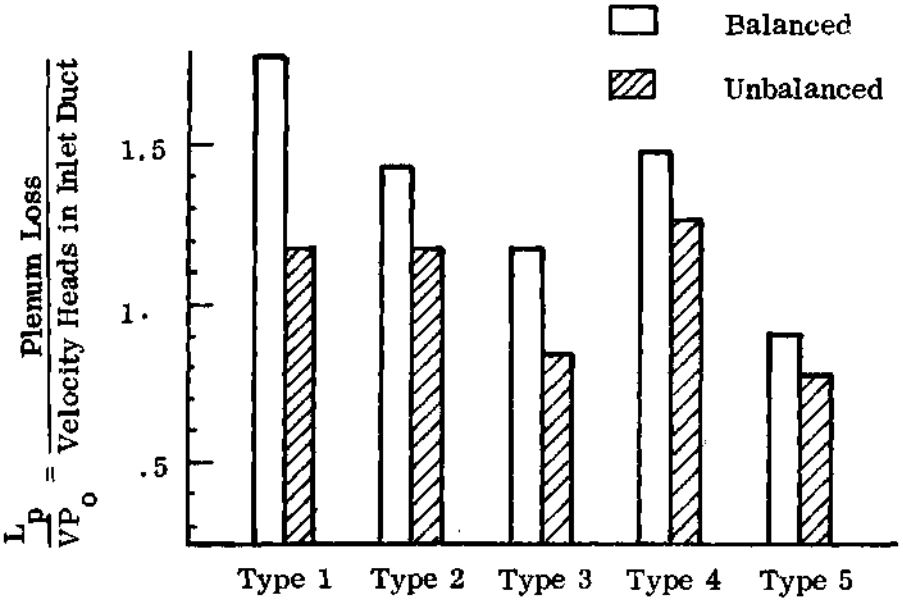

Figure 28. Plenum Loss with Various Entrance Section (Ref. 15, Fig. 5).

unbalanced plenum. A dual duct fan room by nature of the varying cooling flow ratio would be classified as a balanced plenum.

The other study was pointed toward a problem of distributing air from a fan to a bank of filters using a minimum amount of space. This study by Graham (16) was essentially qualitative. The test apparatus included a 49 inch backward inclined D.I.D.W. fan discharging into a 6' x 6' x 8' plenum. The velocity profile downstream of the perforated plate was measured and found to range from 400 to 800 fpm. This variation appears rather large on first examination. But for the filters used in Graham's study the average velocity chosen by a designer would be in the 500 to 1000 fpm range. So a variation of 100 percent in velocity is within the tolerable limits. Furthermore, the performance of a perforated plate in terms of distributing air should be viewed as to how good the high velocity at the fan outlet is broken-up and distributed to coils or filters.

APPENDIX C

INSTRUMENTS AND MEASUREMENT TECHNIQUES

This study of fan rooms required three types of measurements. Of primary importance was the measurement of velocity profiles within the model and prototypes. Measurements of flow rate and pressure were made at various positions in the fan rooms. Measurement techniques used are based on A.S.H.R.A.E. recommendations (25), which apply to the air conditioning industry.

The empirical velocity profiles measured in the fan room are subject to fluctuations due to instability of the flow. In the prototype, visual observations were relied on in many instances. Velocity traverses were made in the fan and coil plenums of both the model and the prototype. As mentioned in Chapter III, there were three velocity measuring techniques used. Only one method was used to any extent, that being a pitot tube and micromanometer. For field tests, a magnehelic gage or inclined manometer were used in lieu of the micromanometer. The other instruments used for velocity measurements were a vaned velometer and a hot wire anemometer.

The accuracy of measurements is limited by the unsteady flow at the point of measurement. The accuracy of the pitot tube used in lab testing is placed at $\pm$ 2 percent (25). The accuracy of the micromanometer exceeds that of the pitot tube, $\pm$ 1 percent at 390 fpm, which is comparable with the hot wire anemometer low range accuracy of $\pm$ 4 fpm. Fan speed was measured to vary $\pm$ 10 rpm at

2700 rpm.

The fluctuating flow rate varied $\pm$ 1 percent of the mean flow rate. A calibration curve for one orifice appears in Figure 29. Note that the flow rate determined by using coil friction loss data is reasonably close to the flow rates determined by duct velocity traverse. Furthermore, the calibration agrees with flow rates measured in the coil plenum.

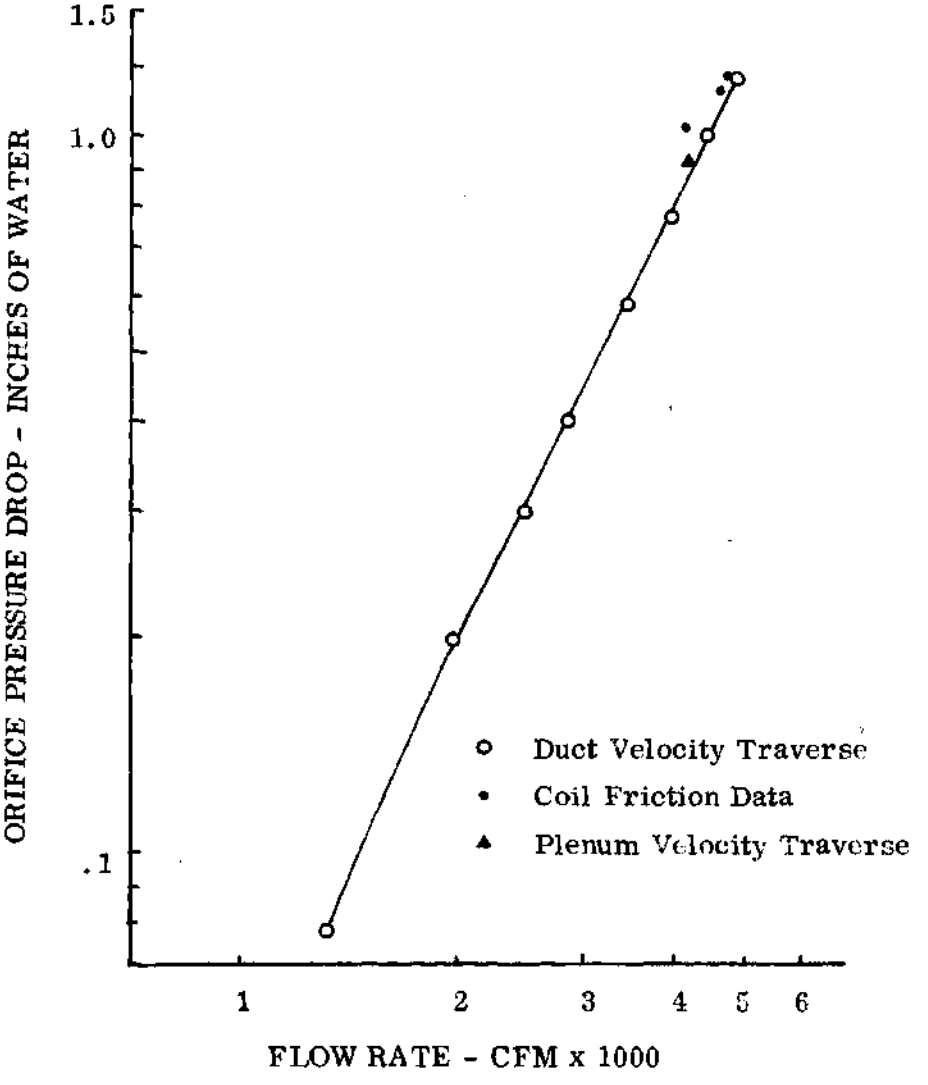

Figure 29. Sample Orifice Calibration Curve.

APPENDIX D

SYSTEM LOSSES

Fan Exit Losses

Several methods of calculating the loss at the abrupt expansion of the fan were available for use. Each method has been considered and compared. Simplifying methods use the same techniques in calculating the losses as in calculating the loss for an abrupt duct expansion (Figure 30). Flow is taken to be one-dimensional, incompressible, and of uniform velocity over the flow cross section.

Borda Equation

Using the steady flow energy equation at constant elevation, an expression for total loss at an expansion can be derived as follows (20),

$$\frac{V_1^2}{2g} + \frac{P_1}{\rho} = \frac{V_2^2}{2g} + \frac{P_2}{\rho} + H_t \qquad (6)$$

or the loss is given by

$$H_t = \frac{V_1^2 - V_2^2}{2g} + \frac{P_{s1} - P_{s2}}{\rho} \qquad (7)$$

A momentum equation without wall shear can be written by assuming velocities are such that wall shear is neglected, and the fluid stream retains its shape and size as it enters the larger section,

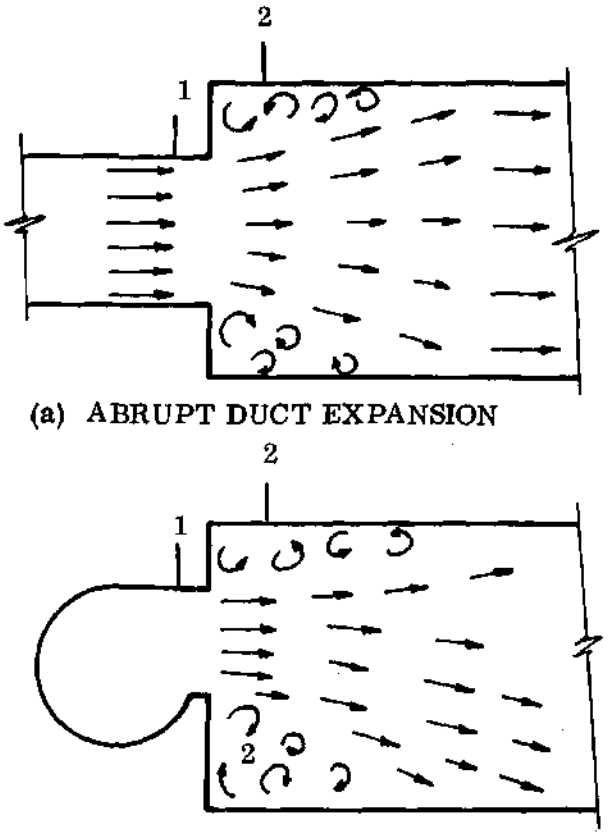

(a) ABRUPT DUCT EXPANSION

(b) ABRUPT FAN DISCHARGE

Figure 30. A Comparison of Abrupt Duct Expansions and Abrupt Fan Discharges.

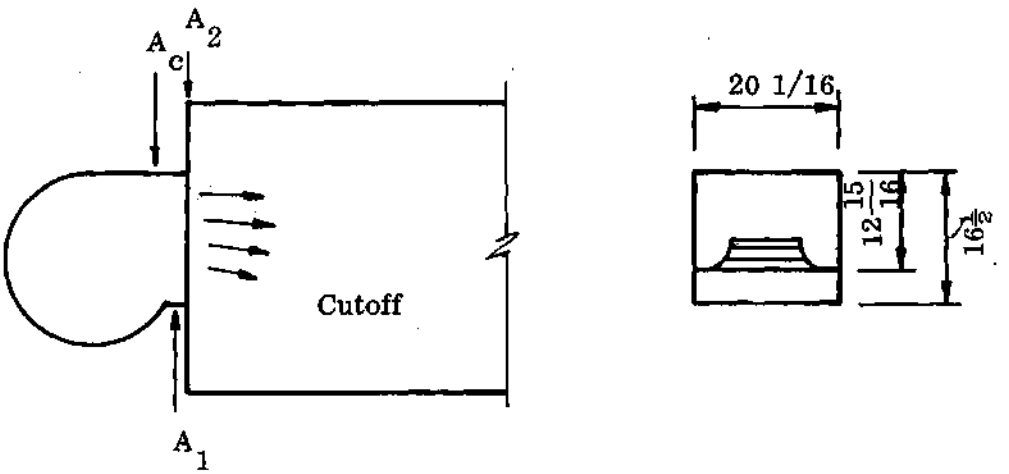

Figure 31. Cutoff and Fan Outlet Abrupt Expansions.

$$A_2P_2 - A_2P_1 = \dot{m}\rho\left(\frac{V_1 - V_2}{g}\right) \tag{8}$$

Dividing by the density ρ and rearranging

$$\frac{P_2-P_1}{\rho} = \frac{\dot{m}}{A_2}\left(\frac{V_1-V_2}{g}\right) \tag{9}$$

and since

$$\dot{m} = V_1A_1\rho = V_2A_2\rho \tag{10}$$

then

$$\frac{P_2-P_1}{\rho} = V_2\left(\frac{V_1-V_2}{g}\right) \tag{11}$$

or

$$\frac{P_1-P_2}{\rho} = -V_2\frac{(V_1-V_2)}{g} \tag{12}$$

putting Eqn. (12) into Eqn. (7)

$$H_t = \frac{V_1^2-V_2^2}{2g} - V_2\frac{(V_1-V_2)}{g} \tag{13}$$

or the general Borda formula for head loss is

$$H_t = \frac{(V_1-V_2)^2}{2g} \tag{14}$$

Since continuity must hold, Eqn. (10), Eqn. (14) can be written in terms of V_1

and areas, and becomes,

$$H_t = \left(V_1 - \frac{V_1 A_1}{A_2}\right)^2 \frac{1}{2g} = \left(1 - \frac{A_1}{A_2}\right)^2 \frac{V_1^2}{2g} \tag{15}$$

For air in a duct the Eqn. (15) using conventional head units of inches of water becomes,

$$h_t = \frac{12\rho_a}{\rho_w}\left(1 - \frac{A_1}{A_2}\right)^2 \frac{V_1^2}{2g_c} \tag{16}$$

Using standard values for density, the area ratio for the general model, and the definition of velocity pressure

$$h_v = \rho \frac{V^2}{2} \tag{17}$$

Equation (16) can be written as

$$h_t = .8412\, h_v \tag{18}$$

Equation (18) is based on uniform flow at the outlet of the fan, but this is not the case. The expansion at the outlet might be thought of as two expansions in series, since the flow expands as it passes the fan cutoff, Fig. 31. At the cut-off of the model fan the area is $0.75\, A_1$ and the equation would be modified to

$$h_t = .879\, h_v \tag{19}$$

Part of the loss of Eqn. (19) is accounted for in the performance data of the fan published by the manufacturer. Therefore, Eqn. (18) is chosen to represent the abrupt expansion loss.

Static Regain

Another method of considering the losses at an abrupt expansion is an expression for the static pressure regain

$$h_r = h_{v1} - h_{v2} - h_t \tag{20}$$

Farquhar (13) used the static regain as a basis of estimating reduction in fan performance due to abrupt expansion losses. The static pressure obtained by rating a fan by the A.M.C.A. test code includes static regain for the expansion at the fan cutoff. In this case the area ratio is 0.75 for the model's fan. Using the static regain curve given by Gilman (15), Fig. 32, the regain is 38 percent of the velocity pressure at the cutoff,

$$h_r = .38\, h_{v_c} \tag{21}$$

This regain is the loss resulting from the abrupt expansion, that can be subtracted from the cataloged fan performance data to arrive at a corrected performance. The results reported by Farquhar dealing with small forward curved fans produced good correlation between predicted "static regain" loss and measured loss. The results indicated 1.1 velocity heads lost as a result of abrupt expansion which agrees closely with recommended losses of 1.0 velocity head (12). For the large backward inclined fans as found in dual duct applications or even the small model

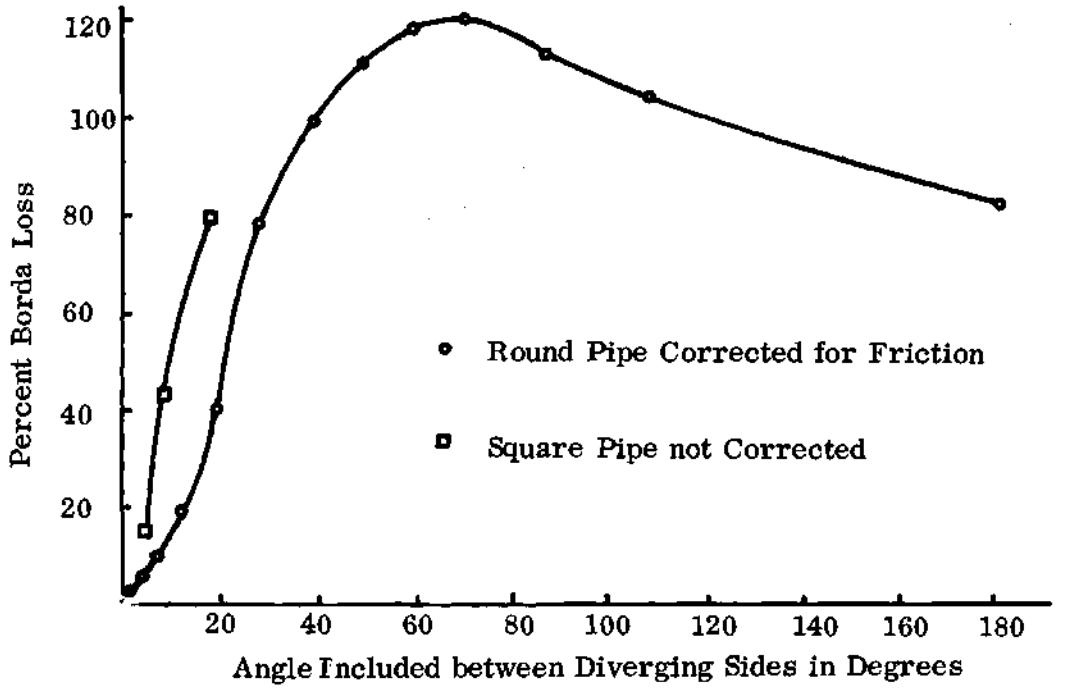

Figure 32. Ratio of Actual Loss in Diverging Sections to Borda Loss from Data of A. H. Gibson (20).

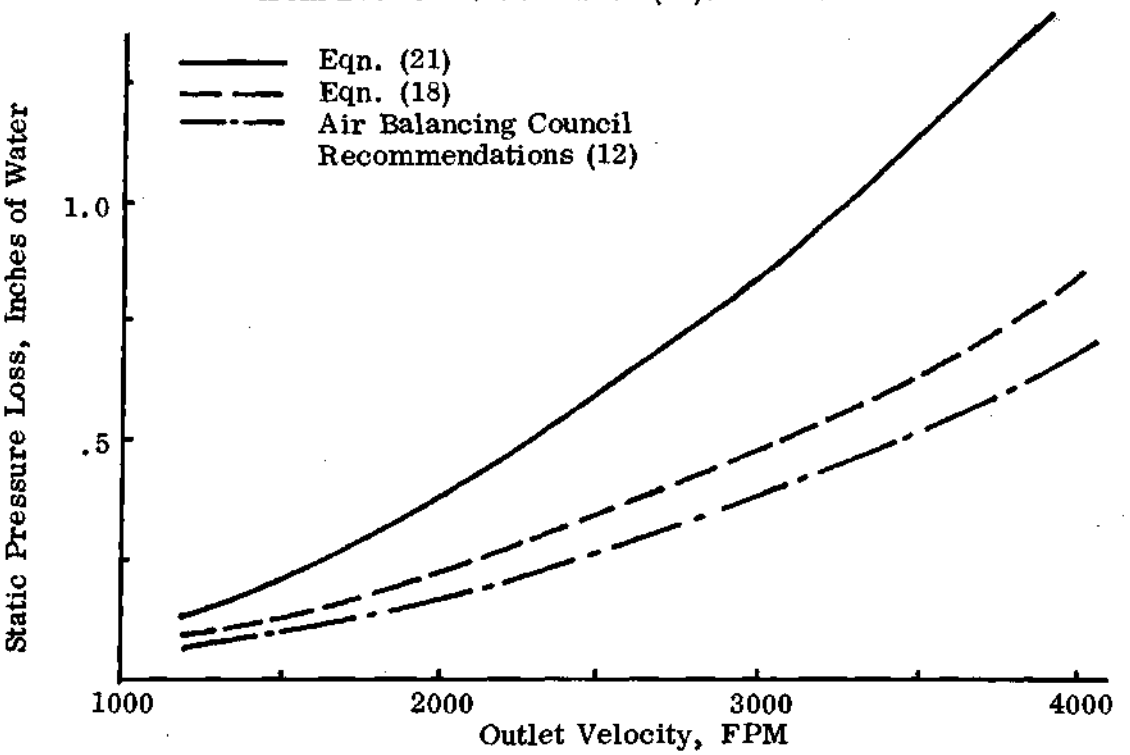

Figure 33. Abrupt Expansion Losses for the Model.

fan, the method of subtracting the static regain from the fan rating would give losses less than those from abrupt expansion calculations.

Recommendations for Fan Applications

The American Air Balancing Council recommend the following corrections for abrupt expansion losses for fans (12): The correction being velocity heads added to the fan static pressure, airfoil backward inclined--1.0, backward inclined--1.5, and forward curved--1.8. These corrections appear somewhat high when plotted with the other loss estimates, (Eqn. 18 and Eqn. 21) Fig. 33.

Turbulent Mixing and Friction Loss

Analytical estimates of the losses for turbulent mixing have not been attempted. The flow is subject to many variations as the system changes for cooling to heating. These variations in percentage of flow going through the coils would make analysis unreasonable. Gilman encountered a similar problem and chose to neglect turbulent mixing. Since friction calculated by normal methods is small, friction at the plenum walls is neglected (21). In the study of box plenums the difference between an abrupt expansion from the fan or a duct between the fan and plenum were not significant. The loss was estimated by the Borda formula, Eqn. (15), to be 0.34 velocity heads. But the measured total plenum loss was found to be 1.17 velocity heads. If the system was balanced for equal flow from all outlet ducts, the loss was 1.77 velocity heads. This loss is about the same as the 1.8 velocity heads for correction in selecting fans published by the American Air Balancing Council (12). It appears that these recommendations might be applied to the dual duct fan room in estimating losses.

Resistance of System Coils

The resistance of the coils is obtained from the manufacturer's data (27). The resistance of the coils is increased by poor entrance conditions (21). The velocity of air wiping the coil face was found to be 3 to 4 times greater than the through flow face velocity. But as previously mentioned this increased resistance has been attributed to turbulence in the fan plenum and was not considered a part of the coil loss. The coil pressure losses and losses of subsequent components to be considered is plotted in Figure 34.

The duct losses are based on accepted friction loss for ducts and fittings (6, 7, 21). The bellmouth fitting losses were calculated using a coefficient of K equal to 0.04 such that

$$\Delta h_t = K \times h_{v_u} = 0.04\ h_{v_u} \tag{22}$$

is the total pressure loss and

$$\Delta h_s = (1 + K) \times h_{v_u} = 1.04\ h_{v_u} \tag{23}$$

is the static pressure loss. The combined friction loss for the ducts and bellmouth fittings, both cooling and heating, is plotted in Figure 34.

The losses through the flow measuring orifice are a function of velocity and the ratio of the duct area to the orifice area. The loss in static pressure is given by,

$$h_s = C_o\ h_v \tag{24}$$

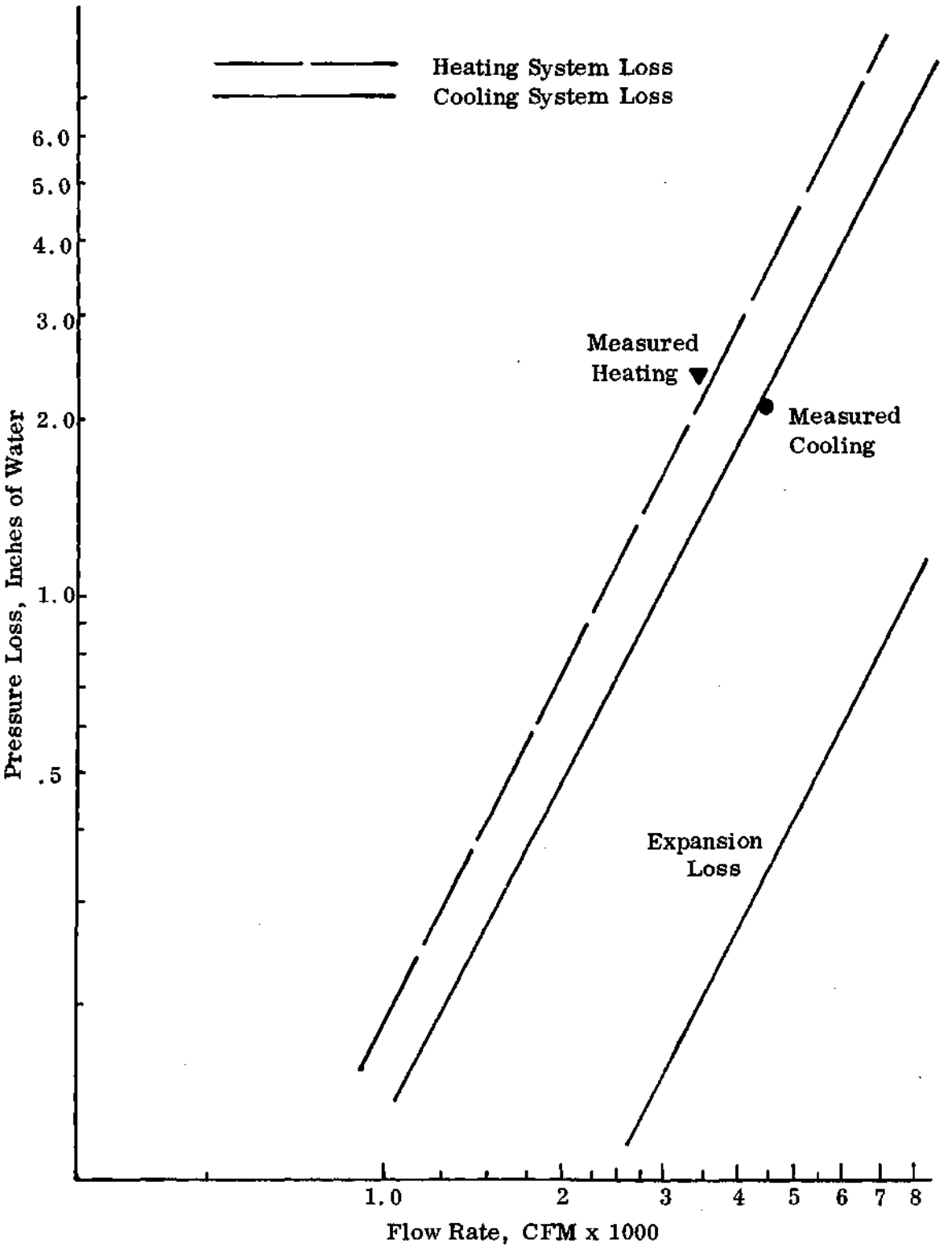

Figure 34. Estimated and Observed System Resistance Curve.

The coefficient C_o, was given as a function of the area ratio (21). For Eqn. (24) the velocity pressure used is that at the Vena Contracta. For the orifices normally used the coefficients for heating and cooling ducts were 0.21 and 0.20, respectively (21). Equation (24) is also applicable for calculating the drop at the damper, which has an orifice over the end of the duct. The coefficients used for the heating and cooling dampers in the open position were 1.7 and 1.66, respectively (21). The losses as a result of flow measurement and control are included in Figure 34.

Air Flow Correction Devices

Diverging Plenum Walls

A diverging transition at the fan outlet improves static regain and reduces turbulent mixing losses (15). Consider first the static pressure regain by going back to Eqn. 14 which is for the ideal situation of 100 percent regain and can be rewritten

$$H_r = \frac{V_1^2}{2g} - \frac{V_2^2}{2g} - \frac{(V_1-V_2)^2}{2g} \qquad (25)$$

for the actual regain

$$H_r = \left(\frac{V_1^2 - V_2^2}{2g}\right) - K\,\frac{(V_1-V_2)^2}{2g} \qquad (26)$$

Kratz (20) used equation (26) and the value of the experimental constant K obtained by a previous investigator to compare angles of divergence. The values of K was obtained from A. H. Gibson's work (20) and are expressed as a percentage of the Borda loss, Figure 32. Figure 35 was given by Kratz based on Eqn. (26) and of K from Fig. 32.

Gilman's study (15) included a comparison of the abrupt expansion inlet to a plenum and a 2 dimension diverging transition inlet to a plenum. For an included

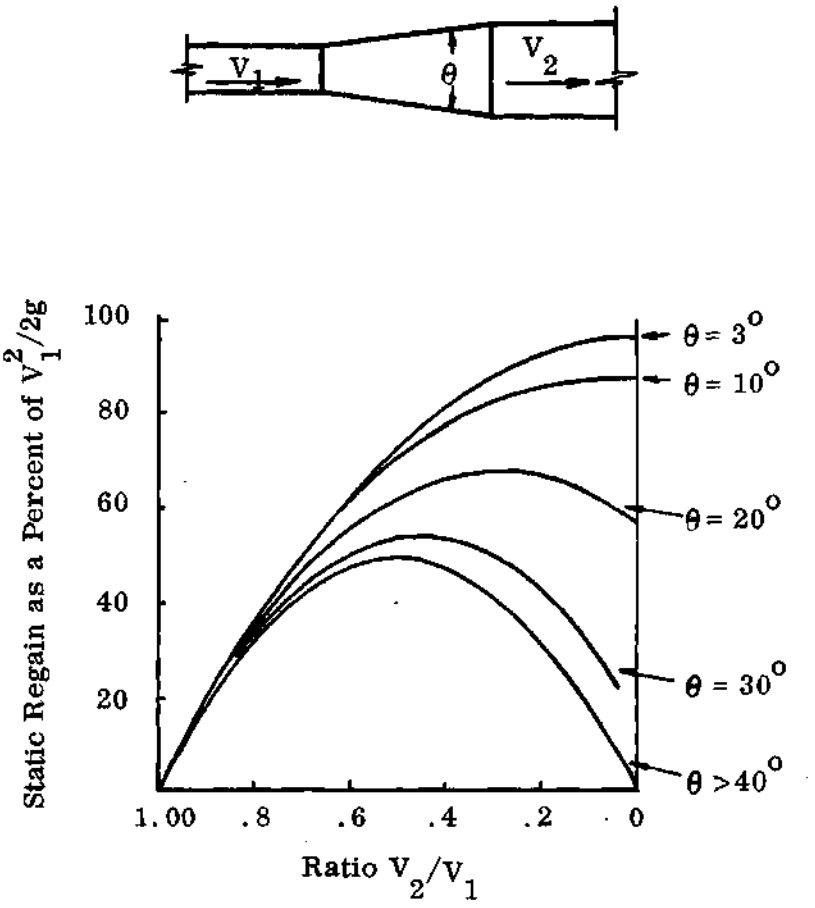

Figure 35. Static Pressure Regain for Diverging Sections in Smooth Circular Ducts (Ref. 20, Fig. 17).

angle of 58° the measured loss was 1.17 velocity heads, which was the same as the abrupt expansion. For the case of balanced flow in the outlet ducts the loss was 1.42 velocity heads as compared to 1.77 for the abrupt expansion. The theoretical static regain should have been about 0.48 velocity heads as computed by methods of this Kratz (20).

For the model fan, the use of a 60° included angle transition would regain less than the estimates for Gilman's arrangement of fan and plenum. For the general model having a Borda loss of 0.8412 velocity heads, the static regain should have been 0.17 velocity heads. Converted into static pressure for an outlet velocity of 3000 fpm, the static regain would be 0.095 inches of water. The static regain for included angles of 40° is about the same regain as an abrupt expansion. The only difference appears to be the reduction of some turbulence in the fan plenum.

Air Diffusing Devices

The vaned diffuser used by Gilman decreased the losses in the box plenum (15). In fact, the plenum losses for the unbalanced situation were 0.78 velocity heads for balanced outlet flow. The use of the diffuser by Gilman eliminated about 50 percent of the box plenum losses. For the model's fan a similar reduction in losses would save 0.5 inches of water. A detailed analysis of diffuser static regain is beyond the scope of this study and will be a part of subsequent studies with the model.

Perforated Plates

The losses resulting from the use of perforated plates can be estimated by

using the techniques of Baines and Peterson (18). The pressure drop through a screen or perforated plate can be expressed by a loss coefficient K,

$$K = \frac{\Delta P}{\rho V_o^2/2} \tag{27}$$

Dimensional analysis (18) gives

$$\frac{\Delta P}{\rho V_o^2/2} = f(Re, A_o/A_t, \text{ pattern}) \tag{28}$$

The Reynolds, $Re = V_o b/2$ has as a characteristic dimension the diameter b of the wire of a screen. Baines uses a solidity ratio, $s = 1 - (A_o/A_t)$, but this is confusing since the air conditioning engineer usually speaks of free area. The free area ratio A_o/A_t, is the ratio of the open area of the plate to the total area.

The flow through a perforated plate is a series of jets that coalesce downstream of the plate. For analytic purposes, a single hole has been isolated from the plate. The velocity and pressure relations for flow through a perforated plate are identified in Fig. 36, (18). An expression for the loss coefficient K has been derived by using a combination of the momentum and energy equation. Neglecting losses,

$$\tfrac{1}{2}\rho V_1^2 + P_1 = \tfrac{1}{2}\rho V_2^2 + P_2 \tag{29}$$

$$\sum \text{Forces} = \rho Q(V_3 - V_2) = P_2 A_2 - P_3 A_3 \tag{30}$$

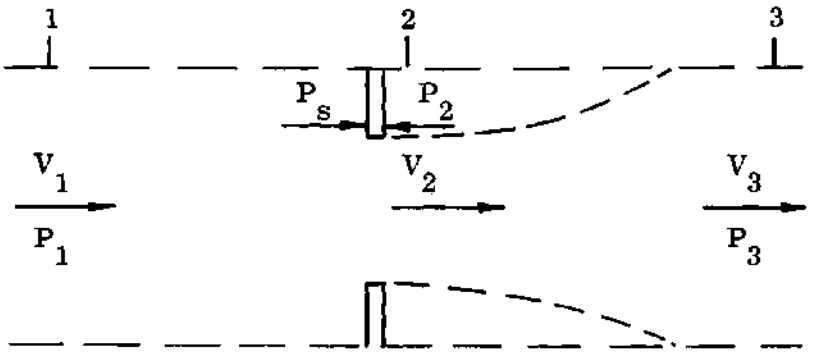

(a) Flow Through One Hole of a Perforated Plate

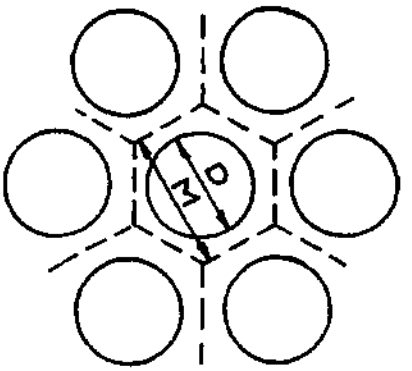

Effective b =

M - 0.95 D

(b) Perforated Plate Dimensions

Figure 36. Perforated Plate Velocity, Pressure and Geometric Relationships.

Assuming a mean velocity of V_o

$$\rho V_o(V_3 - V_2) = P_2 - P_3 \tag{31}$$

Rearranging Eqn. (29) and substituting for P_2 from Eqn. (31),

$$P_1 + \tfrac{1}{2}\rho(V_1^2 - V_2^2) = P_2 \tag{32}$$

$$= P_3 - \rho V_o(V_2 - V_3) \tag{33}$$

assume V_1 and V_3 are at the mean velocity V_o and writing the difference in P_1 and P_3 as ΔP,

$$\Delta P = \frac{\rho}{2}(V_2 - V_o)^2$$

$$= \rho \frac{V_o^2}{2}\left(\frac{V_2}{V_o} - 1\right)^2 \tag{34}$$

Thus the coefficient K can be expressed as

$$K = \frac{\Delta P}{\rho V_o^2/2} = \left(\frac{V_2}{V_o} - 1\right)^2 \tag{35}$$

Since at section 2 the vena contractor occurs, by using the open area, A_o, the total area, A_t, and the contraction coefficient C_c, the continuity equation can be written as,

$$C_c A_o V_2 = A_t V_o \tag{36}$$

or

$$\frac{V_2}{V_o} = \frac{1}{C_c}\left(\frac{A_t}{A_o}\right) = \frac{1}{C_c(A_o/A_t)} \tag{37}$$

substituting for V_2/V_o in Eqn. (35),

$$\frac{\Delta P}{\rho V_o^{\,2}/2} = \left(\frac{1}{C_c(A_o/A_t)} - 1\right)^2 \tag{38}$$

A plot of K versus A_o/A_t from Eqn. (38) for two different values of the contraction conefficient, C_c is given in Fig. 37. The experimental results of several independent investigations is also included in the Figure 37. Most of the investigations of pressure drop across a screen or perforated plate use a uniform approach velocity profile (17, 18). In those cases the value of V_o is simply a mean velocity, easily evaluated. The question of pressure drop across a perforated plate downstream from an abrupt expansion is considered by Lipstein (19). If the mean velocity is used for calculating the loss coefficient, K, in the area of expanding airflow the K will be high. Graham (16) expressed pressure drop across a perforated plate versus a mean velocity downstream of the plate. Recall that Graham had a perforated plate downstream from a fan outlet. In order to correlate Graham's data with Baines and others, the effective velocity correction given by Lipstein was needed, see Fig. 38. By using the effective velocity, the pressure drop measured for perforated plates used in this study has been correlated with analytical predictions, Figure 37.

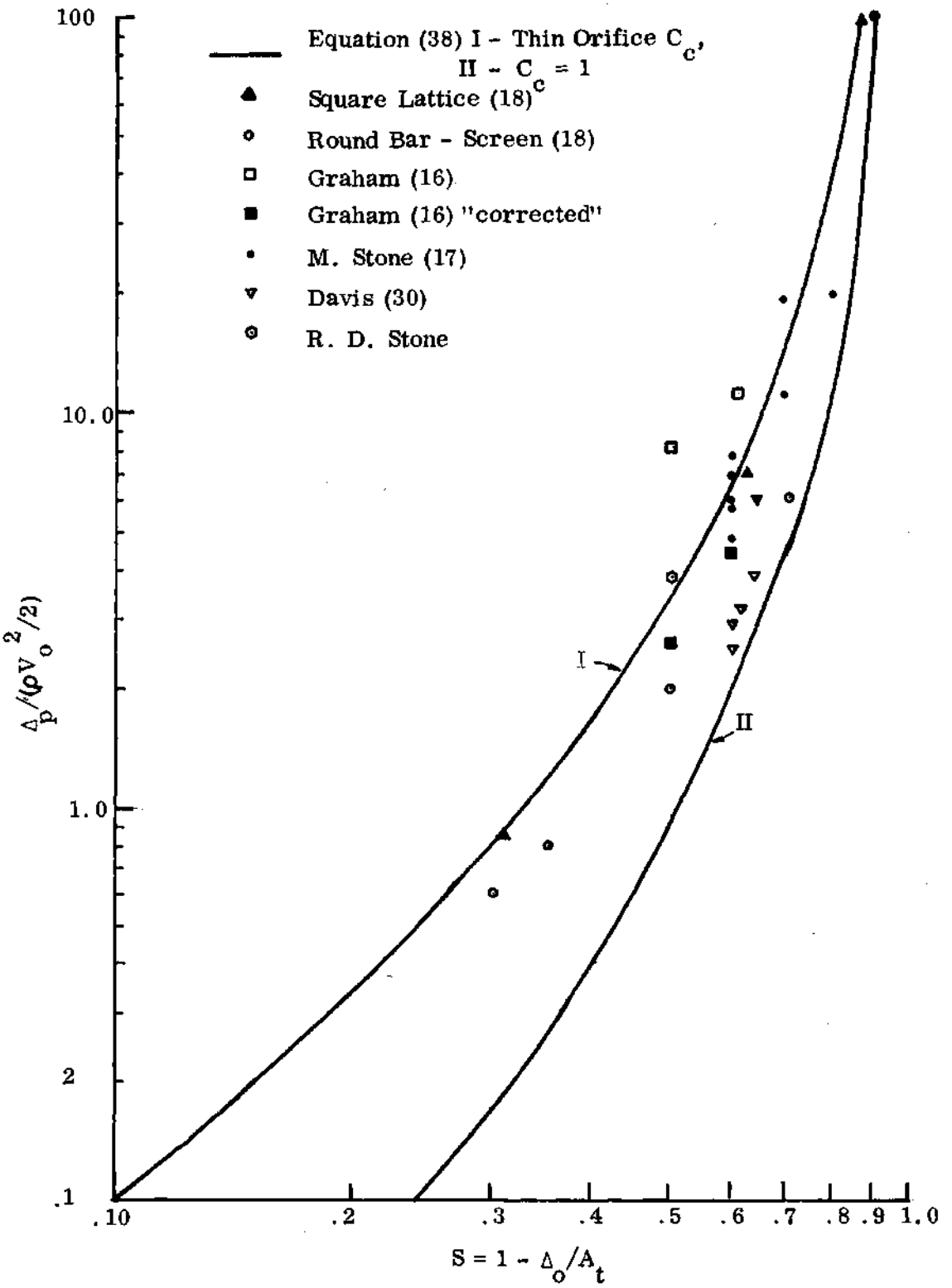

Figure 37. Relative Pressure Loss as a Function of Solidity Ratio.

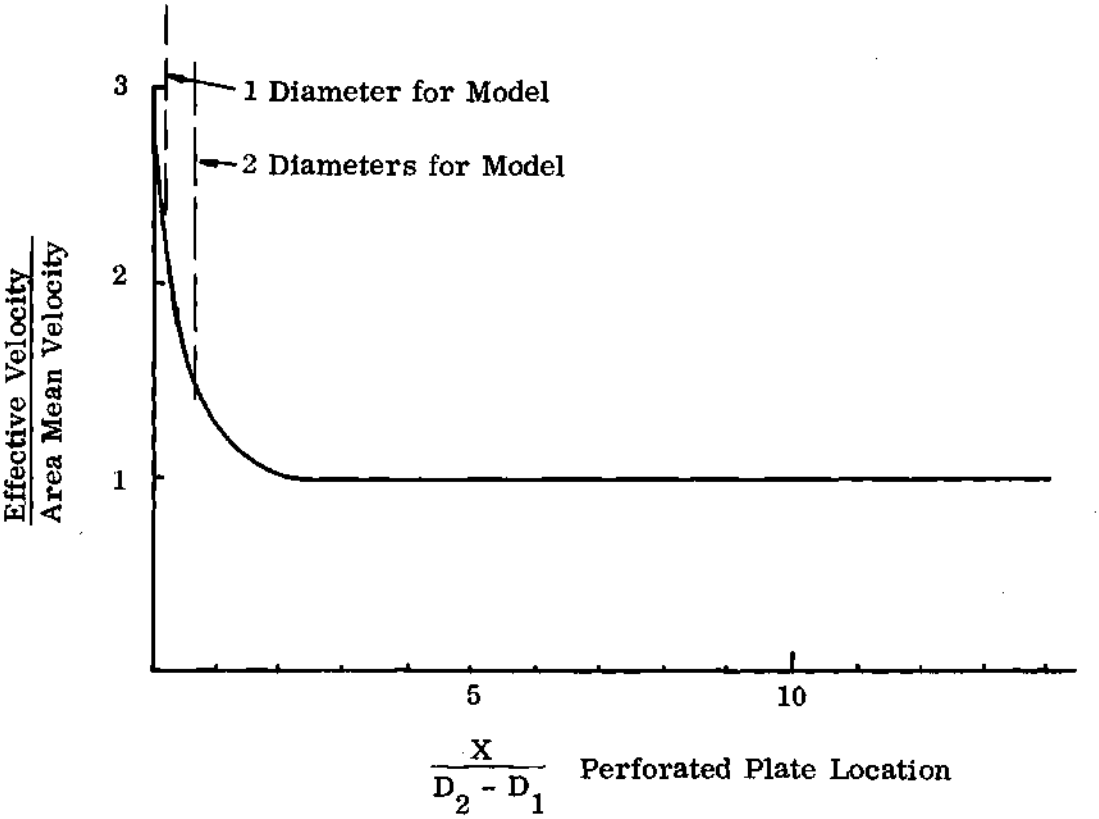

X = Distance from Plate to Outlet

D_2 = Hydraulic Diameter of Plenum

D_1 = Hydraulic Diameter of Fan Outlet

Figure 38. Effective Velocity for Perforated Plates Downstream of an Abrupt Expansion.

APPENDIX E

AIRFLOW ANALYSIS

Velocity Profiles

The outlet velocity profile is nonuniform. Often the velocity profile does not follow the expected trend of high velocity at the outside of the scroll decreasing to low velocity as the cut-off is approached. The results of Graham (16) point this out, and were substantiated by this study. Figure 39 contains profiles reported by Graham for a 49 inch airflow D.W.D.I. fan, discharging into a plenum containing a perforated plate ahead of a bank of filters. Two points should be noted, first, the non-uniformity of the velocity profiles and second, the similarity of profiles for the same fan under different conditions, such as outlet vanes.

The ability of a perforated plate to modify the fan outlet velocity profile, distributing over the entire face of a filter is shown in Figure 39. Note the improvement resulting from using vanes in the fan outlet to deflect the air to the upper portion of the filter. Also the velocity modification was better if the plate has less free area in the blast area of the fan.

Prediction of Flow Regions

The three regions of flow for an abrupt expansion are given in Figure 40 in terms of distance from the expansion interface. Using Figure 40 the flow regions were determined for either Building A or general model, both

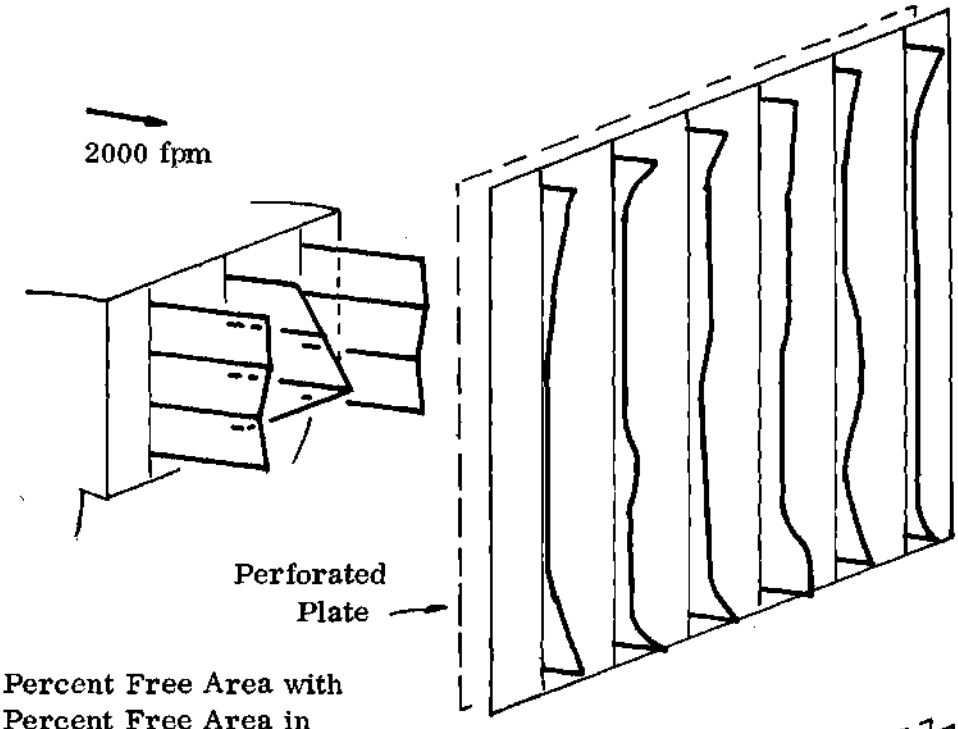

(a) 50 Percent Free Area with 25 Percent Free Area in Fan Blast Area.

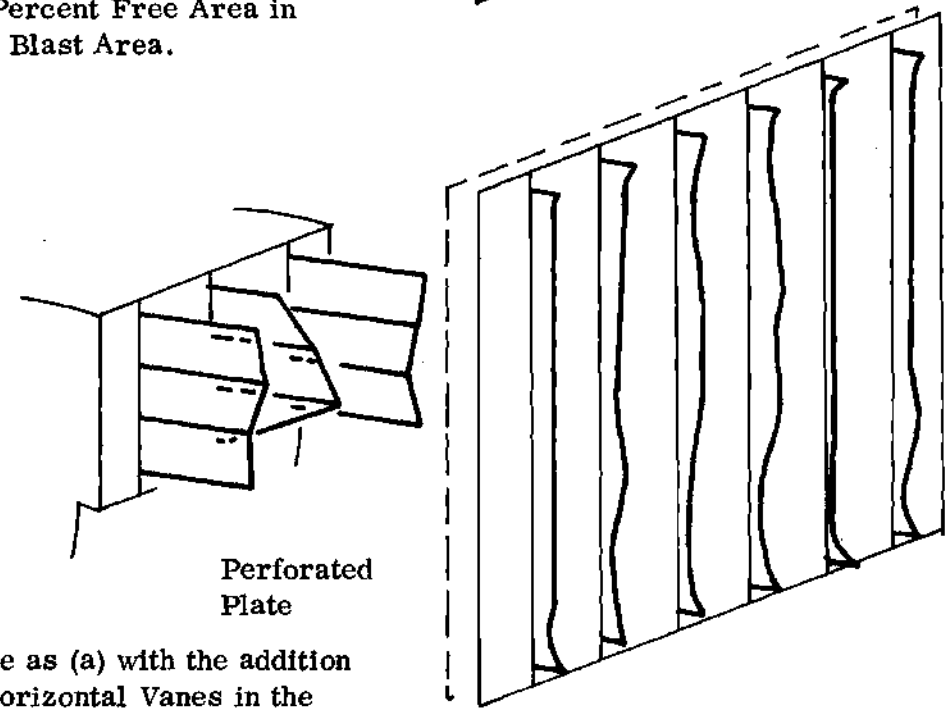

(b) Same as (a) with the addition of Horizontal Vanes in the Outlet

Figure 39. Fan Outlet and Perforated Plate Velocity Profiles

Reported by Graham (16).

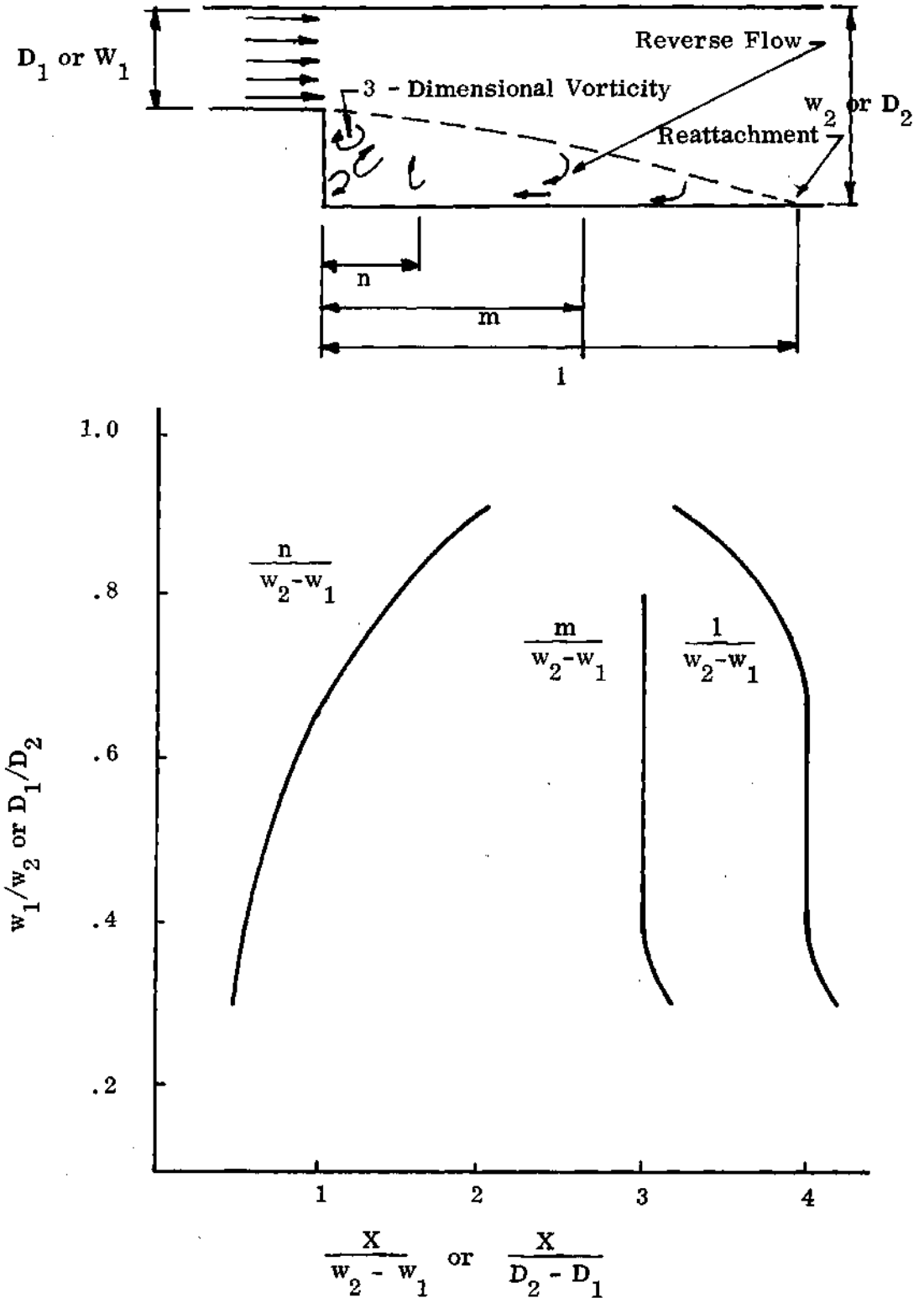

Figure 40. Three Regions of Flow for an Abrupt Expansion, as Reported by Abbott and Kline (26).

have the same W_1/W_2 ratio, 0.39. Recall that the outlet dimension of a fan is a function of the wheel diameter. For double width, double inlet centrifugal fans W_1 ranges from 1.06 D to 1.1 D. The region of three-dimensional vorticity for the model would be up to 14 inches or about one fan wheel diameter from the outlet. The reverse flow would occur up 76 inches or about 5 D. The point of reattachment, if space were available would be 102 inches or 6.8 D. Thus, if the above data is applied to a fan plenum, the characteristic flow regions would appear as shown in Figure 41. Several obvious assumptions were made to apply the two dimensional expansion data to flow in a fan plenum. First of all, the fan plenum is a three-dimensional, not two-dimensional expansion. Secondary, the outlet velocity for the fan plenum is non-uniform. Third, although not in importance, the fan plenum has an obstruction, cooling and heating coils, in the flow expansion region. The obstruction in the form of coils might be offset, as much as one fan wheel diameter is not uncommon. Also the cooling flow ratio is not constant.

Distance Between Fan and Coils

The empirical relationships for maximum velocity pressure at the face of the coils provide one method of estimating the performance of a fan plenum. For the cooling coil the following equation is recommended (12),

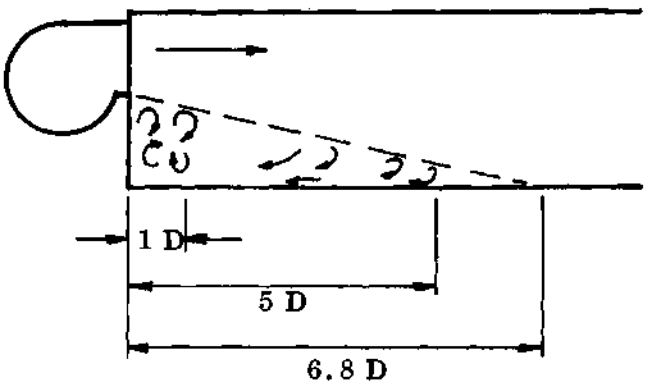

(a) IDEAL

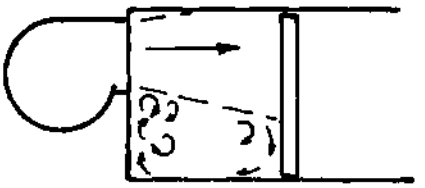

(b) GENERAL MODEL

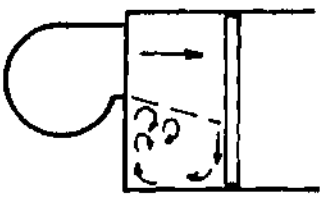

(c) BUILDING A MODEL

Figure 41. Three Flow Regions in Fan Room Models.

$$VP_e \leq 0.4\,(\Delta P_c + VP_c) \tag{39}$$

where $\Delta P_c/VP_c \geq 27$. A similar equation is recommended for the heating coil,

$$VP_e \leq 0.25(\Delta P_c + VP_c) \tag{40}$$

where $\Delta P_c/VP_c \geq 5$. Equations (39) and (40) are used in conjunction with empirical data plotted in Figure 42. By establishing a maximum velocity pressure at the face of the coil with either Eqn. (39) or (40), and knowing the coil average face velocity and pressure drop; the ratio, VP_e/VP_o, can be used in Figure 42 to find the distance L. As an example, the general model is considered. Using a coil face velocity of 500 fpm as a basis for the model airflow, the VP_e/VP_o ratio is 0.216. From Figure 42, the value obtained for L/D is about 2. Since D for the model is 18.4 inches, the minimum L is 36.8 inches or 2.4 fan wheel diameters. If the fan is placed closer than minimum L, a perforated diffusing plate is recommended (12). Comparing this result to the flow at 2.4 D as shown in Figure 41, it appears that the minimum L is not far enough downstream for a good distribution of airflow at the coil face. Results of studies of airflow in the model have shown that a perforated plate will improve the distribution at the cooling coil greatly, for distances of $3\frac{1}{2}$ D and closer. For the heating coil, use of Eqn. (40) in a manner similar to the above example gives a minimum distance of 4.4 D. This appears to be more in line with observations and flow regions (19).

Velocity Modification by Perforated Plates

Experimental observations of perforated plates have shown that the local

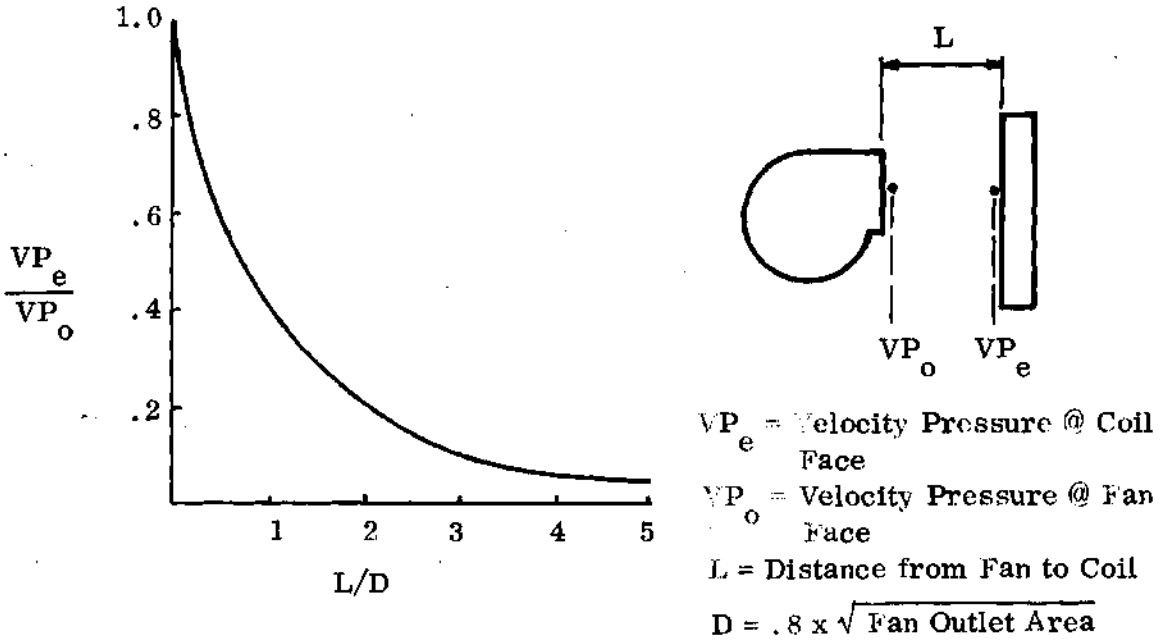

Figure 42. Empirical Relationships for Maximum Velocity Pressure at Coils (Ref. 12, Fig. 100).

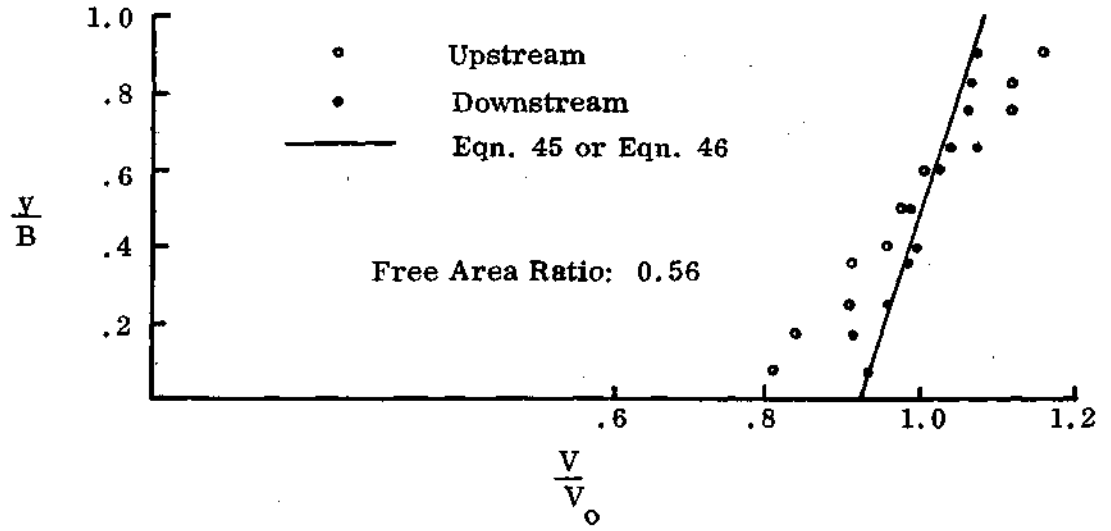

Figure 43. Predictions of Velocity Modification for a Perforated Plate (Ref. 18, of Fig. 4).

pressure drop is essentially constant for any velocity distribution. Therefore, a relationship between V_1 and V_3, see Fig. 11, can be established if the terms $P_s - P_2$ is evaluated (18). Based on the experimental observations of Baines, the upstream energy equation can be written,

$$P_s - P_1 = \frac{\rho V_1^2}{2} \tag{41}$$

and the downstream energy equation,

$$P_2 - P_3 = \left(1 - \frac{K}{1 - A_o/A_t} + K\right) \frac{\rho V_3^2}{2} \tag{42}$$

or

$$P_2 - P_3 = \left(1 - \frac{K}{1 - A_o/A_t}\right) \frac{\rho V_3^2}{2} + \frac{K\rho V_o^2}{2} \tag{43}$$

Equations (41) and (43) can be combined with the perforated plate energy equation,

$$\Delta P - (1 - A_o/A_t)(P_s - P_2) = \frac{\rho}{2}(V_3^2 - V_1^2) \tag{44}$$

to give velocity modification equations,

$$\left(\frac{V_3}{V_o}\right)^2 = \frac{K + (V_1/V_o)^2}{K + 1} \tag{45}$$

and

$$\left(\frac{V_3}{V_o}\right)^2 = \frac{K + A_o/A_t \left(\frac{V_1}{V_o}\right)^2}{K + A_o/A_t} \tag{46}$$

Equation (46) is the more accurate. These equations consider mean flow only. Baines (18) gives four other velocity modification equations used by previous researchers. Equation (45) and (46) predictions of velocity profiles differ less than 2 percent. Experimental results show agreement for high free area ratios, see Figure 43. The data for perforated plates followed similar velocity modification as the screen data. For a jet of air, similar to an abrupt expansion, the velocity modification tend to slightly under-predict the velocity profile correction for screens. But the predictions of perforated plates for the same free area ratio do not agree with experimental observations. Baines gives no apparent reason for the disagreement. The inability of velocity modification equations to accurately predict the improvement in profile tends to discredit their use.

APPENDIX F

PROTOTYPE FIELD TESTS AND SELECTED VELOCITY PROFILES

Table 2. List of Prototype Tests

Test No.	Description	Date
P-1	Building A, Upper West, with Diffuser	4-18-69
P-2	Building A, Upper West, with Diffuser	4-25-69
P-3	Instrument Calibration Check	5-2-69
P-4	Building A, Upper West, without Diffuser	5-6-69
P-5	Building C, Upper East, with Diffuser	5-6-69
P-6	Building A, Upper West, without Diffuser	5-15-69
P-7	Building A, Upper East, with Diffuser	5-15-69
P-8	Building B, Upper East & West, with Diffuser	5-19-69
P-9	Building A, Airflow Measurement	5-19-69
P-10	Building B, Airflow Measurement	5-20-69
P-11	Building A, Upper West, without Diffuser	9-15-70

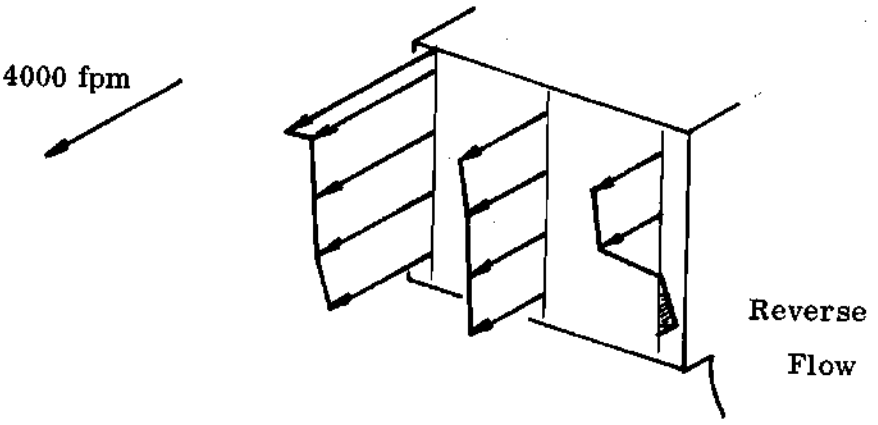

(a) Fan Outlet Profile
Test P. 1, with
Outlet Diffuser.

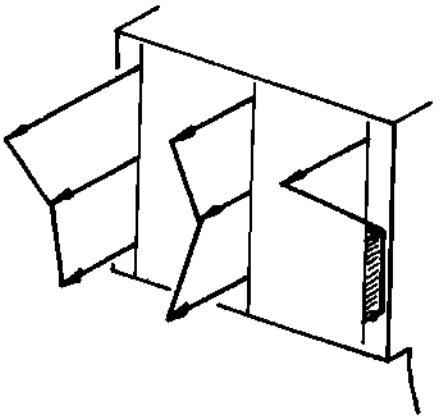

(b) Fan Outlet Profile
Test P. 4, without
Outlet Diffuser.

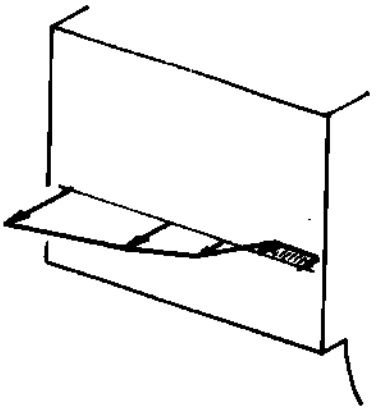

(c) Fan Outlet Profile
Test P. 11, without
Outlet Diffuser.

Figure 44. Fan Outlet Velocity Profiles, Building A
Upper West Fan Room.

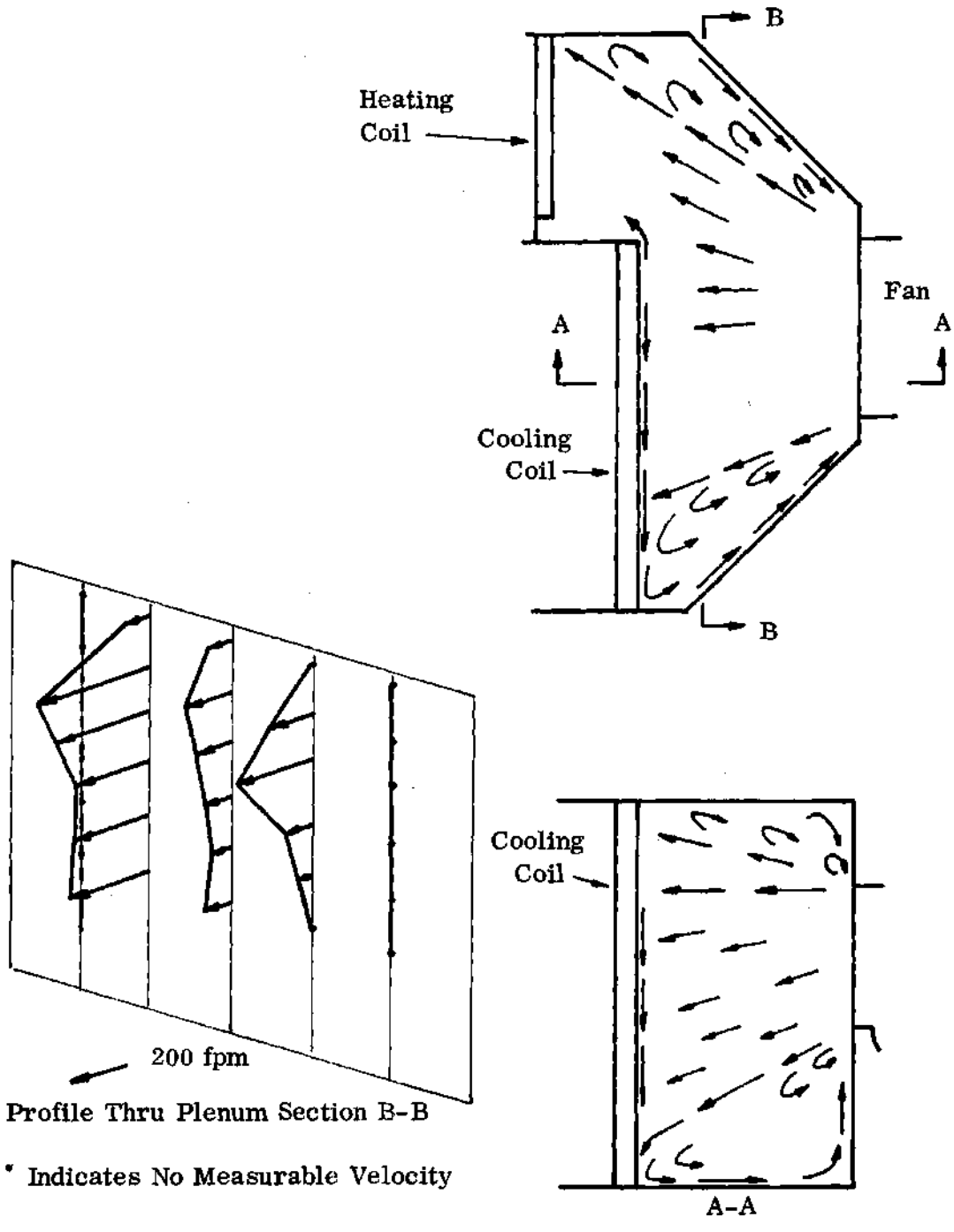

Figure 45. Building A Upper West Fan Room Airflow Patterns in the Fan Plenum.

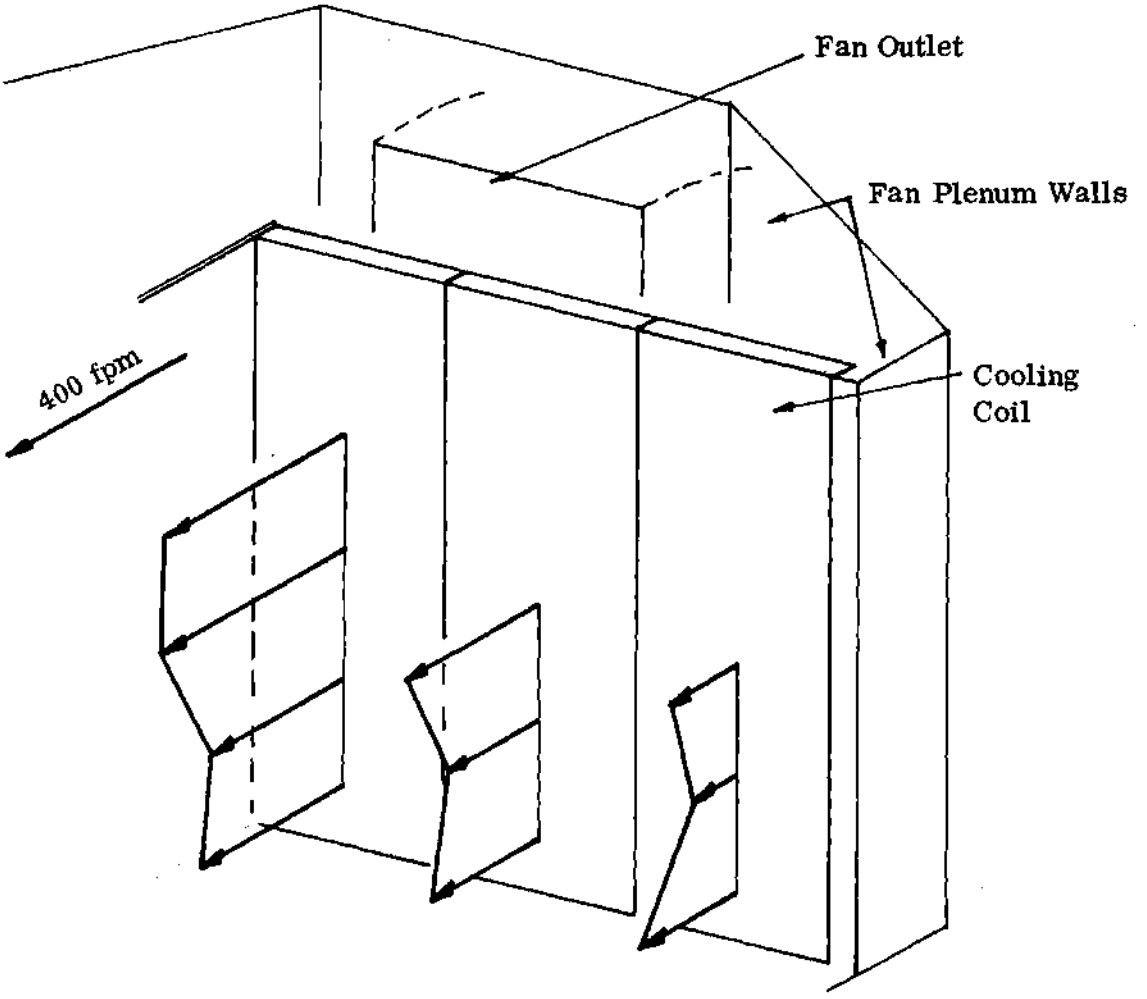

Figure 46. Building A Upper West Fan Room Velocity Profile Downstream of the Cooling Coil.

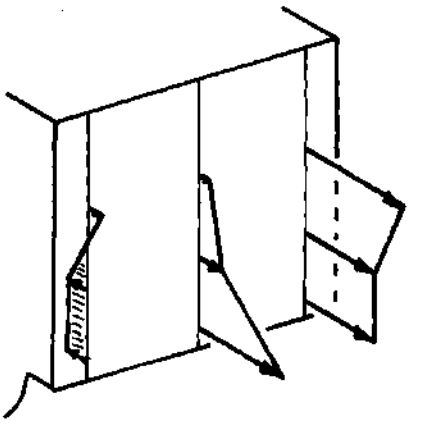

Figure 47. Building A Upper East Fan Room, Fan Outlet Velocity Profile.

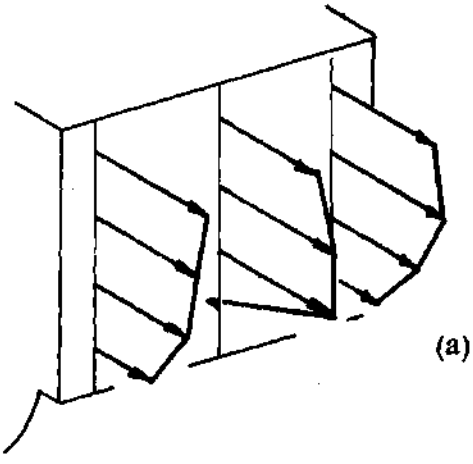

(a) Upper East

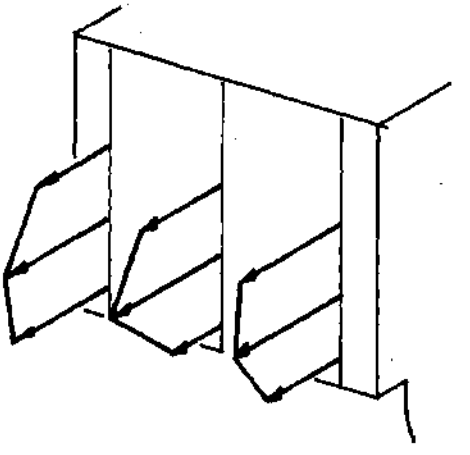

(b) Upper West

Figure 48. Building B Fan Room, Fan Outlet Velocity Profile.

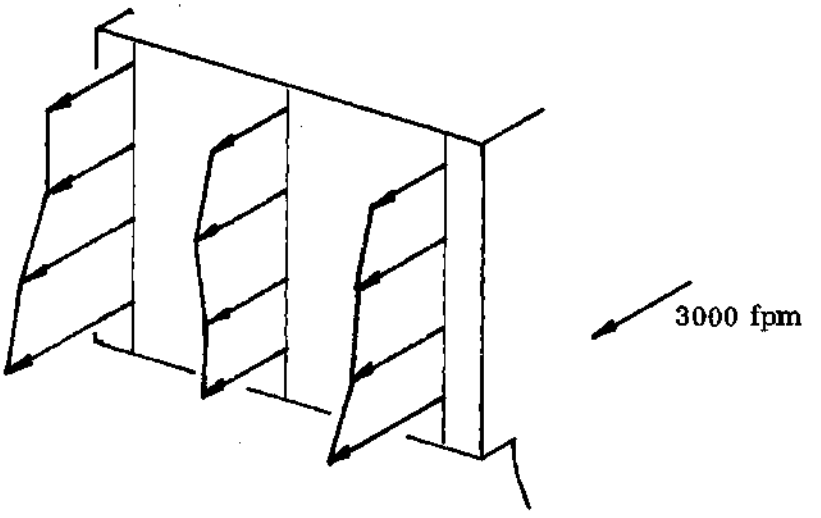

(a) Fan Outlet Velocity Profile.

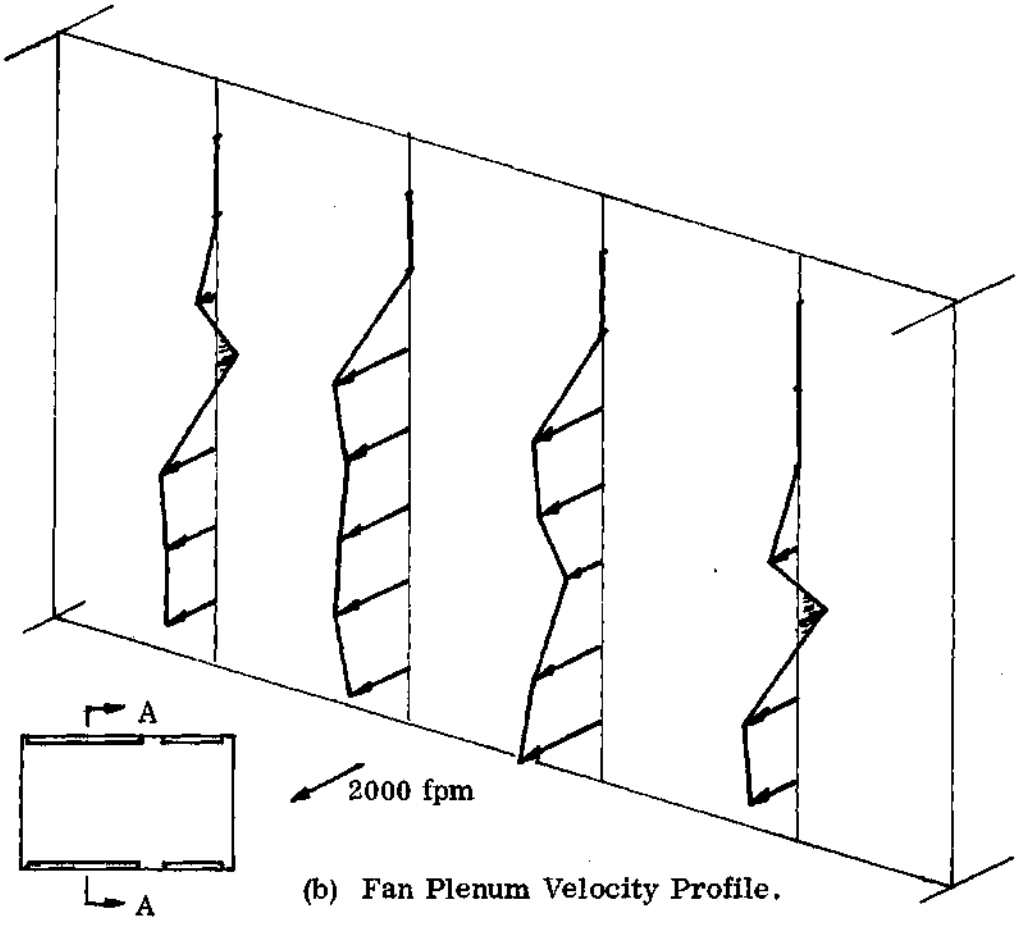

(b) Key Plan

(b) Fan Plenum Velocity Profile.

Note: Refer to Fig. 18 for details of fan room arrangement.

Figure 49. Building C Fan Room Velocity Profiles.

APPENDIX G

MODEL TESTS AND SELECTED DATA

Table 3. Tests Using the Building A Model

Test No.	Description
1	Fan Outlet Velocity Profile
2	Recheck of Test No. 1 w/Coil Velocity Profile & Observations
3	Evaluation of Anti-Wipe Baffle
4	Perforated Plate Evaluation for 0.25 Cooling Flow Ratio
5	Same as Test No. 4, but with 0.75 Cooling Flow Ratio
6	Removal of Diverging Wall for 0.75 Cooling Flow Ratio
7	Repeat of Test No. 6 for 0.25 Cooling Flow Ratio
8	Perforated Plate Position Evaluation 0.75 Cooling Flow Ratio
9	Abrupt Expansion, 0.75 Cooling Flow Ratio
10	Abrupt Expansion, 0.25 Cooling Flow Ratio

Table 4. Preliminary Tests with the General Model

Test No.	Description
11	Fan Outlet Velocity Profile
12	Recheck of Test No. 11
13	Fan Plenum Velocity Profiles
14	Same as Test No. 11 and 13, with Varying Cooling Flow Ratio
15	Evaluation of Fan Head-Flow Characteristics
16	Fan Plenum Air Motion Observations for Varying Cooling Flow Ratio

Table 5. Velocity Profile Tests with the General Model *

Test No.	Description
17	Cooling Coil; 3.33 D; 0.55; None
18	Cooling Coil; 3.33 D; 0.55; Vaned Diffuser
19	Cooling Coil; 3.33 D; 0.55; Perforated Plate No. 1 @ 2 D
20	Cooling and Heating Coils; 2.33 D; 0.55 Perforated Plate No. 1 @ 1 D

* Tests are velocity profiles measured at the leaving side of the cooling and heating coils, described as follows: coil or coils tested, distance from fan to coil surface, cooling flow ratio, correction device, distance from coil to bellmouth duct connection, if other than 3 duct diameters.

Table 5 (Continued). Velocity Profile Tests with the General Model

Test No	Description
21	Cooling and Heating Coils; 2.33 D; 0.55; None
22	Cooling and Heating Coils; 2.33 D; 0.55; Vaned Diffuser
23	Heating Coil; 2.33 D; 0.77; None
24	Heating Coil; 2.33 D; 0.77; Perforated Plate No. 1@1D
25	Cooling and Heating Coils; 1.33 D; 0.55; Perforated Plate No. 1 @ 1 D
26	Cooling and Heating Coils; 1.33 D; 0.55; None
27	Cooling and Heating Coils; 1.33 D; 0.55; Vaned Diffuser
28	Cooling and Heating Coils; 2.33 D; Varying Cooling Flow Ratio; None; 1 Diameter
29	Cooling and Heating Coils; 2.33 D; Varying; Perforated Plate No. 1 @ 2 D; 1 Diameter
30	Recheck of Test 28
31	Heating Coil; 2.33 D; 0.55; Perforated Plate No. 1 @ 1 D; 2 Diameters
32	Heating Coil; 2.33 D; 0.55; None; 2 Diameters
33	Heating Coil; 2.33 D; 0.55; Perforated Plate No. 1 @ 2 D; 2 Diameters
34	Heating Coil; 2.33 D; 0.55; Perforated Plate No. 1 @ 2 D; 3 Diameters
35	Cooling Coil; 2.33 D; 0.55; Perforated Plate No. 1 @ 2 D; 1 Diameter
36	Cooling Coil; 2.33 D; 0.55; Perforated Plate No. 1 @ 2 D; 3 Diameters

Table 5 (Continued). Velocity Profile Tests with the General Model

Test No.	Description
37	Cooling and Heating Coils; 2.33 D; 0.55 Perforated Plate No. 1 @ 1.5 D
38	Cooling and Heating Coils; 2.33 D; 0.55 Perforated Plate No. 1 @ 0.5 D
39	Cooling Coil; 2.33 D; 0.55; Perforated Plate No. 2 @ 1.5 D
40	Cooling Coil; 2.33 D; 0.55; Perforated Plate No. 3 @ 1.5 D
41	Cooling Coil; 2.33 D; 0.55; Perforated Plate No. 4 @ 1.5 D

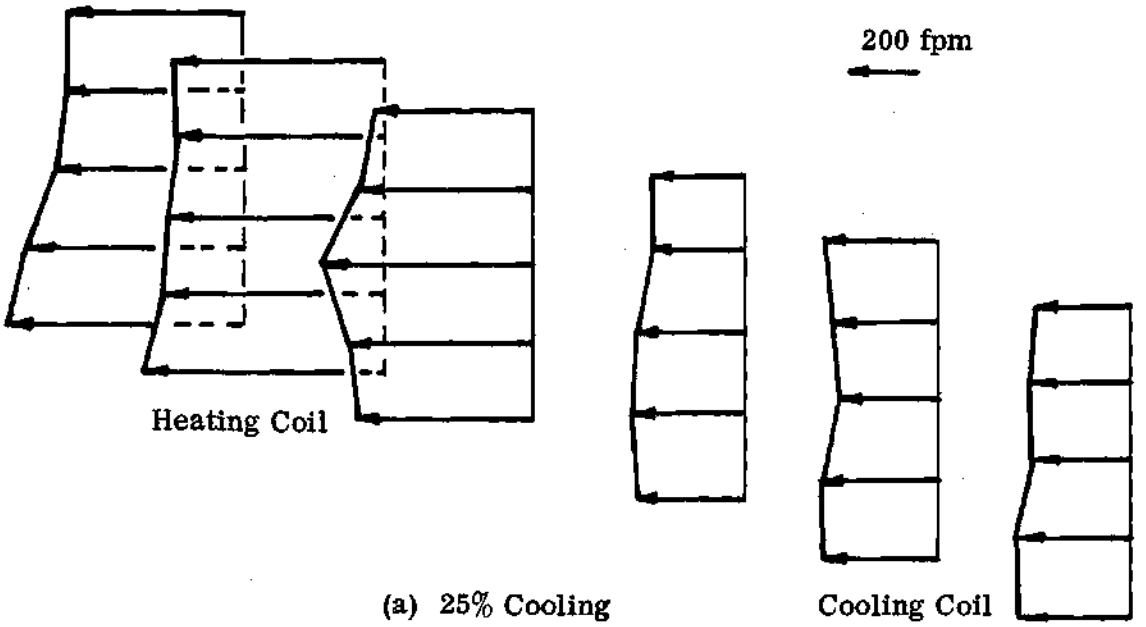

(a) 25% Cooling

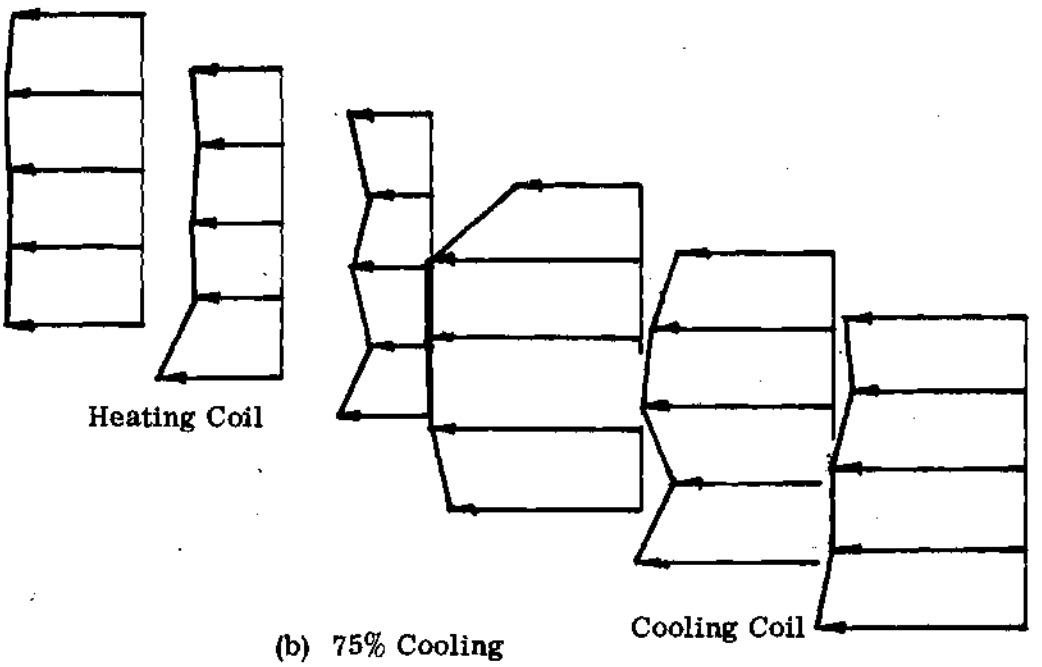

(b) 75% Cooling

Figure 50. Building A Fan Room Model, Downstream Heating and Cooling Coil Velocity Profiles.

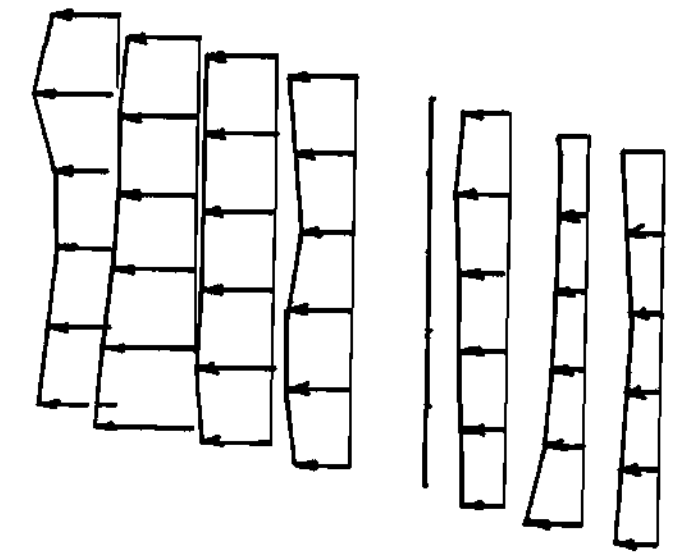

(a) Cooling Coil

500 fpm

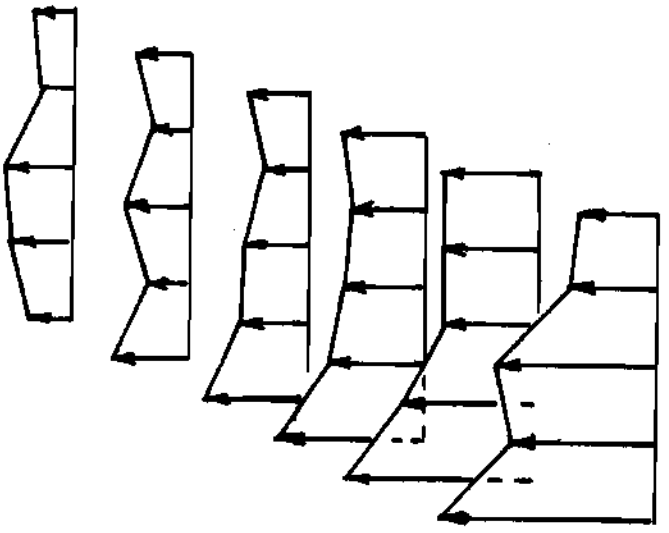

(b) Heating Coil

Figure 51. General Model, Typical Cooling and Heating Coil Velocity Profile without a Corrective Device.

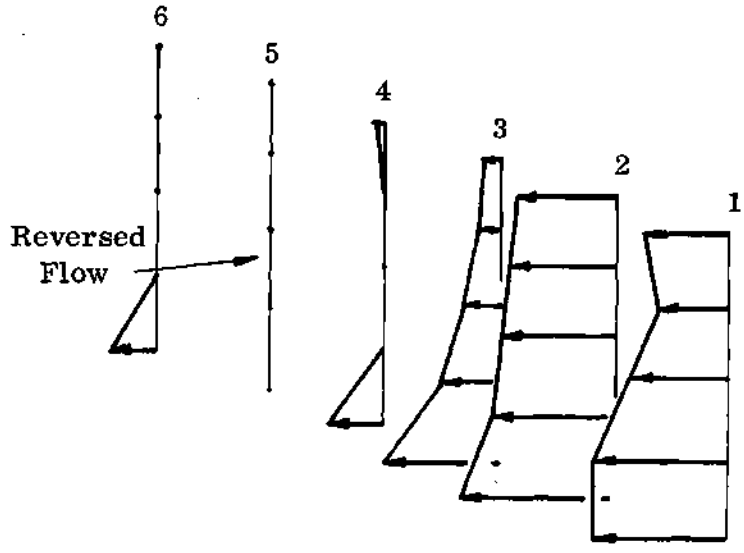

(a) 23% Heating

500 fpm

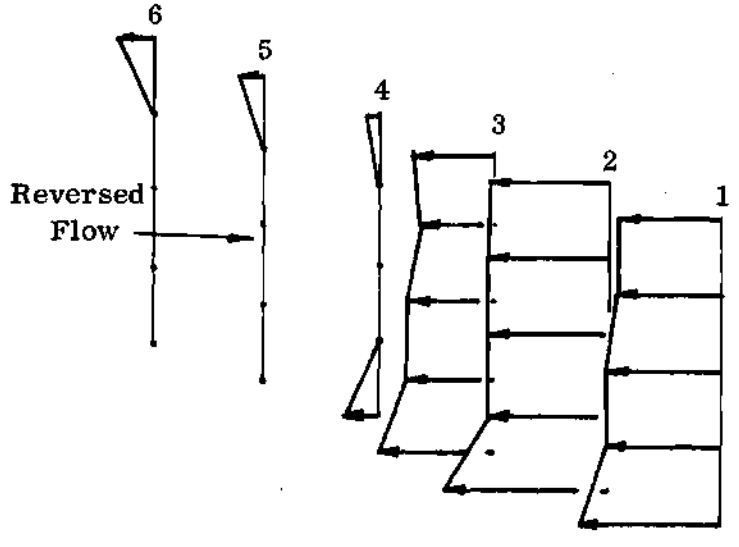

(b) 5% Heating

Figure 52. General Model, Heating Coil Velocity Profiles for Low Heating Flow Rates without a Corrective Device.

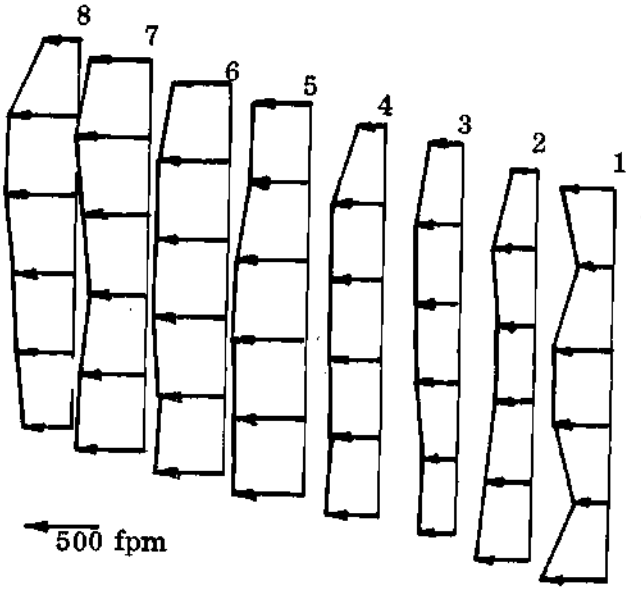

(a) Cooling Coil

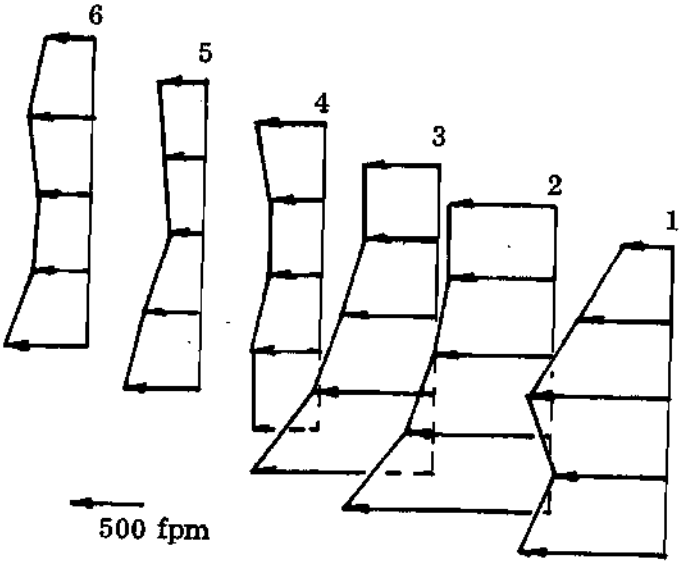

(b) Heating Coil

Figure 53. General Model, Cooling and Heating Coil Velocity Profiles with a Vaned Diffuser.

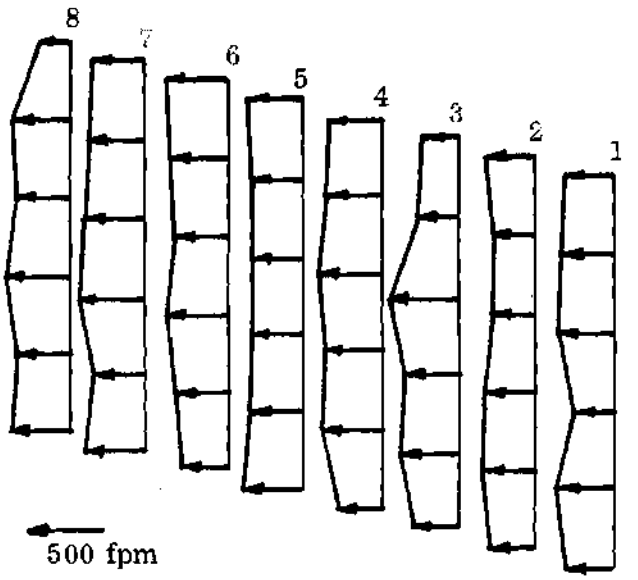

(a) Cooling Coil

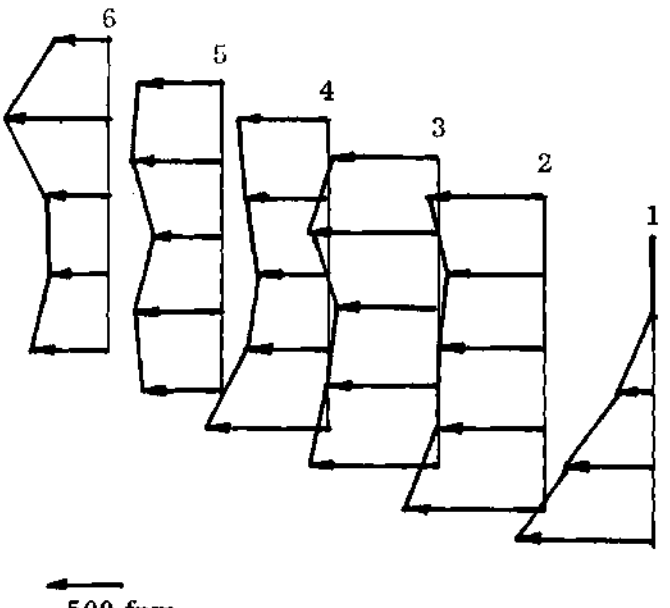

(b) Heating Coil

Figure 54. General Model, Cooling and Heating Coil Velocity Profile Using a Perforated Plate with the Fan at 1-1/3 Diameters from the Coils.

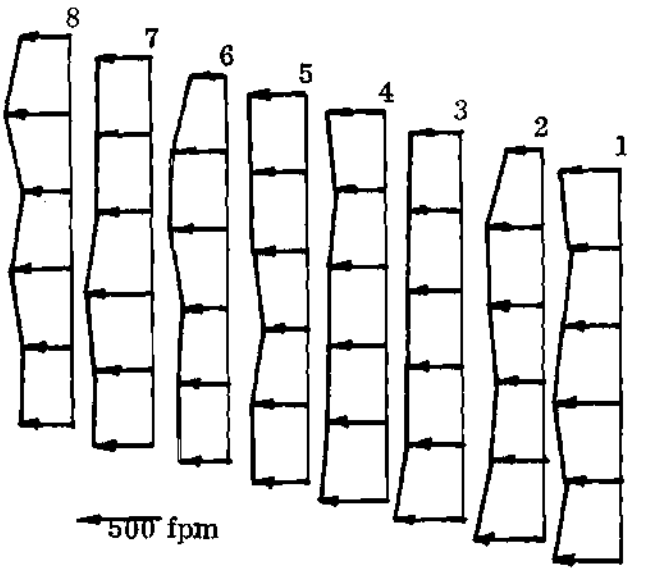

(a) Cooling Coil

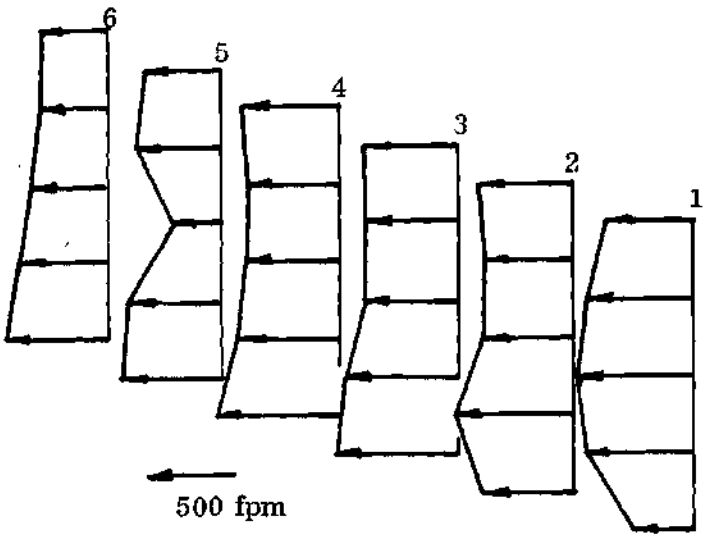

(b) Heating Coil

Figure 55. General Model, Heating and Cooling Coil Velocity Profile Using a Perforated Plate with the Fan at 2-1/3 Diameters from the Coils.

Table 6. Test No. 20

Fan Position from Coils: 2.33 D

Correction Device: Perforated Plate No. 1

Position of Plate from Fan: 1 D

Cooling Coil Velocity Profile:*

	1	2	3	4	5	6	7	8
A	300	320	270	400	350	300	260	360
B	370	320	390	400	280	300	320	290
C	300	310	410	410	340	310	310	280
D	420	420	350	360	360	340	300	330
E	310	330	380	400	350	340	310	320
F	360	380	300	370	380	390	340	300

Average Velocity: 368 fpm, Flow Rate: 4050 cfm.

Heating Coil Velocity Profile:

	1	2	3	4	5	6
A	360	400	500	490	490	450
B	350	430	430	480	470	540
C	400	250	490	480	480	580
D	460	490	540	600	620	520
E	530	540	620	630	470	300

Average Velocity: 550 fpm, Flow Rate: 4120 cfm.

*Profile is taken looking into the leaving side of the coils for all data in Appendix G.

Table 7. Test No. 21

Fan Position from Coils: 2.33 D

Correction Device: None

Cooling Coil Velocity Profile:

	1	2	3	4	5	6	7	8
A	440	470	430	420	0	270	210	250
B	560	520	470	390	0	330	200	230
C	460	510	470	360	0	290	210	210
D	410	540	470	460	0	290	210	230
E	440	600	490	450	0	280	230	250
F	460	610	450	380	0	210	350	240

Average Velocity: 355 fpm, Flow Rate: 3905 cfm.

Heating Coil Velocity Profile:

	1	2	3	4	5	6
A	230	290	310	430	500	400
B	190	190	230	390	490	440
C	370	340	310	410	490	820
D	340	200	340	480	680	740
E	220	380	490	740	1000	1100

Average Velocity: 500 fpm, Flow rate: 3755 cfm.

Table 8. Test No. 22

Fan Position from Coils: 2.33 D

Correction Device: Vaned Diffuser

Cooling Coil Velocity Profile:

	1	2	3	4	5	6	7	8
A	200	420	330	420	200	260	200	290
B	440	480	440	440	290	290	290	250
C	420	410	450	430	320	310	230	310
D	380	390	480	460	290	290	290	310
E	350	430	440	410	310	250	290	200
F	250	430	390	450	310	360	340	320

Average Velocity: 376 fpm, Flow Rate: 4140 cfm.

Heating Coil Velocity Profile:

	1	2	3	4	5	6
A	270	270	350	400	550	250
B	340	210	280	390	550	470
C	270	190	290	490	630	720
D	310	310	310	610	770	600
E	420	380	310	930	1070	760

Average Velocity: 498 fpm, Flow Rate: 3740 cfm.

Table 9. Test No. 36

Fan Position from Coils: 2.33 D

Correction Device: Perforated Plate No. 1

Position of Correction Device from Fan: 2 D

Cooling Coil Velocity Profile:

	1	2	3	4	5	6	7	8
A	320	330	280	340	180	170	200	350
B	580	370	340	340	160	230	280	220
C	460	350	340	320	190	320	250	310
D	500	340	310	340	290	320	280	290
E	390	390	310	350	240	320	280	340
F	290	460	270	360	0	410	380	280

Average Velocity: 338 fpm, Flow Rate: 3720 cfm.

Heating Coil Velocity Profile:

	1	2	3	4	5	6
A	540	570	570	600	730	400
B	490	420	510	590	670	90
C	340	300	480	550	700	560
D	220	430	420	620	700	480
E	620	640	710	760	830	950

Average Velocity: 605 fpm, Flow Rate: 4537 cfm.

Table 10. Test No. 37

Fan Position from Coils: 2.33 D

Correction Device: Perforated Plate No. 1

Position of Plate from Fan: 1.5 D

Cooling Coil Velocity Profile:

	1	2	3	4	5	6	7	8
A	260	230	350	380	360	300	200	310
B	430	390	390	400	340	240	320	320
C	380	350	370	400	340	350	300	330
D	430	340	340	380	340	340	310	360
E	380	380	380	380	370	370	350	260
F	350	360	400	390	320	410	360	320

Average Velocity: 378 fpm, Flow Rate: 4160 cfm.

Heating Coil Velocity Profile:

	1	2	3	4	5	6
A	380	400	530	530	490	220
B	360	420	440	470	490	460
C	400	420	440	440	470	500
D	450	450	500	560	310	560
E	490	560	650	410	220	460

Average Velocity: 494 fpm, Flow rate: 3700 cfm.

Table 11. Test No. 38

Fan Position from Coils: 2.33 D

Correction Device: Perforated Plate No. 1

Position of Plate from Fan: 0.5 D

Cooling Coil Velocity Profile:

	1	2	3	4	5	6	7	8
A	360	290	370	190	300	330	410	300
B	390	410	310	450	310	380	360	430
C	400	390	330	390	300	350	290	310
D	420	420	410	380	390	310	350	320
E	350	390	300	390	350	350	310	300
F	390	420	300	430	390	410	370	280

Average Velocity: 358 fpm, Flow Rate: 3940 cfm.

Heating Coil Velocity Profile:

	1	2	3	4	5	6
A	440	460	370	370	460	500
B	410	420	540	440	470	550
C	410	420	460	600	560	620
D	370	470	520	580	490	0
E	470	500	470	280	360	0

Average Velocity: 462 fpm, Flow Rate: 3465 cfm.

BIBLIOGRAPHY

1. N.S. Shataloff, "High Velocity Dual Duct Systems," Air Conditioning, Heating and Ventilating, Dec. 1964.

2. American Society of Heating, Refrigerating, and Air Conditioning Engineers, Guide and Data Book, Systems, Chapters 1 and 2, 1970.

3. R. W. Waterfill, "Air Conditioning of Multi-Room Buildings," A.S.H.R.A.E. Transactions, 1955.

4. N. S. Shataloff, "Elements of Dual-Duct Design and Performance," A.S.H.R.A.E. Transactions, 1956.

5. D. Rickelton, "Psychrometrics of Dual-Duct Systems," Heating, Piping and Air Conditioning, March 1964.

6. United Sheet Metal, Engineering Design Manual, 1970.

7. United Sheet Metal, "Design of High Velocity Systems for Minimum Energy Loss," May 1967.

8. Kazim Abbud and Wayne E. Long, "An Experimental Study of the Behavior of High Velocity Air in Round Sheet Metal Ducts of Field Construction," A.S.H.R.A.E. Transactions, 1966.

9. R. G. Nevins and A. C. Kent, "Heat Losses from Horizontal Ducts Carrying High Velocity Air," A.S.H.R.A.E. Transactions, No. 1865, 1964.

10. Vito V. Cerami, H. S. Shataloff, "Quiet High-Velocity Air Distribution," Air Conditioning, Heating, and Ventilating, Aug. 1964.

11. J. W. Spradling, "Controlling Noise in High-Velocity Air Distribution Systems," Air Conditioning, Heating, and Ventilating, Nov. 1962.

12. The Trane Co., Fans in Air Conditioning, Aug. 1970.

13. Farquhar, "Off-Performance of Fan With and Without Outlet Ducts," A.S.H.R.A.E. Symposium, Jan. 1970.

14. J. B. Graham, "Selecting Fans for Field Fabricated Air Handling Units," Heating, Piping and Air Conditioning, March, 1969.

15. S. F. Gilman, R. J. Martin, and S. Konzo, "Pressure Loss and Airflow Characteristics of a Box Plenum," A.S.H.R.A.E. Transactions, Vol. 55, No. 1367, 1949, pp. 299-320.

16. J. B. Graham, "A Method of Distributing Fan Outlet Velocity to Produce a Smooth Velocity Profile in Plenum Chamber," unpublished report, Buffalo Forge Co., 1969.

17. Martin L. Stone, "Pressure Losses of Perforated Plates," unpublished special problem M.E. 490, Georgia Institute of Technology, 19

18. W. D. Baines, and E. G. Peterson, "An Investigation of Flow Through Screens," A.S.M.E. Transactions, 1950.

19. N. J. Lipstein, "Low Velocity Sudden Expansion Pipe Flow," A.S.H.R.A.E. Transactions, No. 1789, 1962.

20. A. P. Kratz and J. R. Fellows, "Pressure Losses Resulting for Changes in Cross-Sectional Area in Air Ducts," University of Illinois, Engineering Experiment Station Bulletin, No. 300, 1938.

21. A.S.H.R.A.E. Guide and Data Book, Equipment, Chapters 3, 4, 6, and 9, 1969.

22. H. L. Langhaar, Dimensional Analysis and Theory of Models, John Wiley and Sons, 1951.

23. V. L. Streeter, Fluid Mechanics, McGraw-Hill, N.Y. 1966.

24. Air Moving and Conditioning Association, "Standard Test Code for Air Moving Devices," Bulletin 21, 1962.

25. A.S.H.R.A.E., Handbook of Fundamentals, Chapters 5 and 13, 1967.

26. D. E. Abbott, S. J. Kline, "Experimental Investigation of Subsonic Turbulent Flow over Single and Double Backward Facing Steps," A.S.M.E. Paper 61-Hyd-15.

27. The Trane Co., Cooling and Heating Coil Catalogs, 1960.

28. R. D. Stone, S. Simmons, C. Price, M. Williams, "Fan Room Airflow Characteristics," unpublished report for M.E. 455, Georgia Institute of Technology, 1969.

29. N. S. Shataloff, "Architect's Guide Dual Duct Air Conditioning," Buensod-Stacey Corp., New York, 1960.

30. G. de Vahl Davis, "Flow of Air Through Wire Screens," Proceedings of the First Australian Conference of Hydraulics and Fluid Mechanics, 1962.